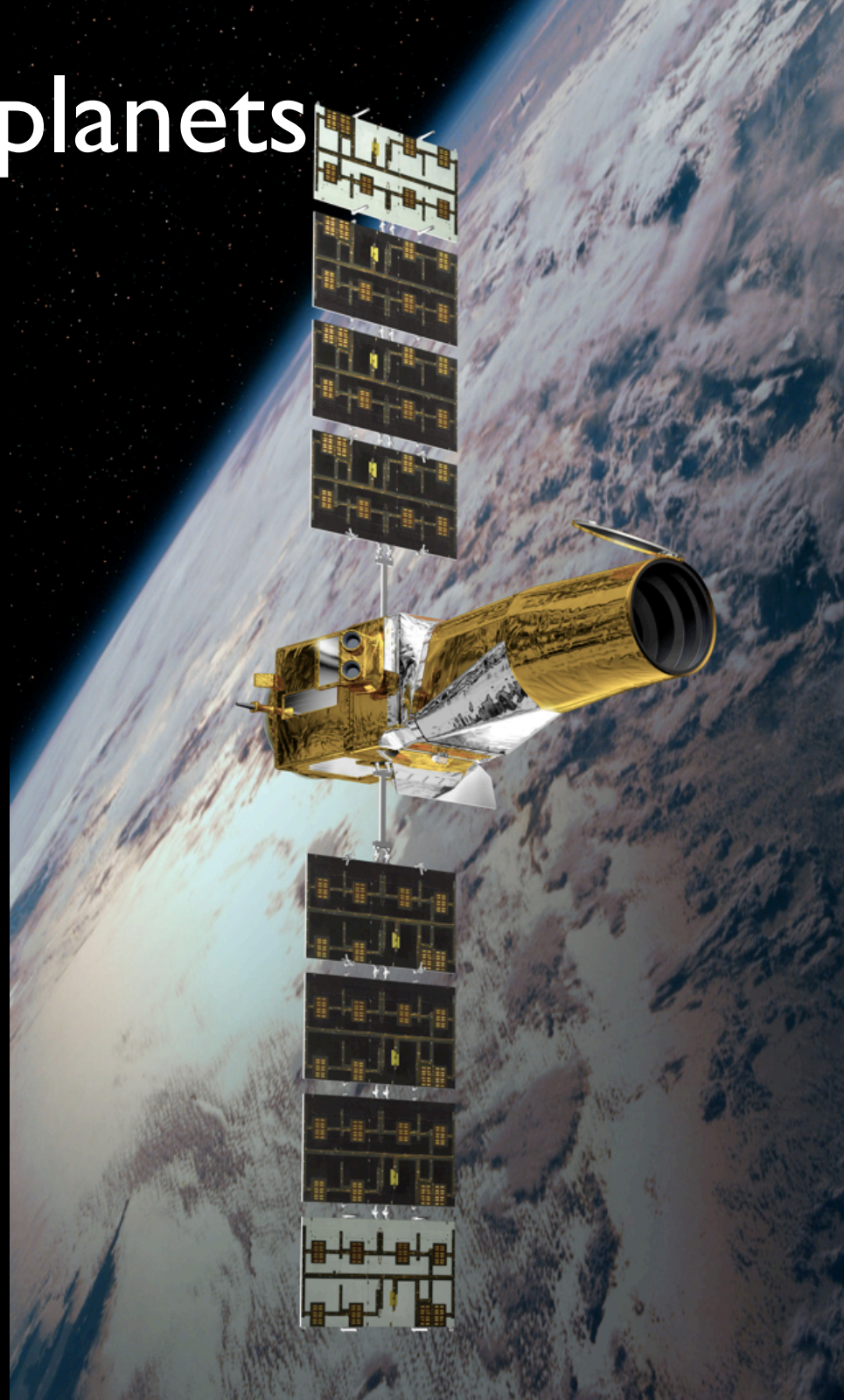


Transiting extrasolar planets with CoRoT

Suzanne Aigrain
University of Exeter

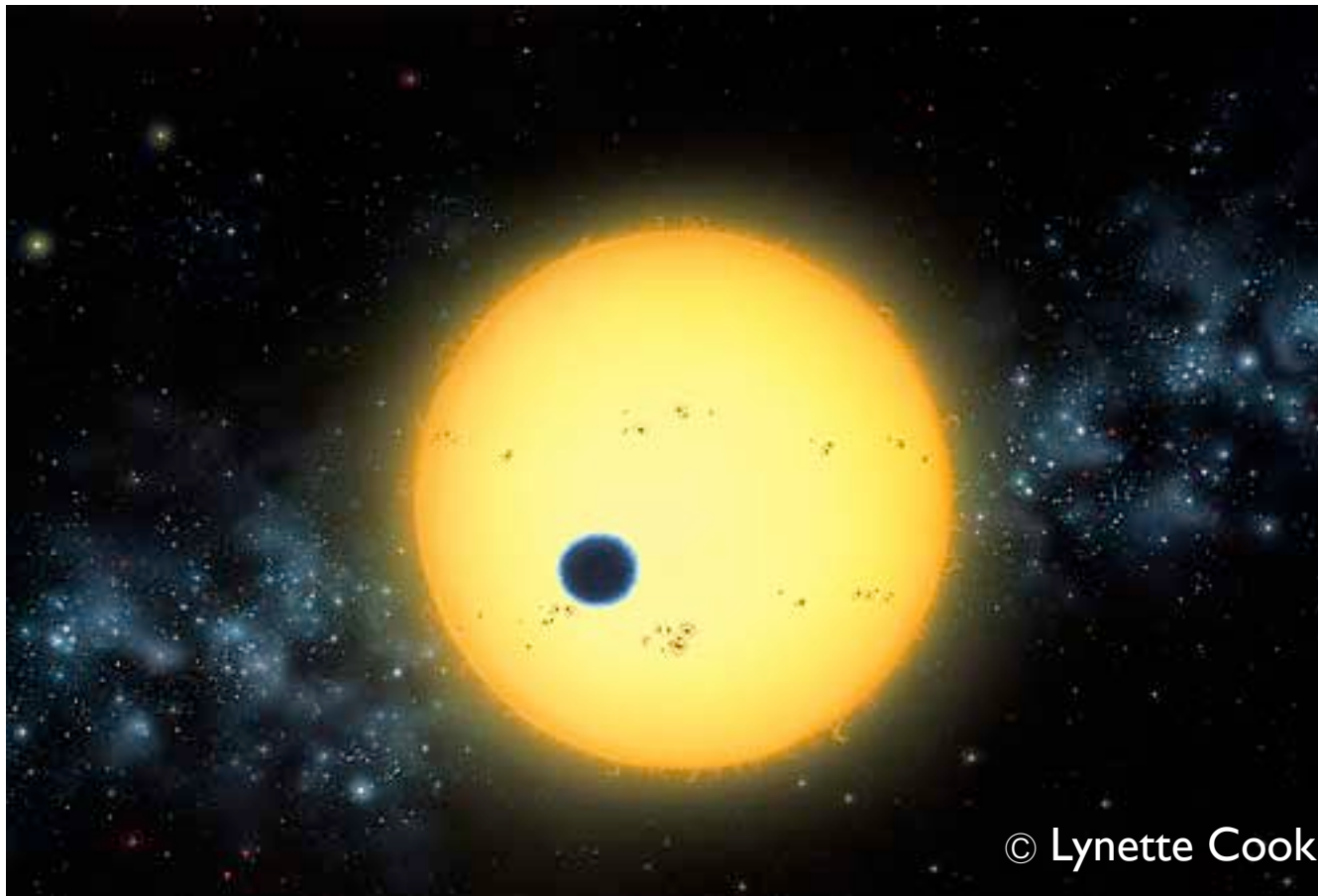
and the CoRoT Exoplanet Science Team

Annie Baglin (PI), A. Alapini, J. Almenara, R. Alonso, M. Auvergne, M. Barbieri, P. Barge, P. Borde, F. Bouchy, J. Cabrera, L. Carone, H. Deeg, J. De La Reza, M. Deleuil, R. Dvorak, A. Erikson, F. Fressin, M. Fridlund, M. Gillon, P. Gondoin, T. Guillot, A. Hatzes, G. Hebrard, L. Jorda, P. Kabath, H. Lammer, A. Leger, A. Llebaria, B. Loeillet, P. Magain, T. Mazeh, M. Mayor, C. Moutou, M. Ollivier, M. Patzold, F. Pepe, F. Pont, D. Queloz, H. Rauer, S. Renner, D. Rouan, J. Schneider, A. Shporer, B. Stecklum, Q. Triaud, G. Wuchterl, S. Udry, S. Zucker...



Outline

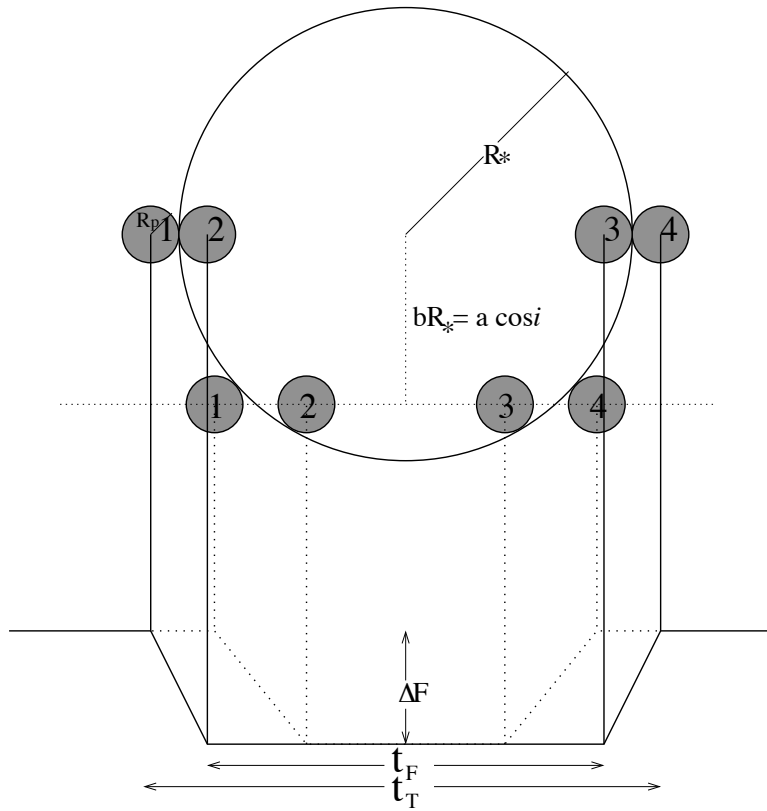
- Why build a space mission to search for transits?
- Brief introduction to the CoRoT mission
- Early results - CoRoT-exo-1b and CoRoT-exo-2b
- A few speculative teasers



Modelling transits

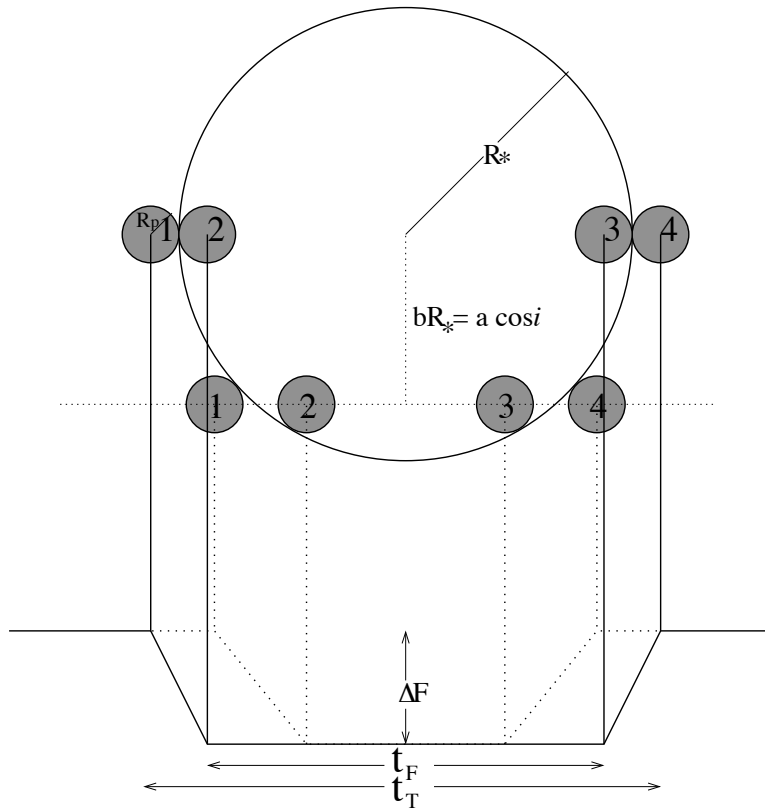
Modelling transits

Seager & Mallen-Ornelas (2003)



Modelling transits

Seager & Mallen-Ornelas (2003)



Ignoring limb-darkening and third light,

$$R_p = R_* \sqrt{\frac{\Delta F}{F}}$$

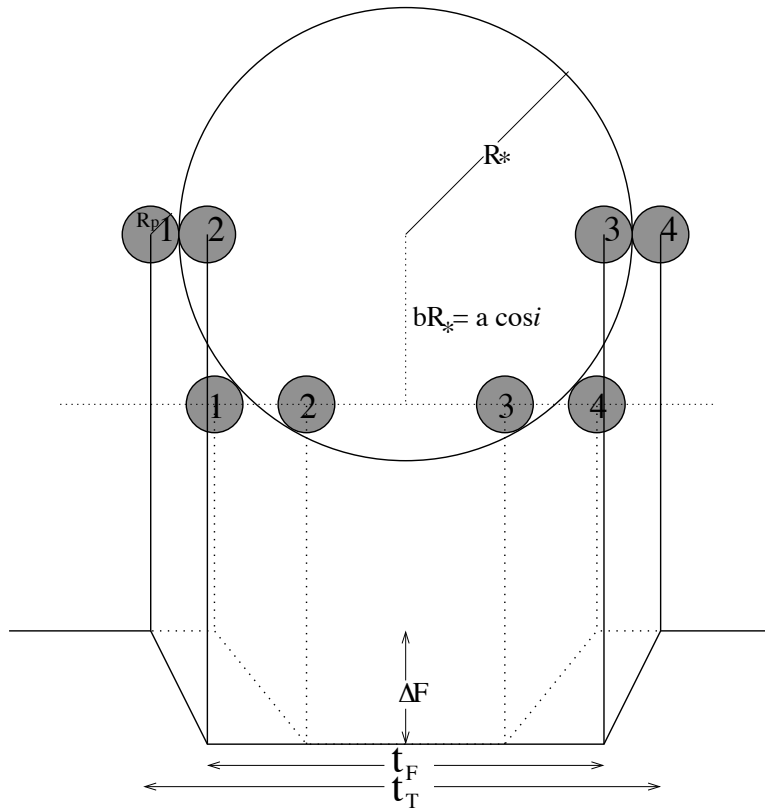
$$b \equiv \frac{a}{R_*} \cos i = \left[\frac{(1 - \sqrt{\Delta F})^2 - \frac{\sin^2 \frac{t_F \pi}{P}}{\sin^2 \frac{t_T \pi}{P}} (1 + \sqrt{\Delta F})^2}{1 - \frac{\sin^2 \frac{t_F \pi}{P}}{\sin^2 \frac{t_T \pi}{P}}} \right]^{1/2}$$

$$\frac{a}{R_*} = \left[\frac{(1 + \sqrt{\Delta F})^2 - b^2 (1 - \sin^2 \frac{t_T \pi}{P})}{\sin^2 \frac{t_T \pi}{P}} \right]^{1/2}$$

In practice, use more complex transit models (e.g. Mandel & Agol 2002) incorporating limb-darkening.

Modelling transits

Seager & Mallen-Ornelas (2003)



Ignoring limb-darkening and third light,

$$R_p = R_* \sqrt{\frac{\Delta F}{F}}$$

$$b \equiv \frac{a}{R_*} \cos i = \left[\frac{(1 - \sqrt{\Delta F})^2 - \frac{\sin^2 \frac{t_F \pi}{P}}{\sin^2 \frac{t_T \pi}{P}} (1 + \sqrt{\Delta F})^2}{1 - \frac{\sin^2 \frac{t_F \pi}{P}}{\sin^2 \frac{t_T \pi}{P}}} \right]^{1/2}$$

$$\frac{a}{R_*} = \left[\frac{(1 + \sqrt{\Delta F})^2 - b^2 (1 - \sin^2 \frac{t_T \pi}{P})}{\sin^2 \frac{t_T \pi}{P}} \right]^{1/2}$$

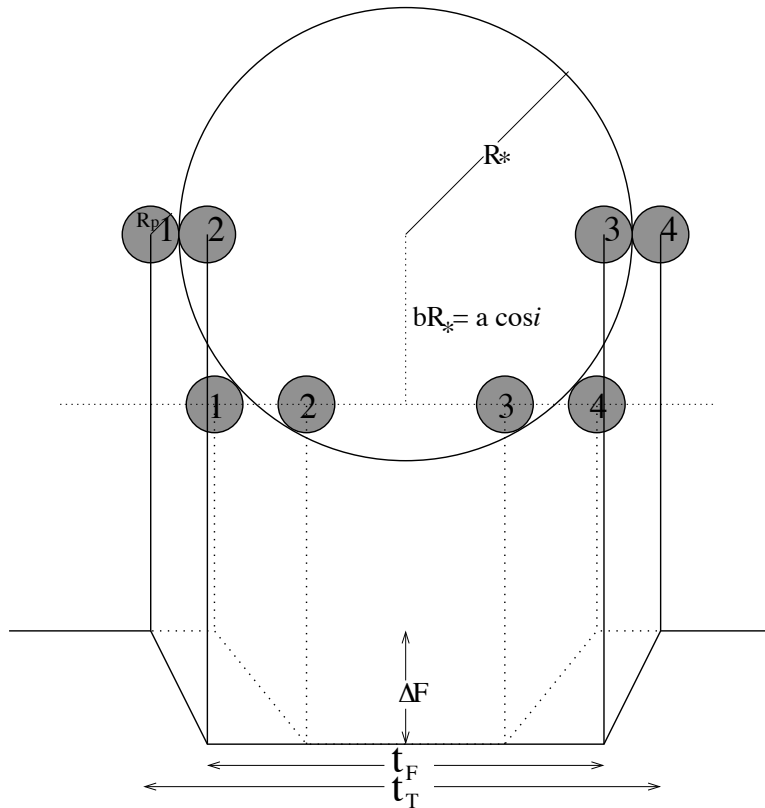
In practice, use more complex transit models (e.g. Mandel & Agol 2002) incorporating limb-darkening.

For circular orbits,

$$M_p = M_*^{\frac{2}{3}} \frac{K}{\sin i} \left(\frac{P}{4\pi G} \right)^{\frac{1}{3}}$$

Modelling transits

Seager & Mallen-Ornelas (2003)



For circular orbits,

$$M_p = M_*^{\frac{2}{3}} \frac{K}{\sin i} \left(\frac{P}{4\pi G} \right)^{\frac{1}{3}}$$

Ignoring limb-darkening and third light,

$$R_p = R_* \sqrt{\frac{\Delta F}{F}}$$

$$b \equiv \frac{a}{R_*} \cos i = \left[\frac{(1 - \sqrt{\Delta F})^2 - \frac{\sin^2 \frac{t_F \pi}{P}}{\sin^2 \frac{t_T \pi}{P}} (1 + \sqrt{\Delta F})^2}{1 - \frac{\sin^2 \frac{t_F \pi}{P}}{\sin^2 \frac{t_T \pi}{P}}} \right]^{1/2}$$

$$\frac{a}{R_*} = \left[\frac{(1 + \sqrt{\Delta F})^2 - b^2 (1 - \sin^2 \frac{t_T \pi}{P})}{\sin^2 \frac{t_T \pi}{P}} \right]^{1/2}$$

In practice, use more complex transit models (e.g. Mandel & Agol 2002) incorporating limb-darkening.

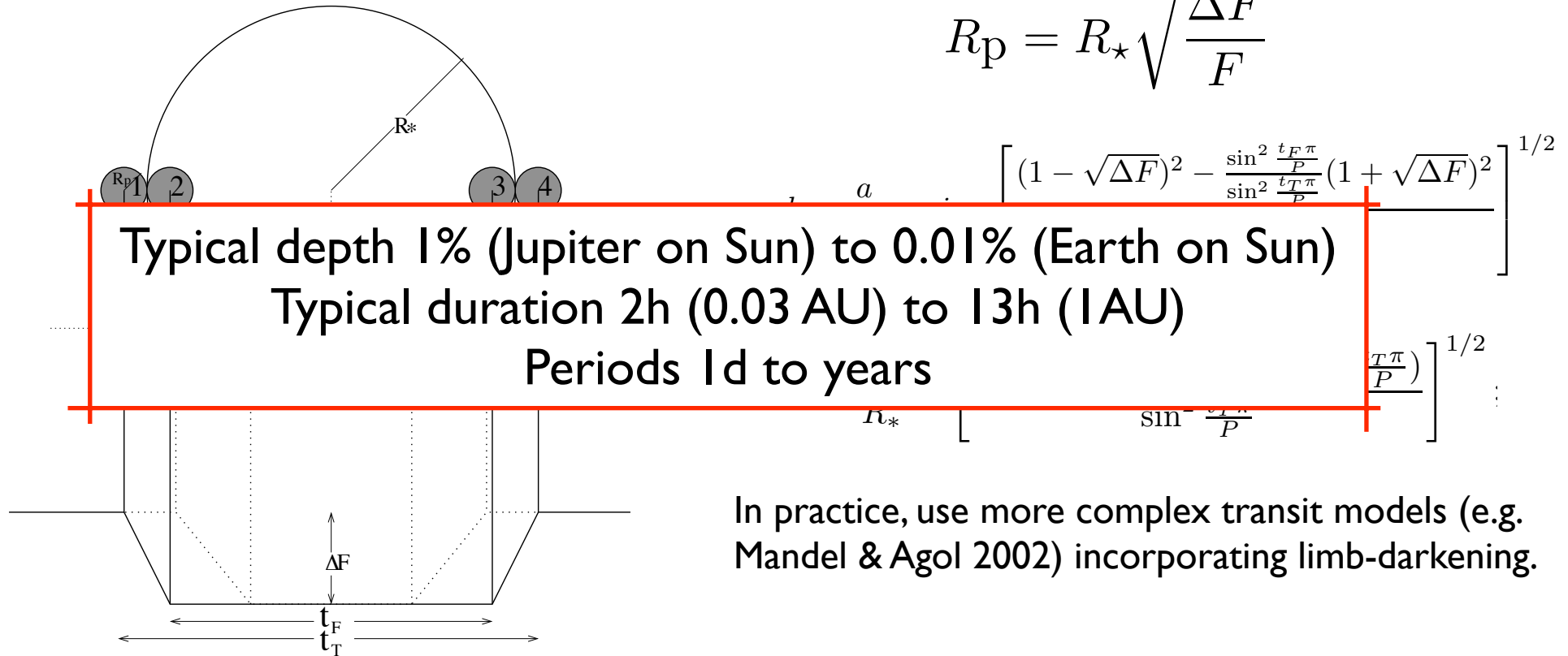
Only break degeneracy between inclination and star radius with ultra-precise (space-based) light curves. Otherwise, star radius as well as mass obtained by modelling high-SNR spectra

Modelling transits

Seager & Mallen-Ornelas (2003)

Ignoring limb-darkening and third light,

$$R_p = R_\star \sqrt{\frac{\Delta F}{F}}$$



In practice, use more complex transit models (e.g. Mandel & Agol 2002) incorporating limb-darkening.

For circular orbits,

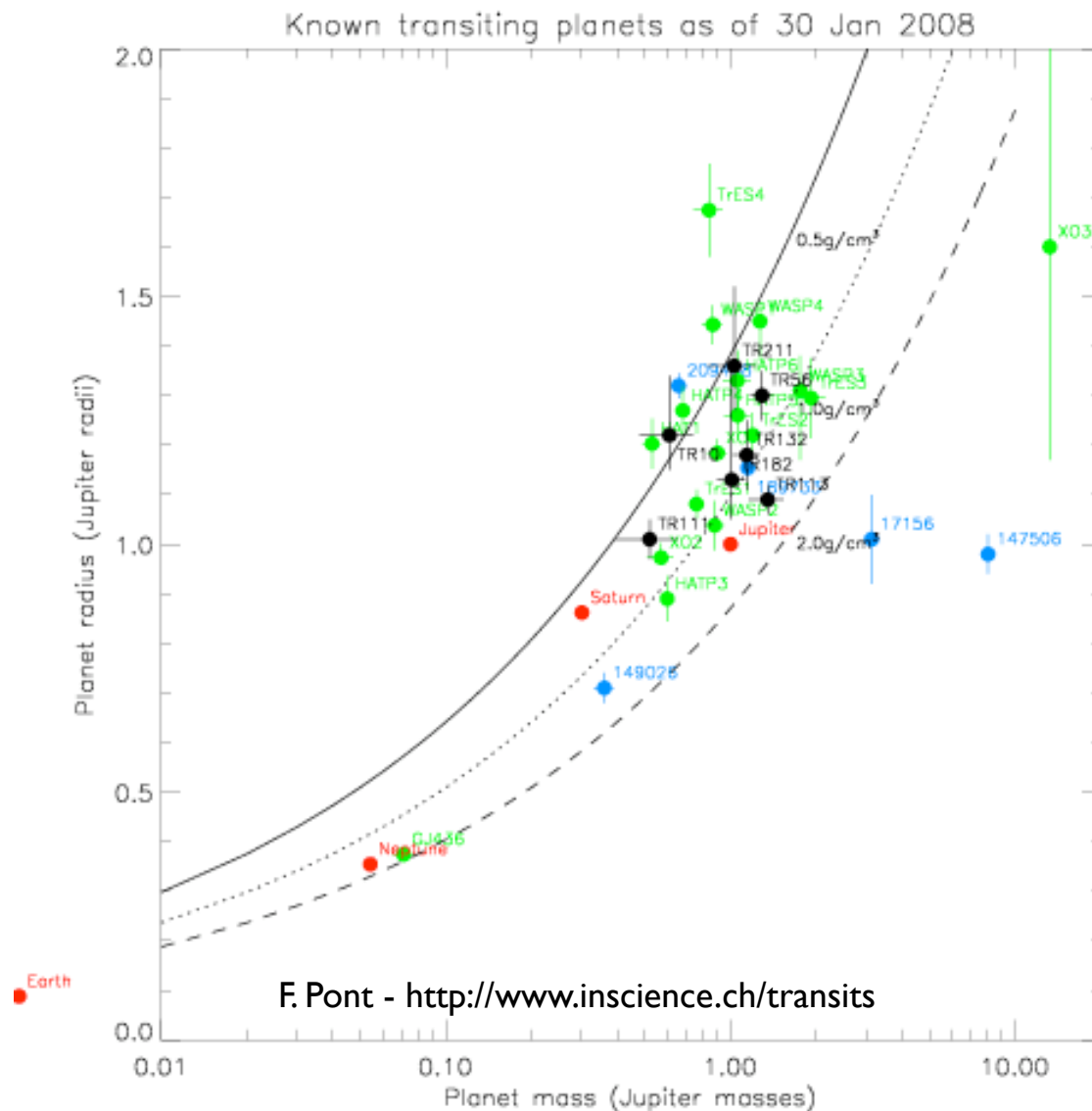
$$M_p = M_\star^{\frac{2}{3}} \frac{K}{\sin i} \left(\frac{P}{4\pi G} \right)^{\frac{1}{3}}$$

Only break degeneracy between inclination and star radius with ultra-precise (space-based) light curves. Otherwise, star radius as well as mass obtained by modelling high-SNR spectra

Why build CoRoT?

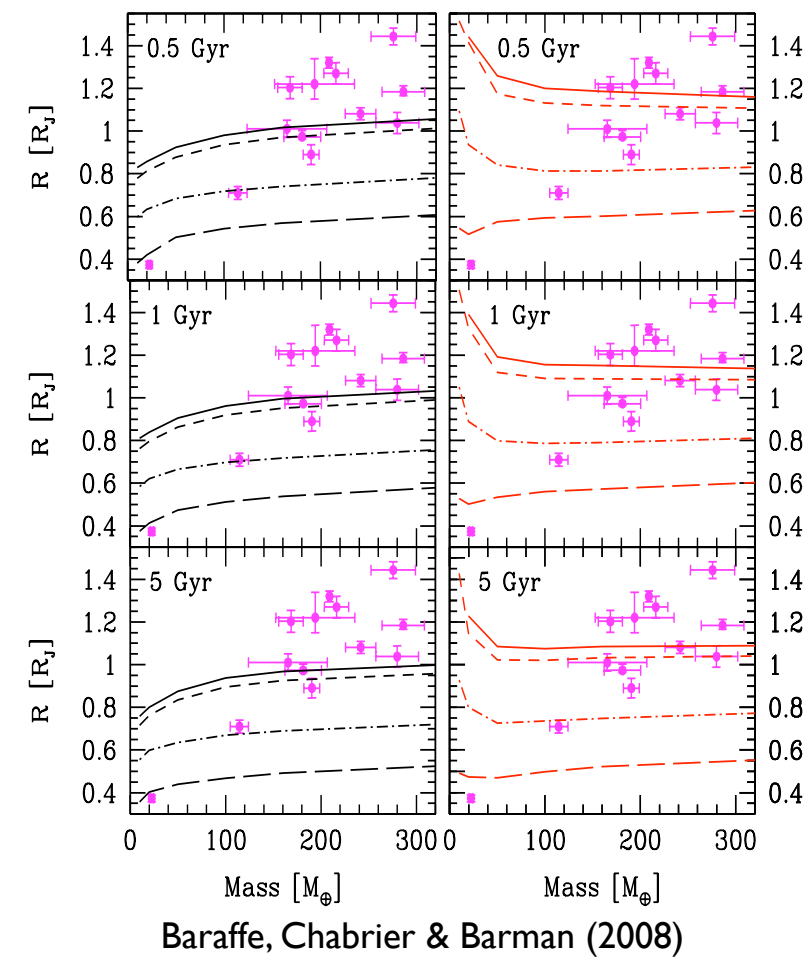
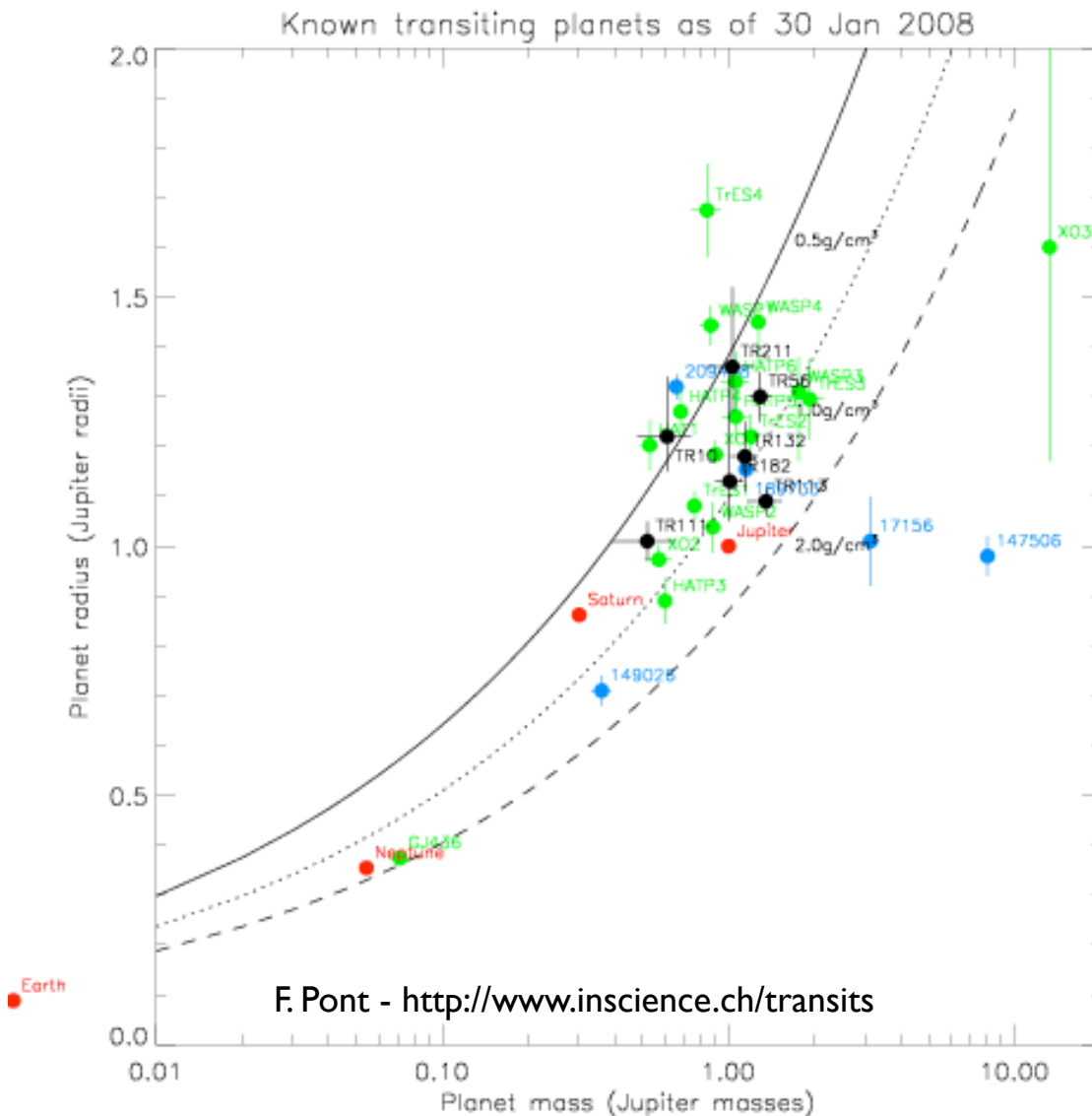
l. transits = physics

Structure and composition



Structure and composition

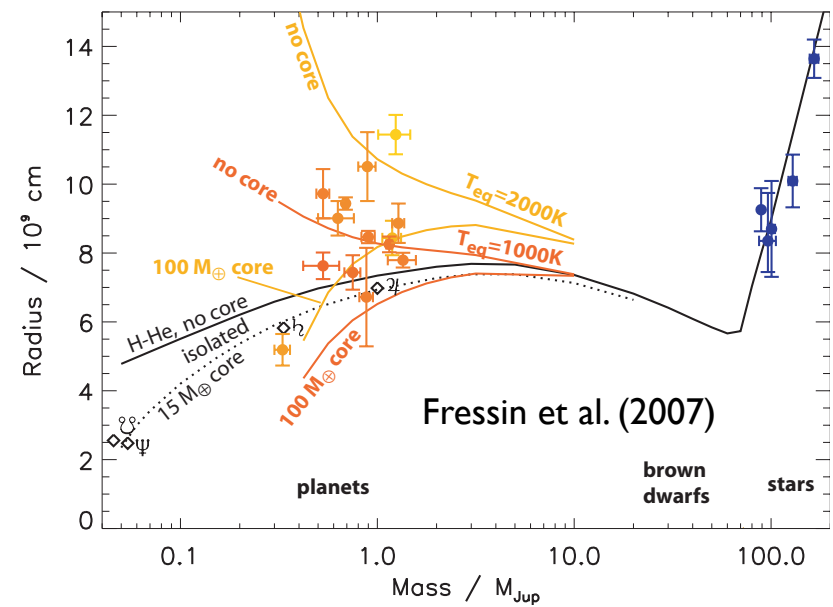
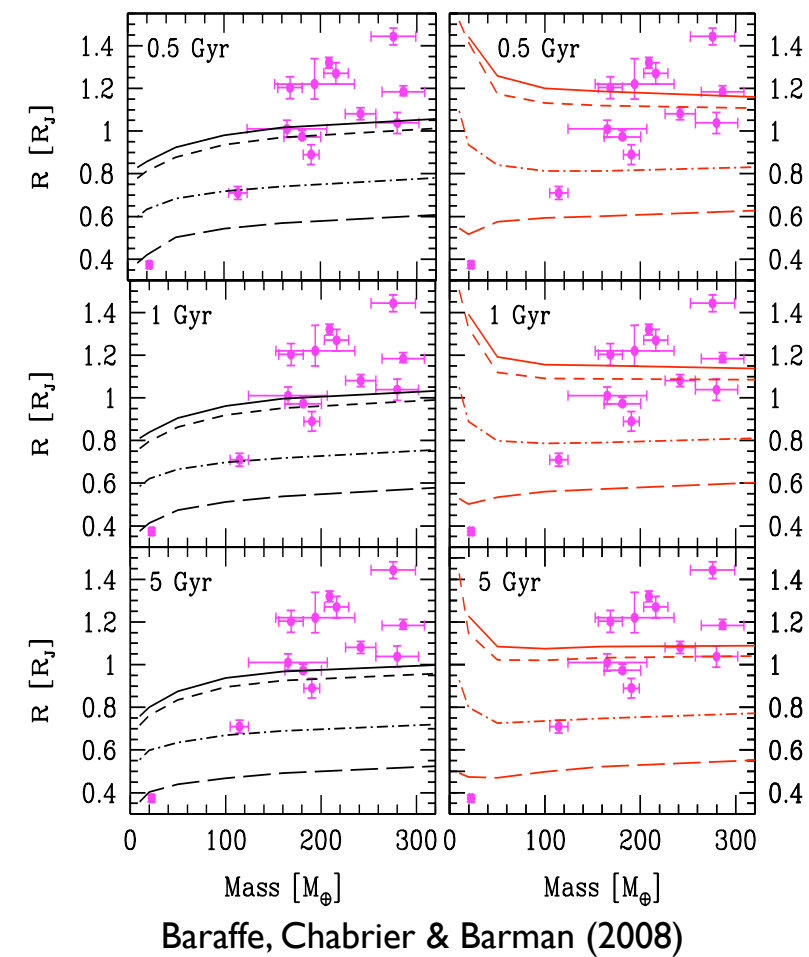
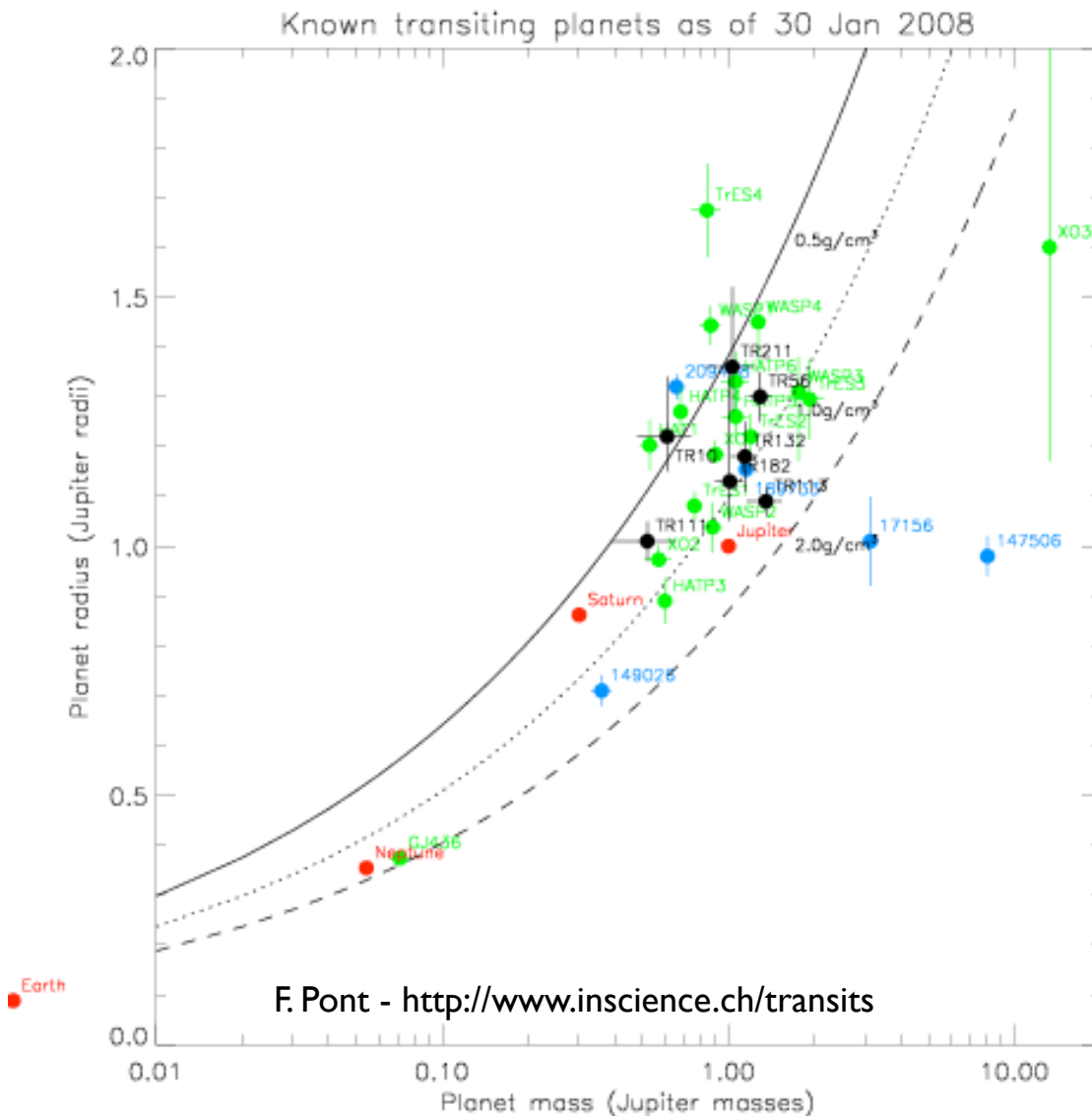
Of the known planets, several are (very) **inflated** - additional **heat source**?



Structure and composition

Of the known planets, several are (very) **inflated** - additional **heat source**?

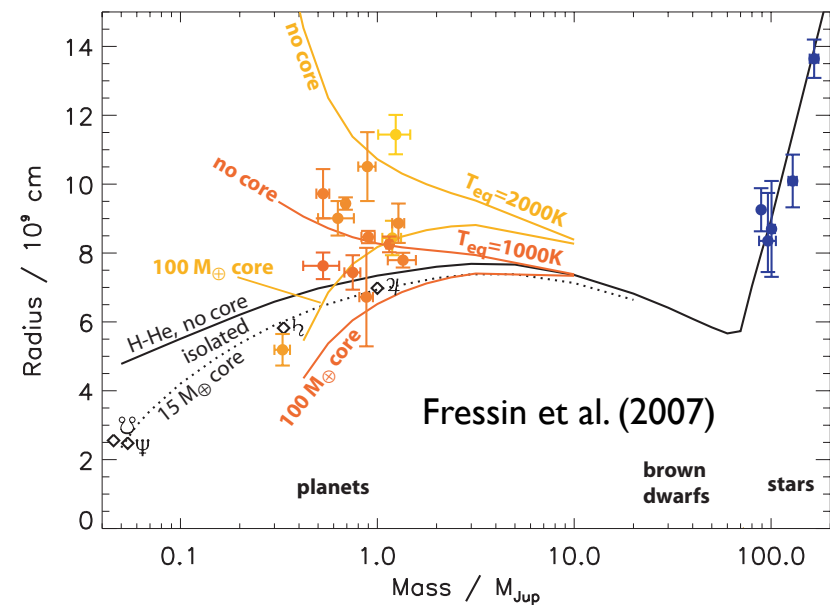
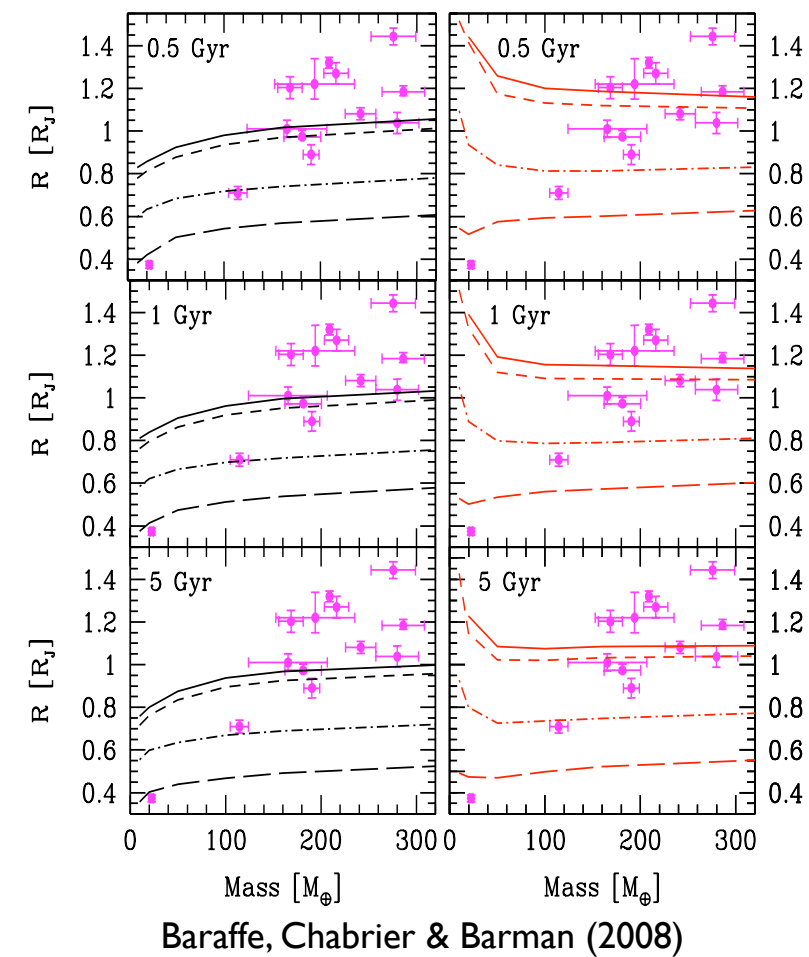
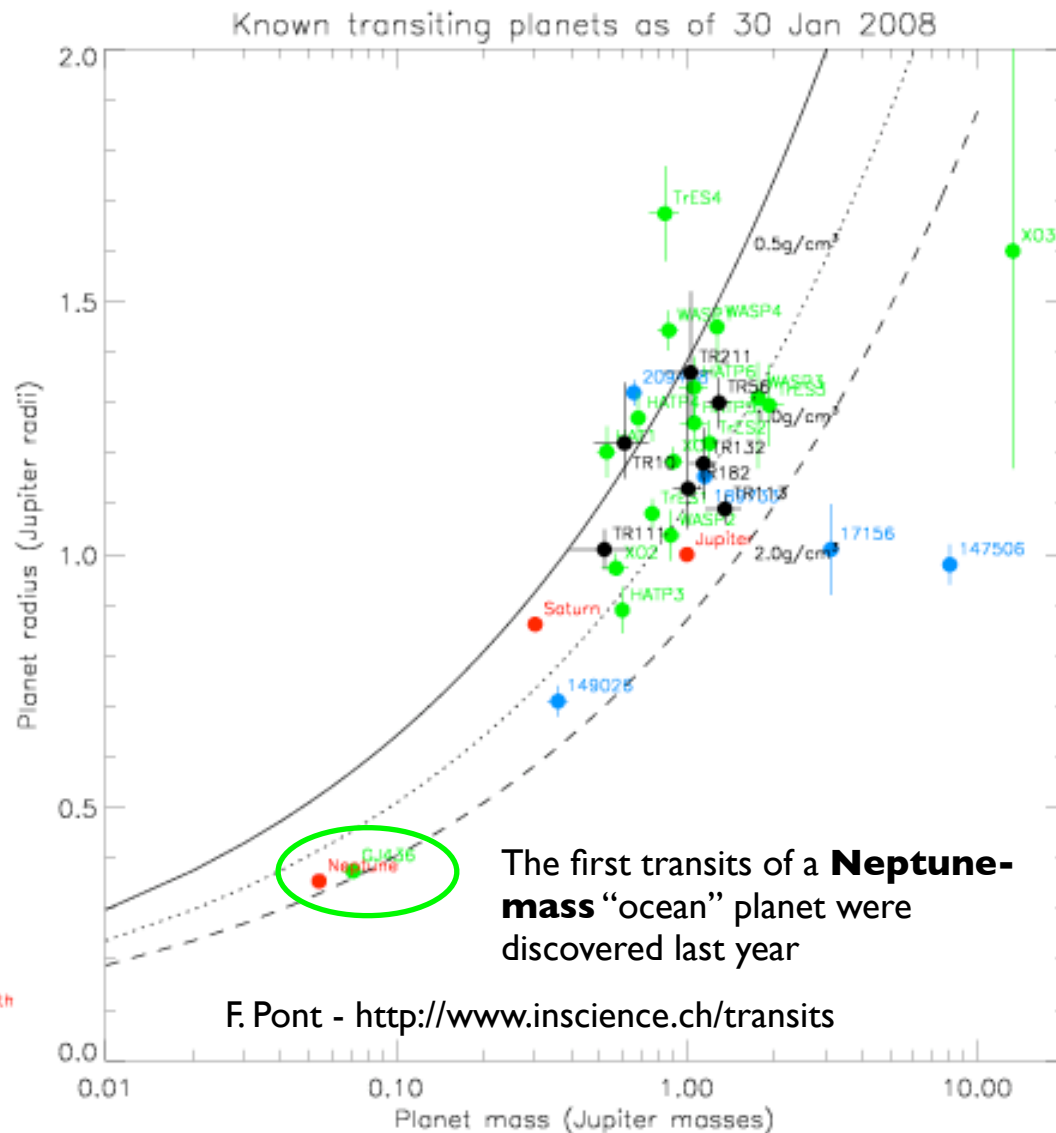
Others are very **dense** - high **core mass**?



Structure and composition

Of the known planets, several are (very) **inflated** - additional **heat source**?

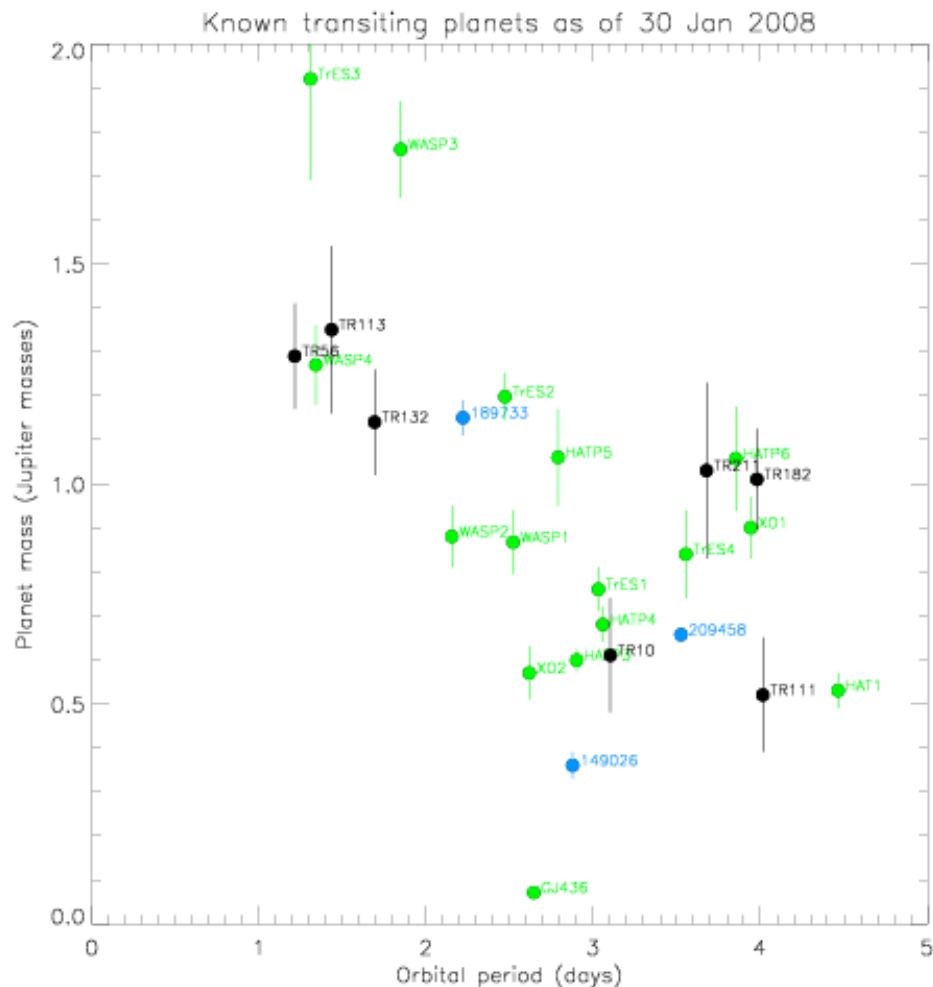
Others are very **dense** - high **core mass**?



Formation and evolution

Formation and evolution

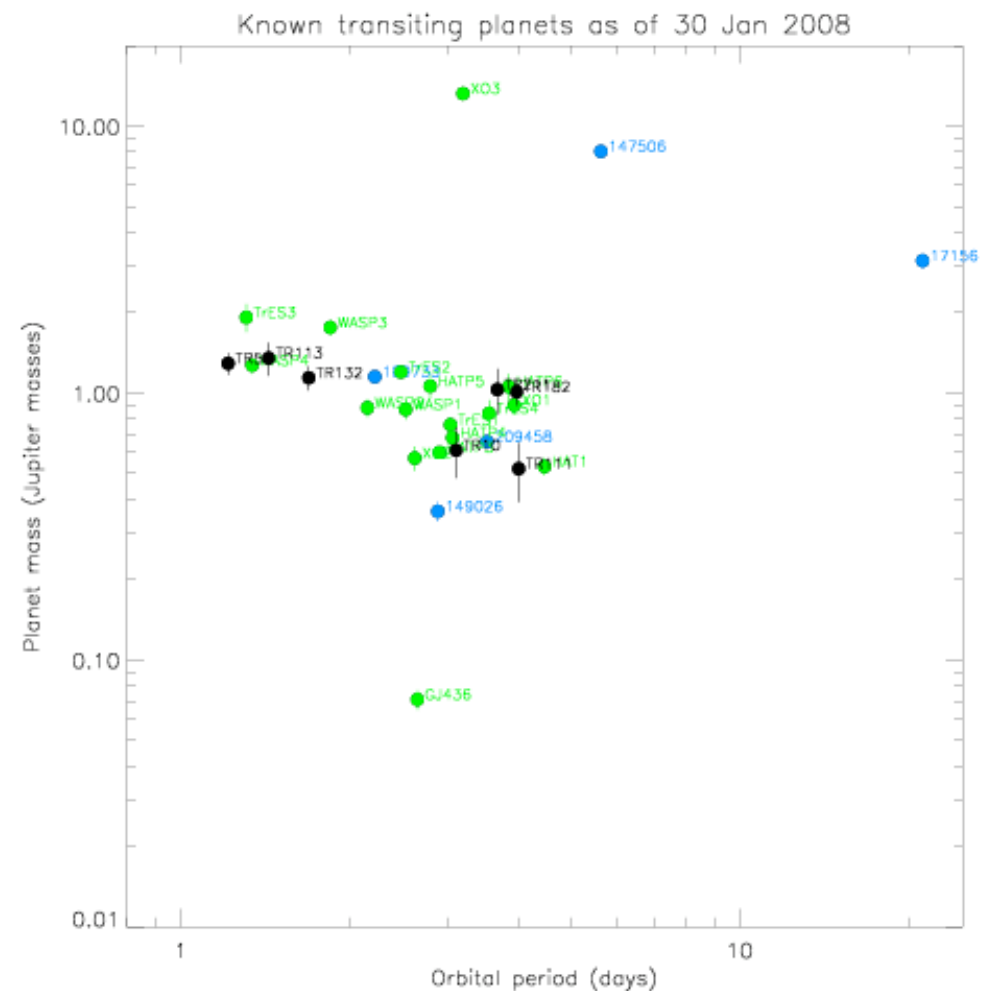
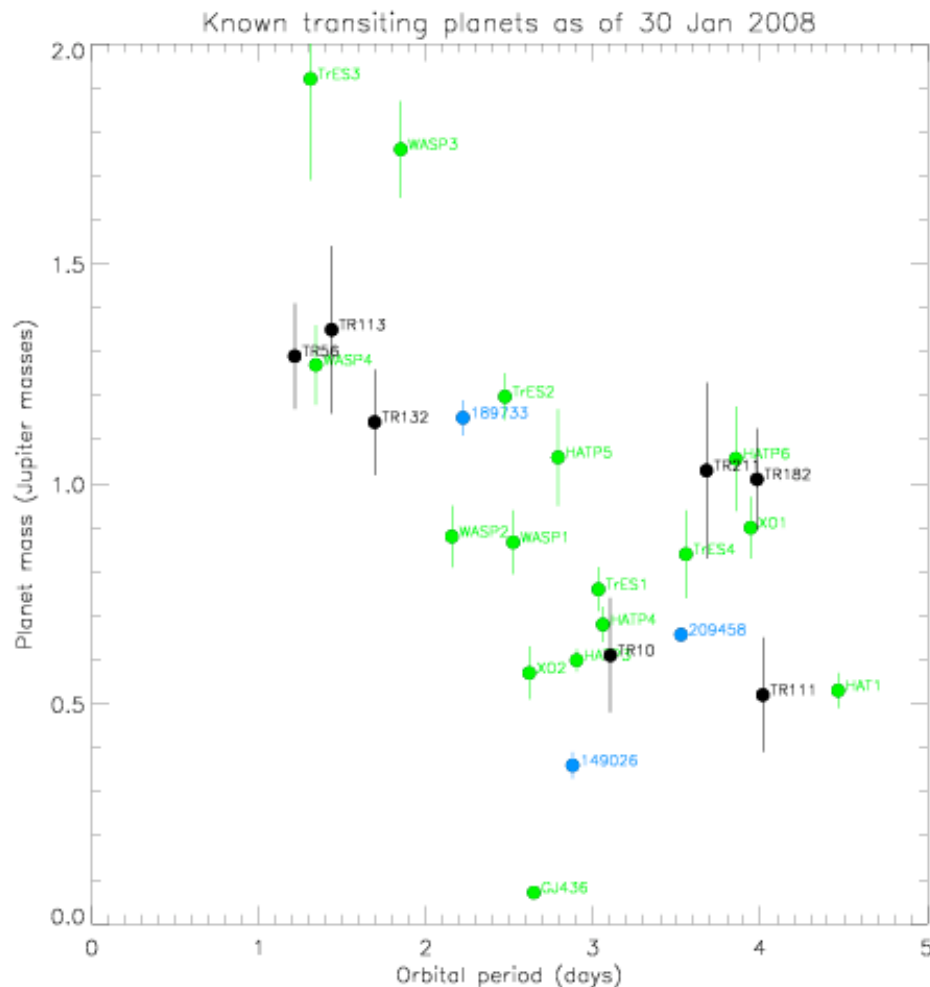
Mazeh & Zucker (2005) first pointed out a correlation between the true mass and period of transiting planets. Today, for giant planets it remains suggestive of a **minimum mass at a given period** - signature of evolutionary processes such as ***tidal evolution*** or ***evaporation***?



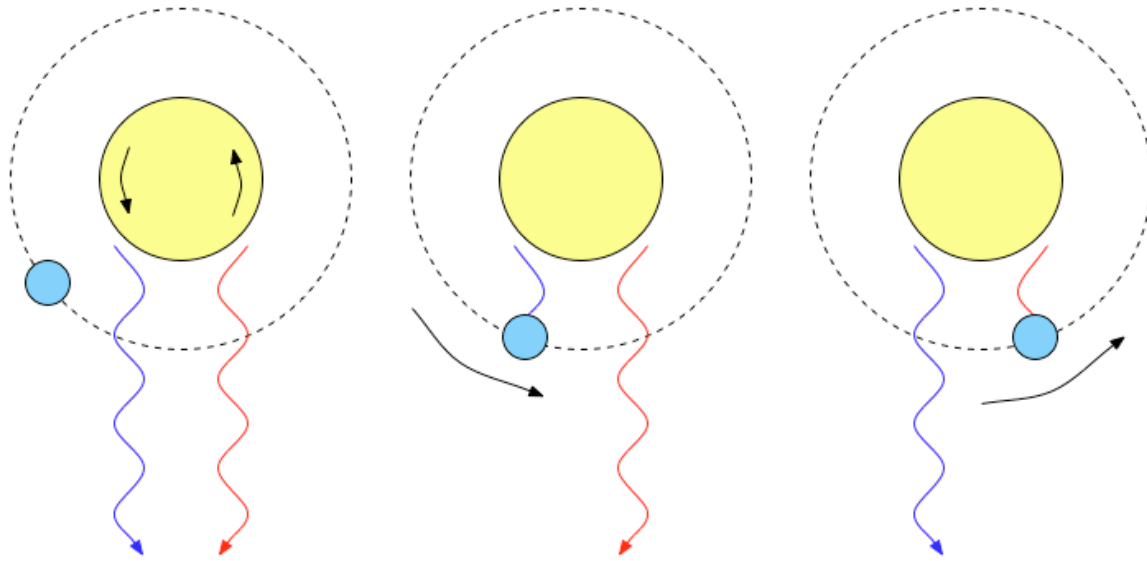
Formation and evolution

Mazeh & Zucker (2005) first pointed out a correlation between the true mass and period of transiting planets. Today, for giant planets it remains suggestive of a **minimum mass at a given period** - signature of evolutionary processes such as **tidal evolution** or **evaporation**?

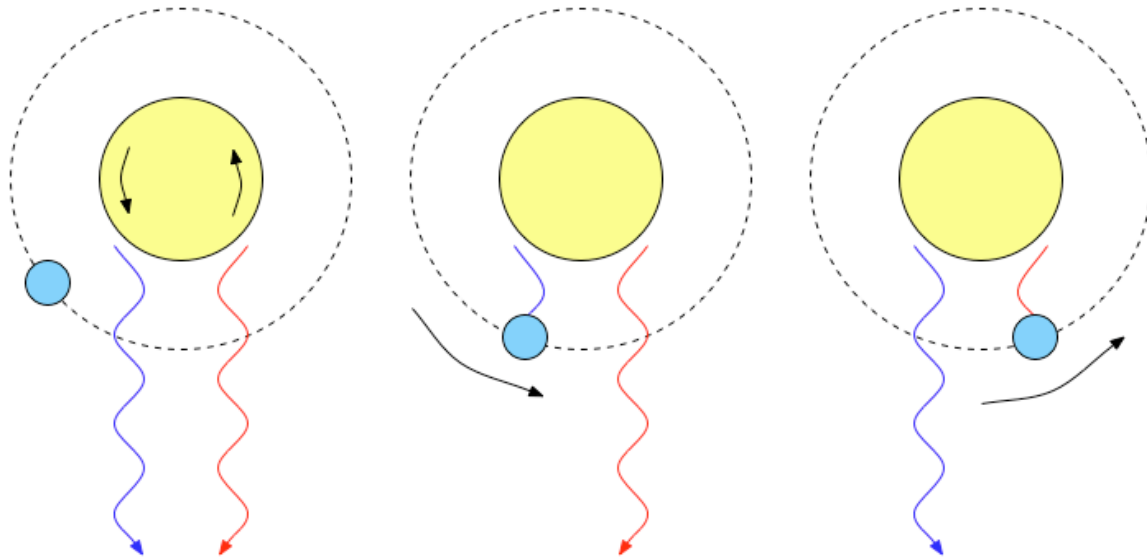
With recent discoveries of low and high mass transiting planets, we are starting to see **3 very distinct classes of planets** in this diagram: normal (very) hot Jupiters, supermassive hot Jupiters, and hot Neptunes. Could this indicate **distinct formation and/or evolution mechanisms**?



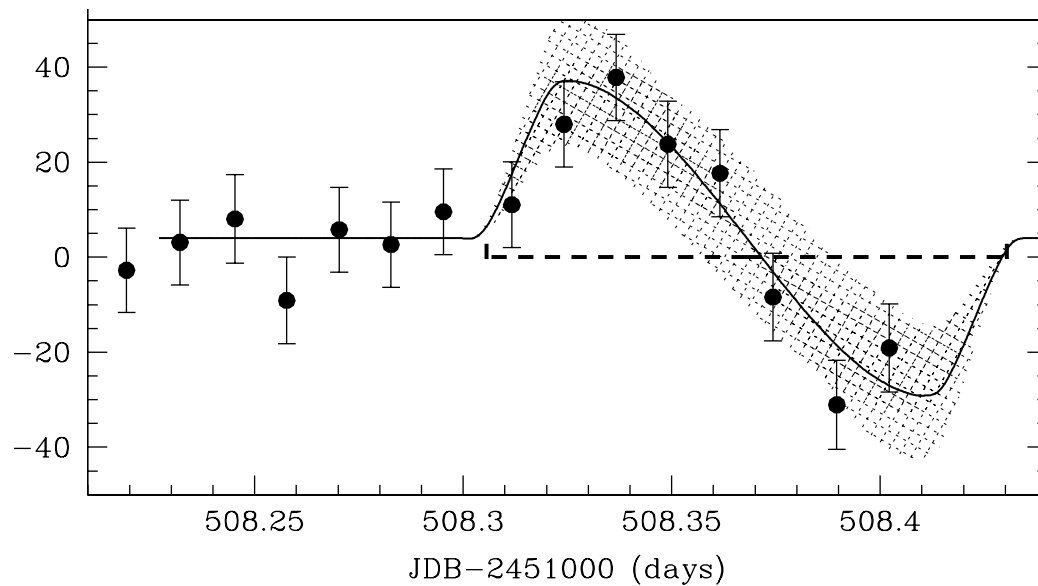
Formation and star-planet interaction



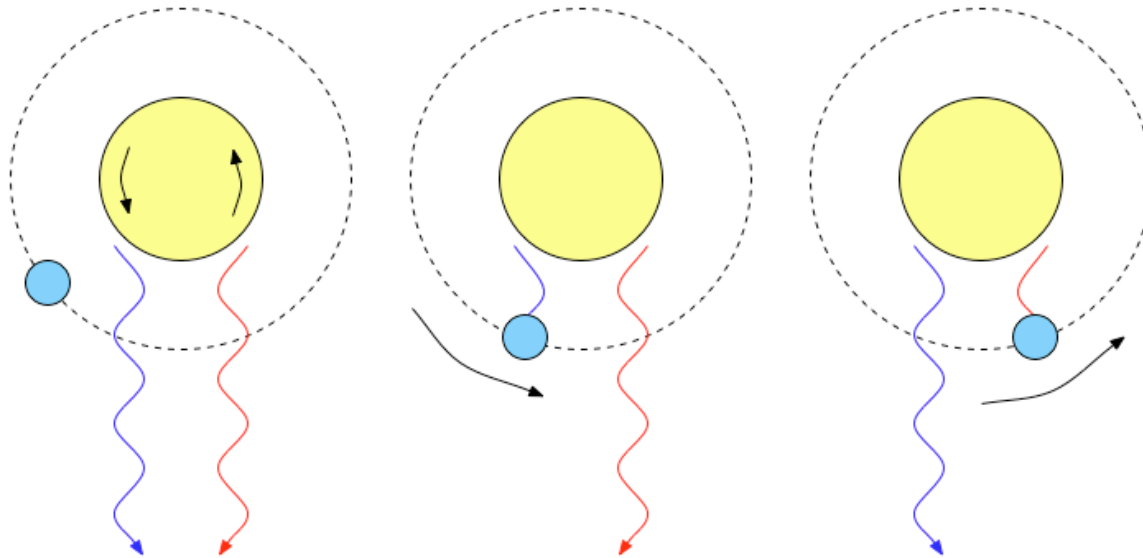
Formation and star-planet interaction



Queloz et al. (2000) - HD 209458b

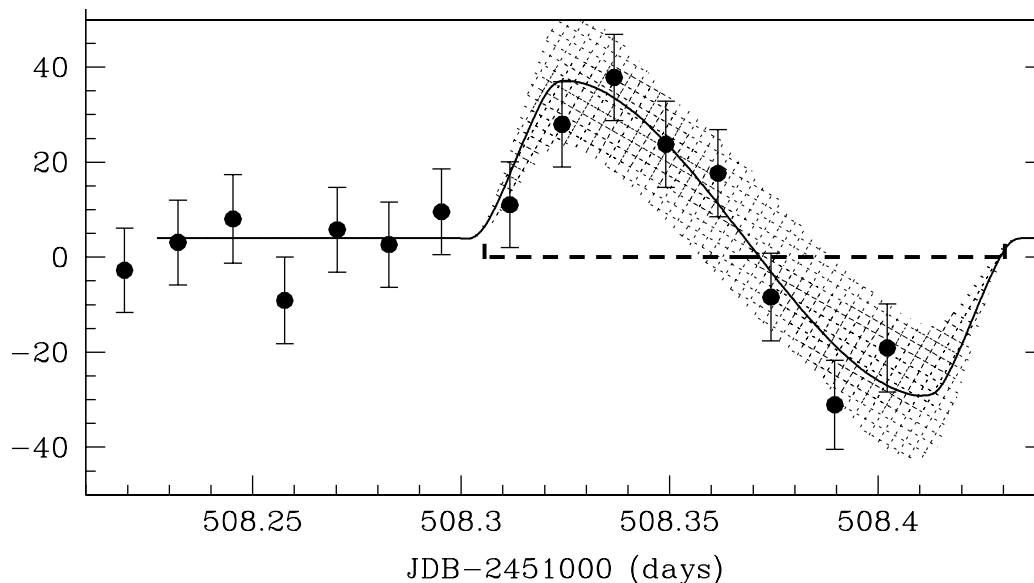


Formation and star-planet interaction



The **Rossiter-McLaughlin effect**, or spectroscopic transit, is primarily sensitive to **relative inclination** of the planet's orbit and the star rotational equator.

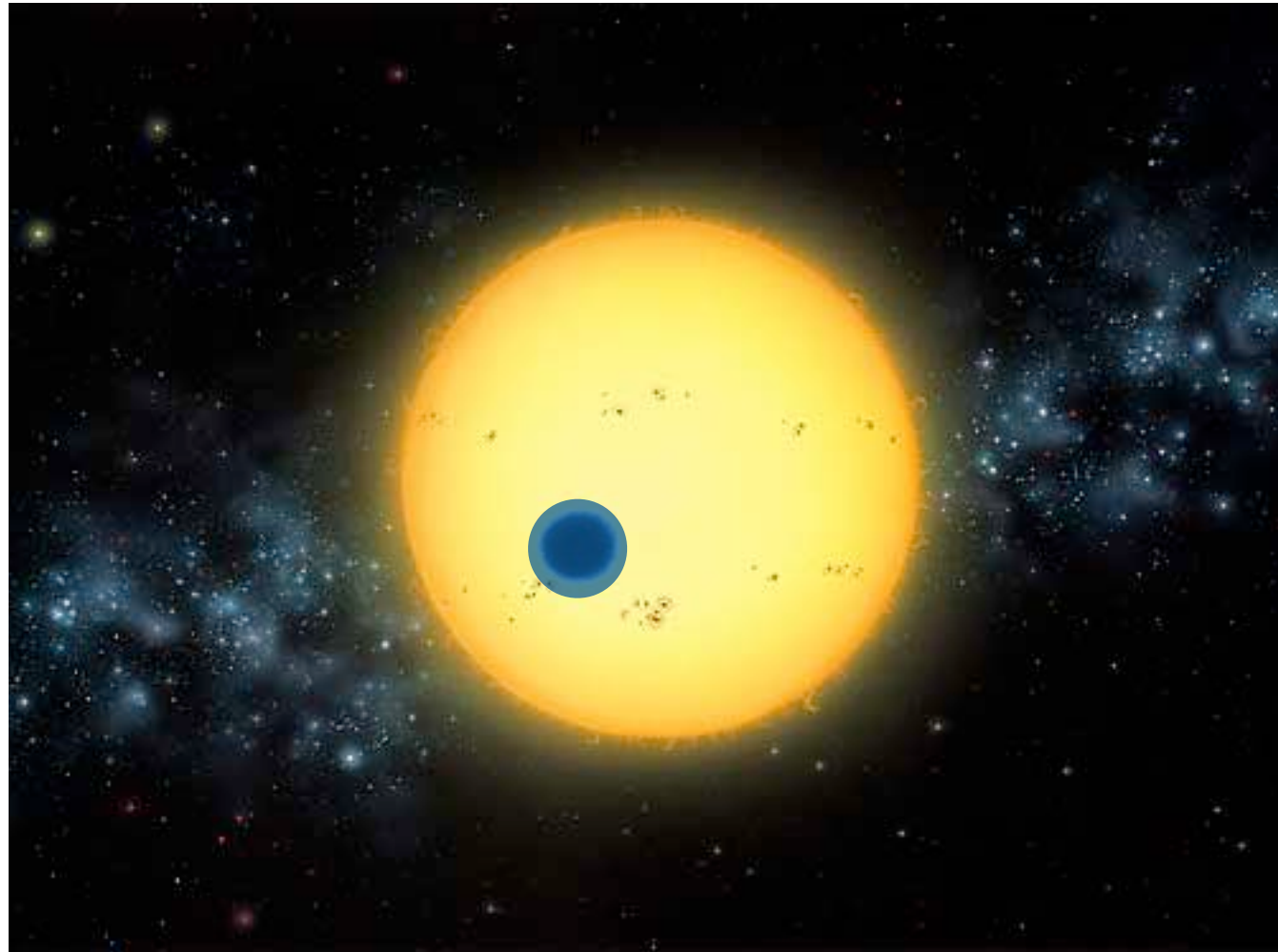
Queloz et al. (2000) - HD 209458b



All measurements to date (a handful of planets) are consistent with **coplanarity** or very small relative inclination. A significant deviation from co-planarity would be challenging to formation models.

Atmospheric composition and dynamics

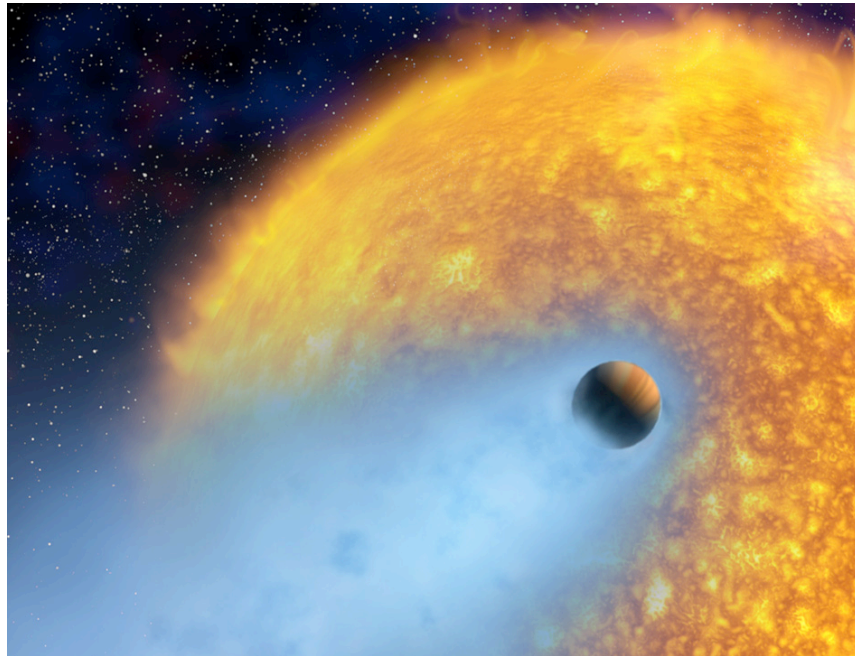
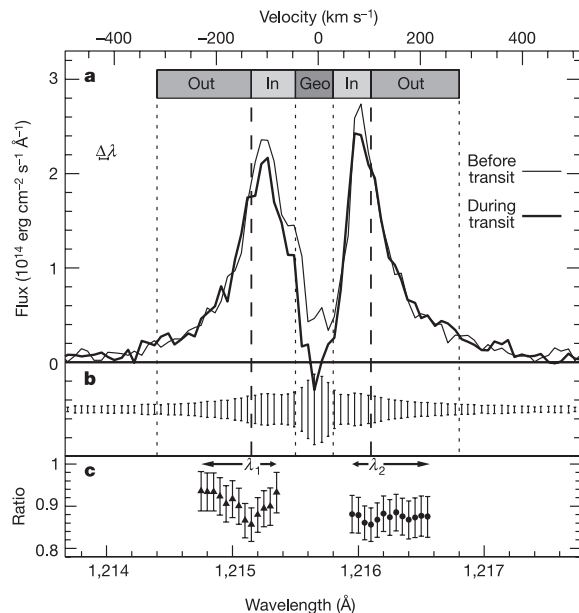
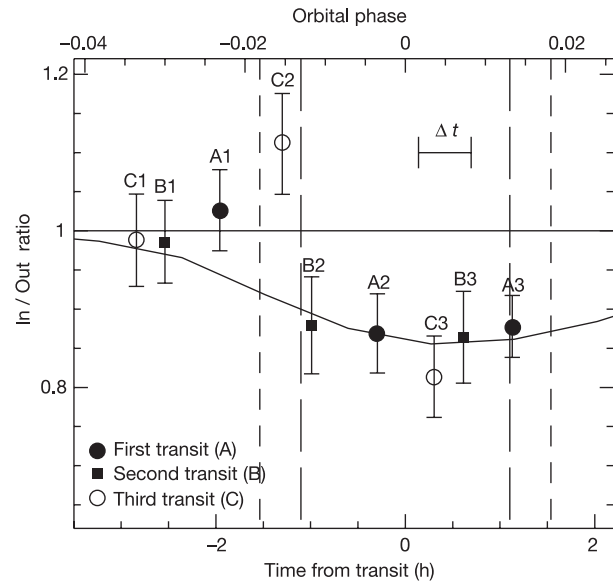
Transmission spectroscopy probes the **atmospheric transparency gradient** near the limb (i.e. at the day-night terminator).



Atmospheric composition and dynamics

Transmission spectroscopy probes the **atmospheric transparency gradient** near the limb (i.e. at the day-night terminator).

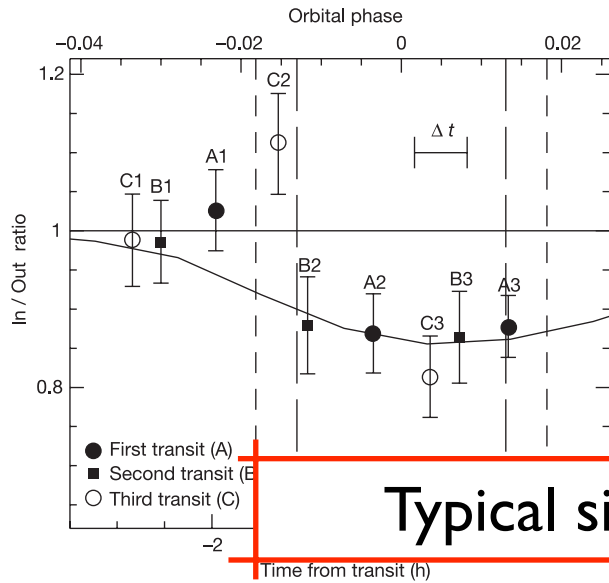
Vidal-Madjar et al. (2003, 2004) - evaporating exosphere



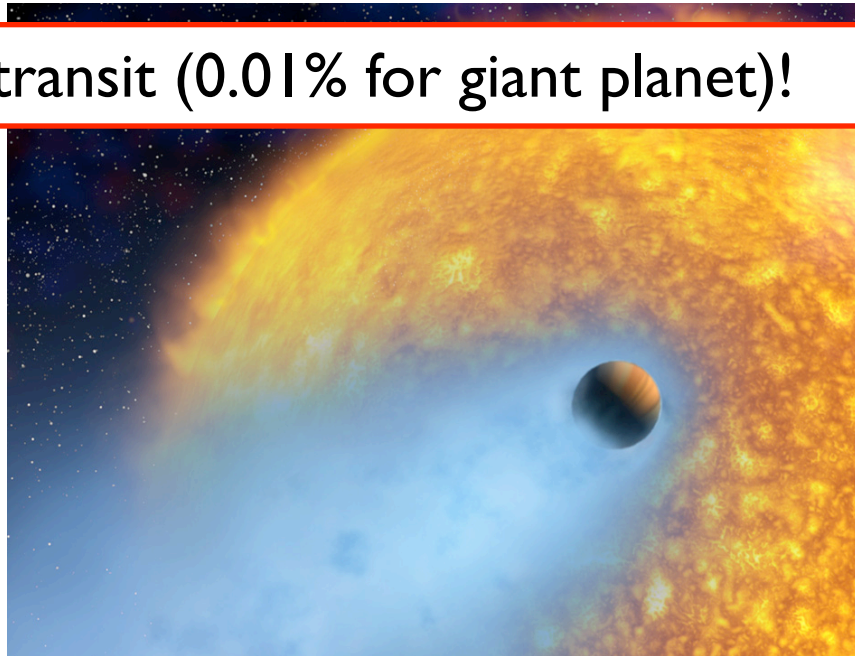
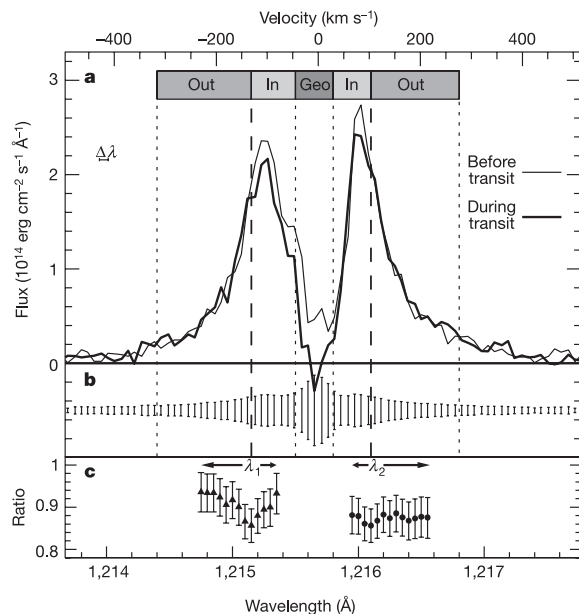
Atmospheric composition and dynamics

Transmission spectroscopy probes the **atmospheric transparency gradient** near the limb (i.e. at the day-night terminator).

Vidal-Madjar et al. (2003, 2004) - evaporating exosphere



Typical signal 1% of transit (0.01% for giant planet)!

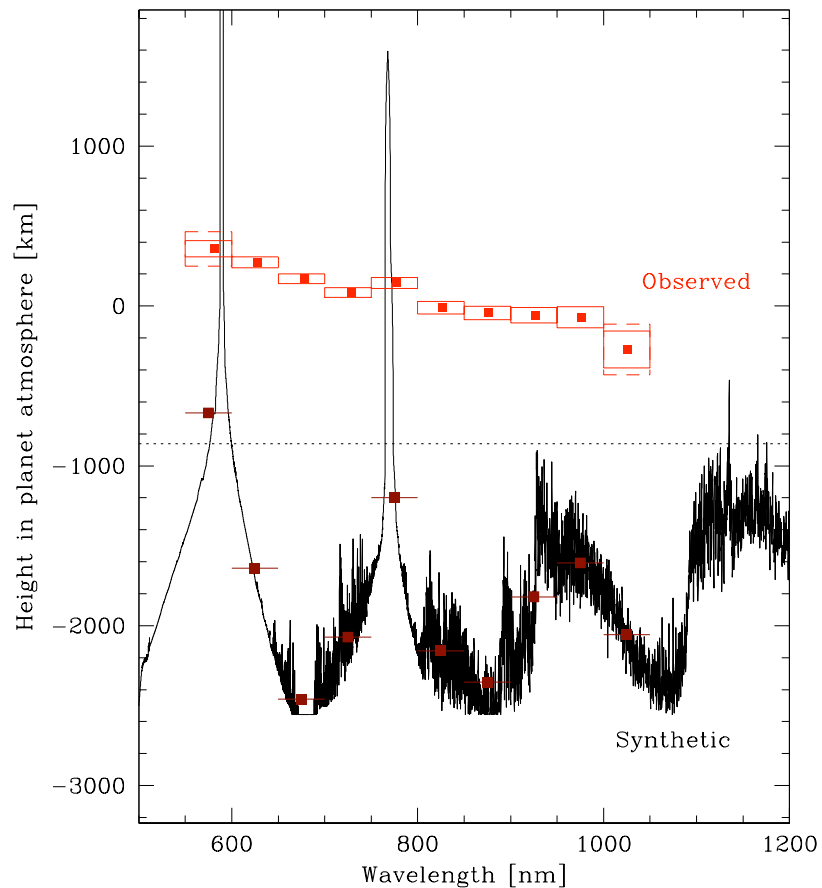


Atmospheric composition and dynamics

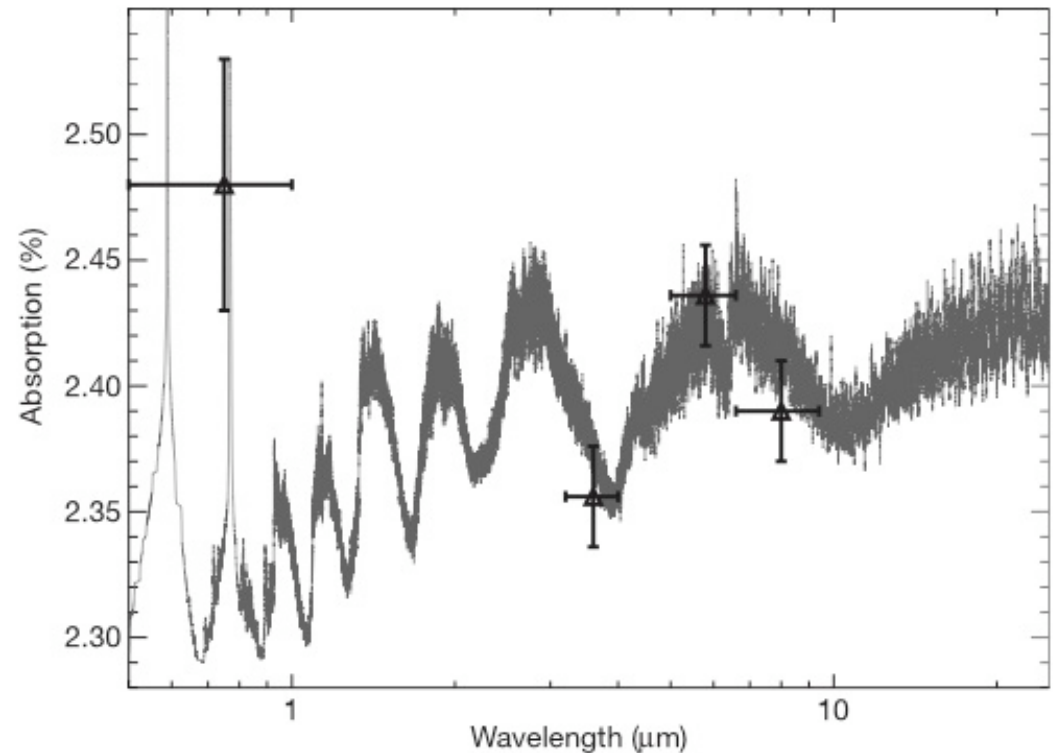
Transmission spectroscopy probes the **atmospheric transparency gradient** near the limb (i.e. at the day-night terminator).

Vidal-Madjar et al. (2003, 2004) - evaporating exosphere

Pont et al. (2007) - visible - \sim micron size haze

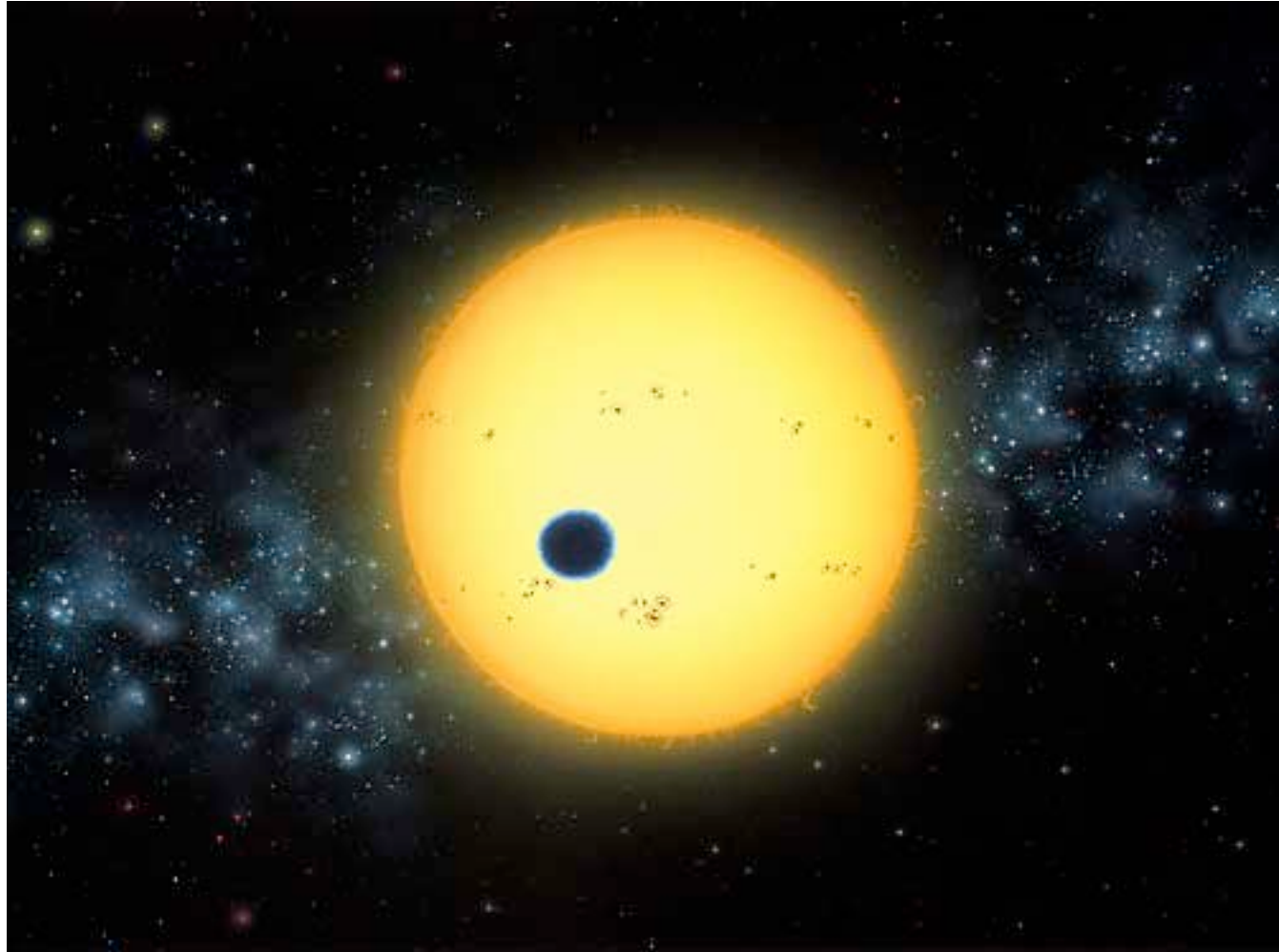


Tinetti et al. (2007) - IR - H_2O (?)



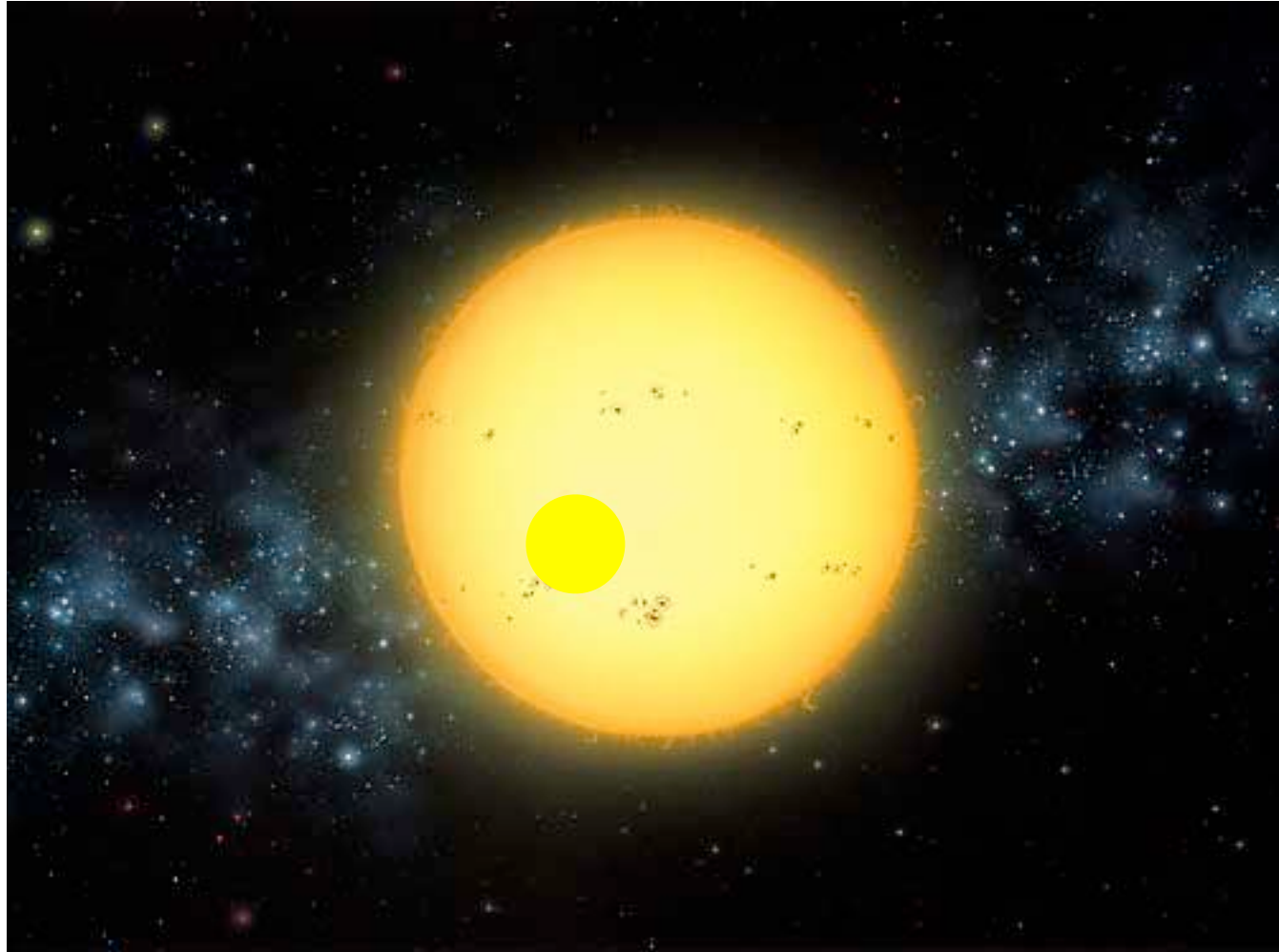
Atmospheric composition and dynamics

Anti-transits, or secondary eclipses, probe **thermal (IR) emission** or **reflected light (optical)** emission from the top of the atmosphere.



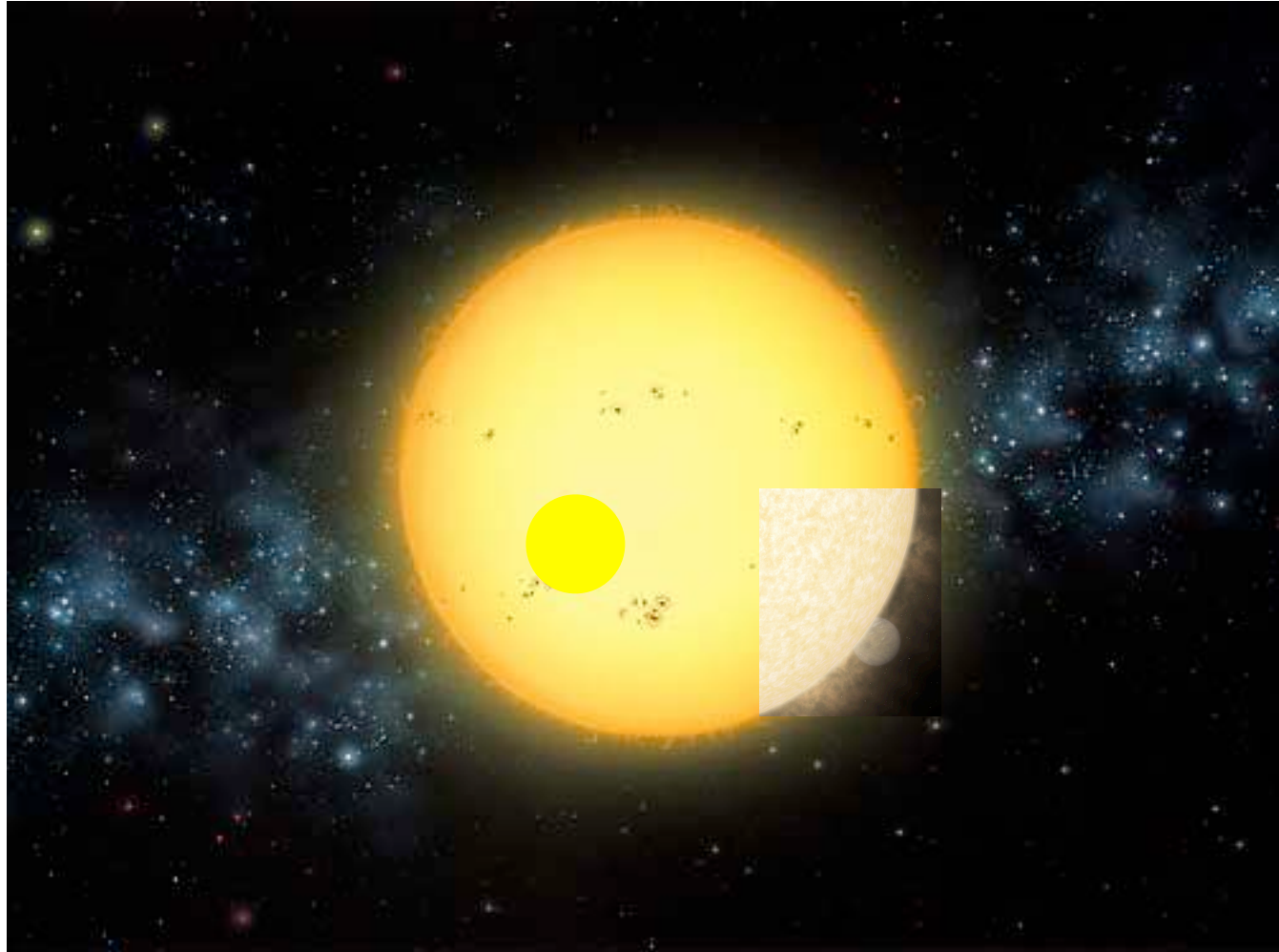
Atmospheric composition and dynamics

Anti-transits, or secondary eclipses, probe **thermal (IR) emission** or **reflected light (optical)** emission from the top of the atmosphere.



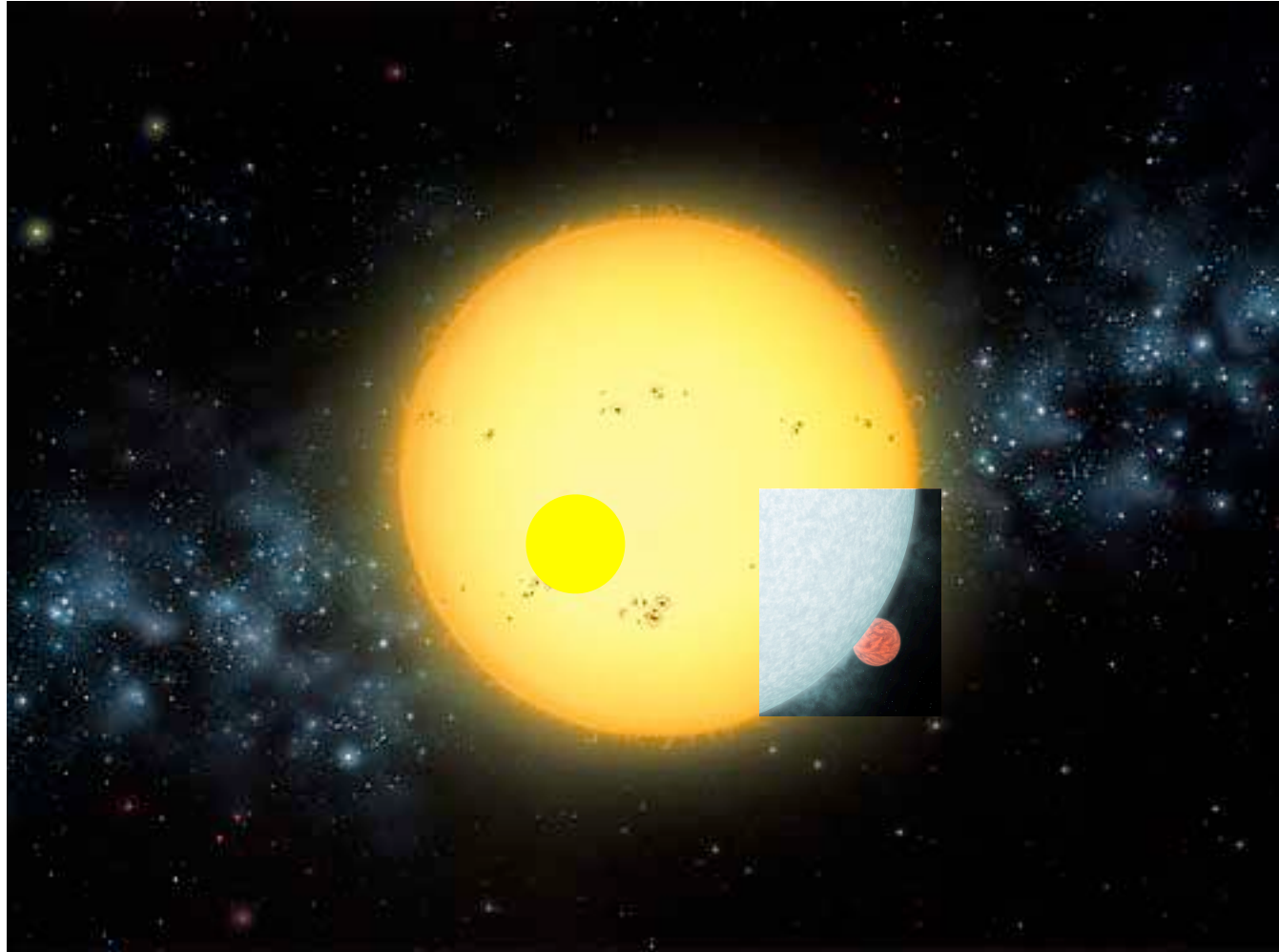
Atmospheric composition and dynamics

Anti-transits, or secondary eclipses, probe **thermal (IR) emission** or **reflected light (optical)** emission from the top of the atmosphere.



Atmospheric composition and dynamics

Anti-transits, or secondary eclipses, probe **thermal (IR) emission** or **reflected light (optical)** emission from the top of the atmosphere.



Atmospheric composition and dynamics

Anti-transits, or secondary eclipses, probe **thermal (IR) emission** or **reflected light (optical)** emission from the top of the atmosphere.

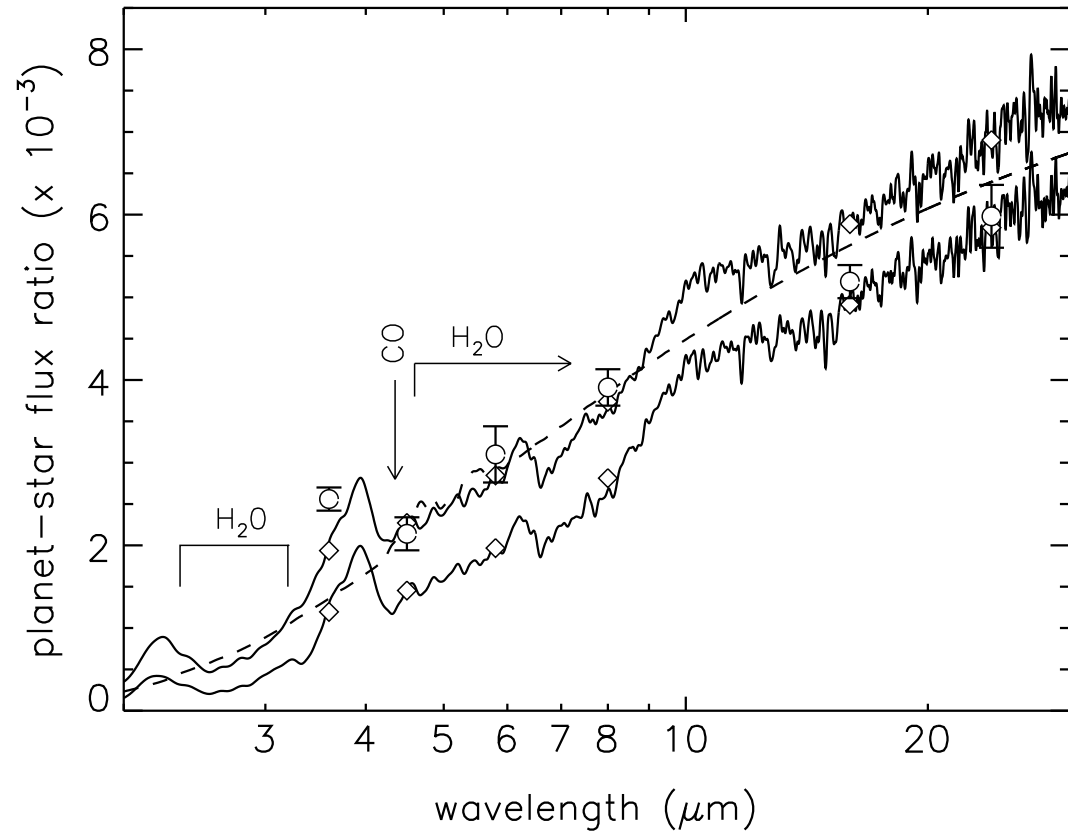
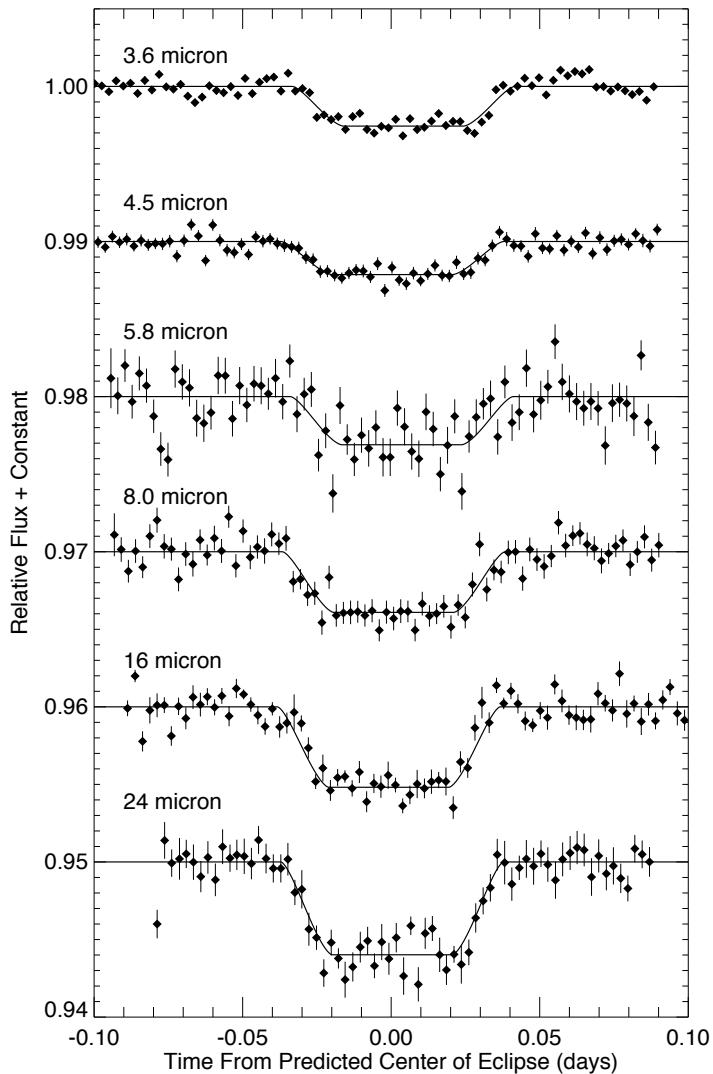
The background image is a composite of three astronomical scenes. The top half shows a bright yellow star with a soft, glowing halo against a dark space filled with distant stars. The bottom half shows a similar star, but with a large, pale blue planet partially obscuring it on the right side. A small, reddish-orange sphere is visible in transit across the lower right edge of the blue planet. A white rectangular box with a red border is superimposed over the center of the image, containing text.

Typical signal 10% of transit in IR, 1% in visible
(0.1 and 0.01% for giant planet)

Atmospheric composition and dynamics

Anti-transits, or secondary eclipses, probe **thermal (IR) emission** or **reflected light (optical)** emission from the top of the atmosphere.

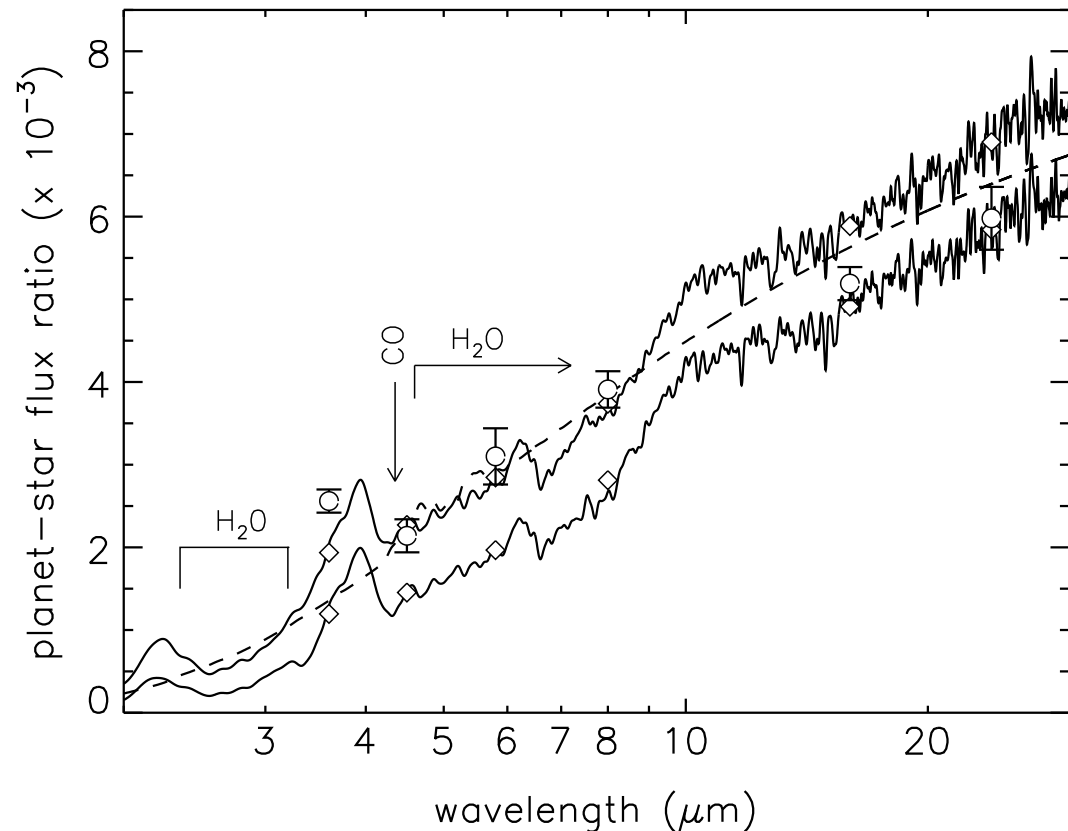
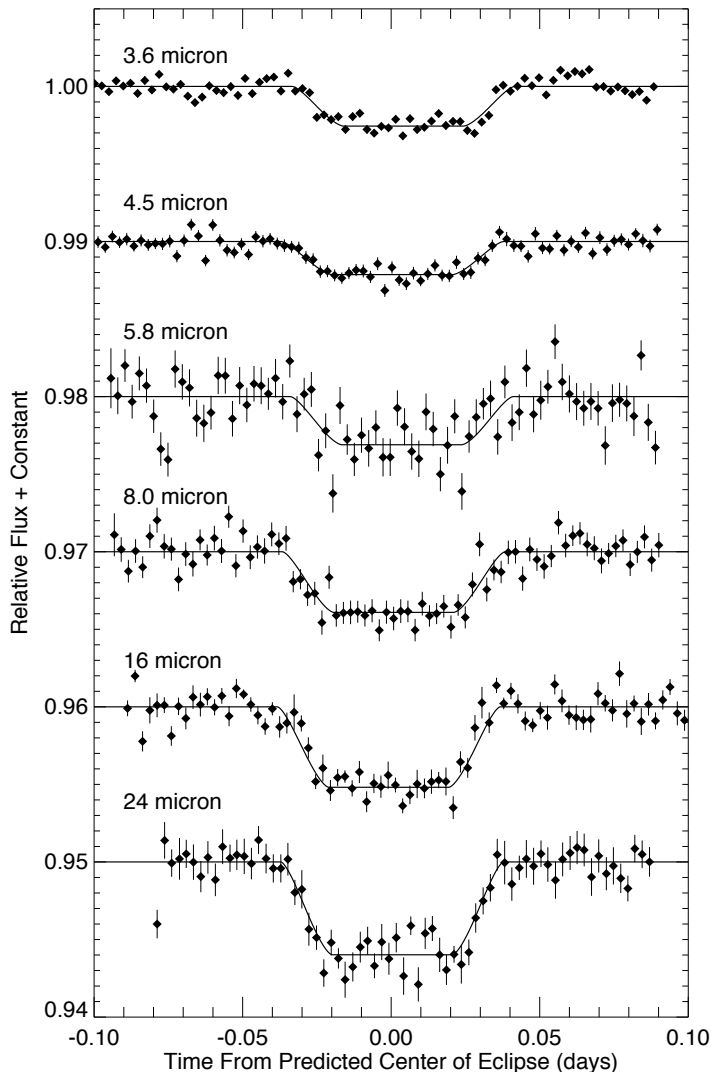
IR detections (e.g. Charbonneau et al. 2008 below): hot Jupiters are really **hot (1000-2000K)**



Atmospheric composition and dynamics

Anti-transits, or secondary eclipses, probe **thermal (IR) emission** or **reflected light (optical)** emission from the top of the atmosphere.

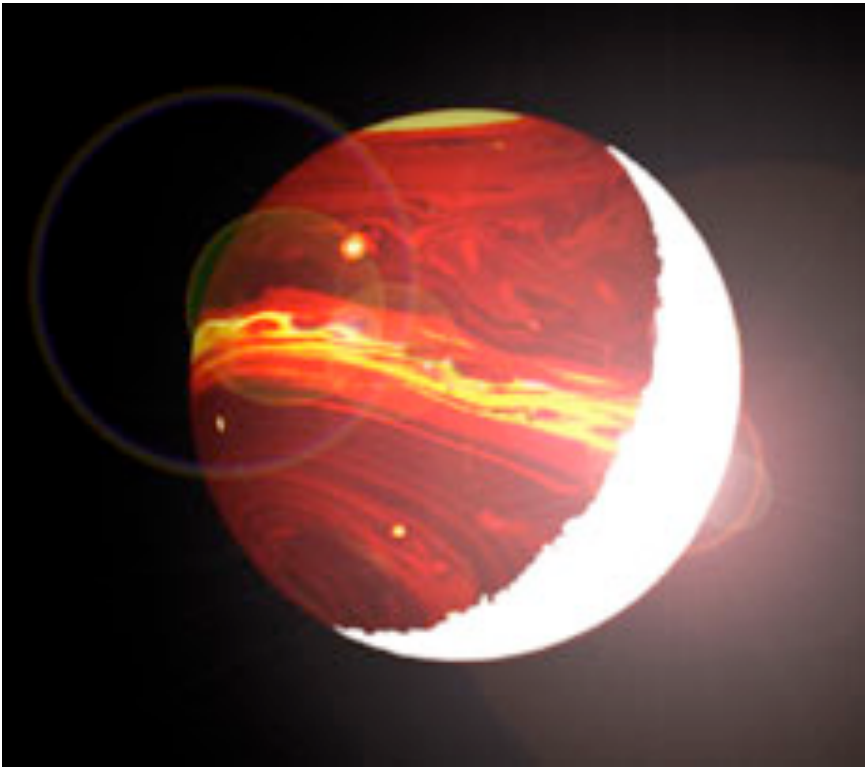
IR detections (e.g. Charbonneau et al. 2008 below): hot Jupiters are really **hot (1000-2000K)**



Visible non-detections (MOST satellite - Rowe et al. 2006): Hot Jupiters are really **dark**.

Atmospheric composition and dynamics

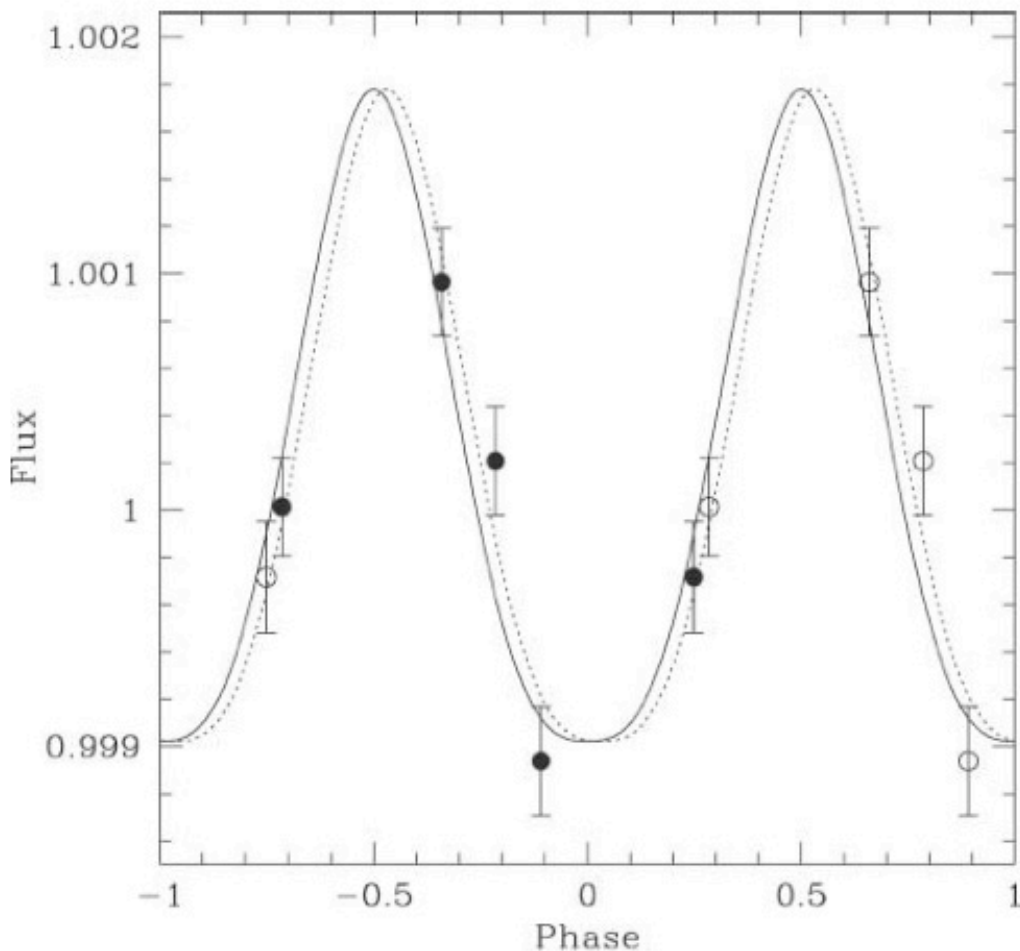
Phase curves, which can be measured for transiting and non-transiting planets, probe **thermal emission (IR)** or **reflected and scattered light (visible)**.



Atmospheric composition and dynamics

Phase curves, which can be measured for transiting and non-transiting planets, probe **thermal emission (IR)** or **reflected and scattered light (visible)**.

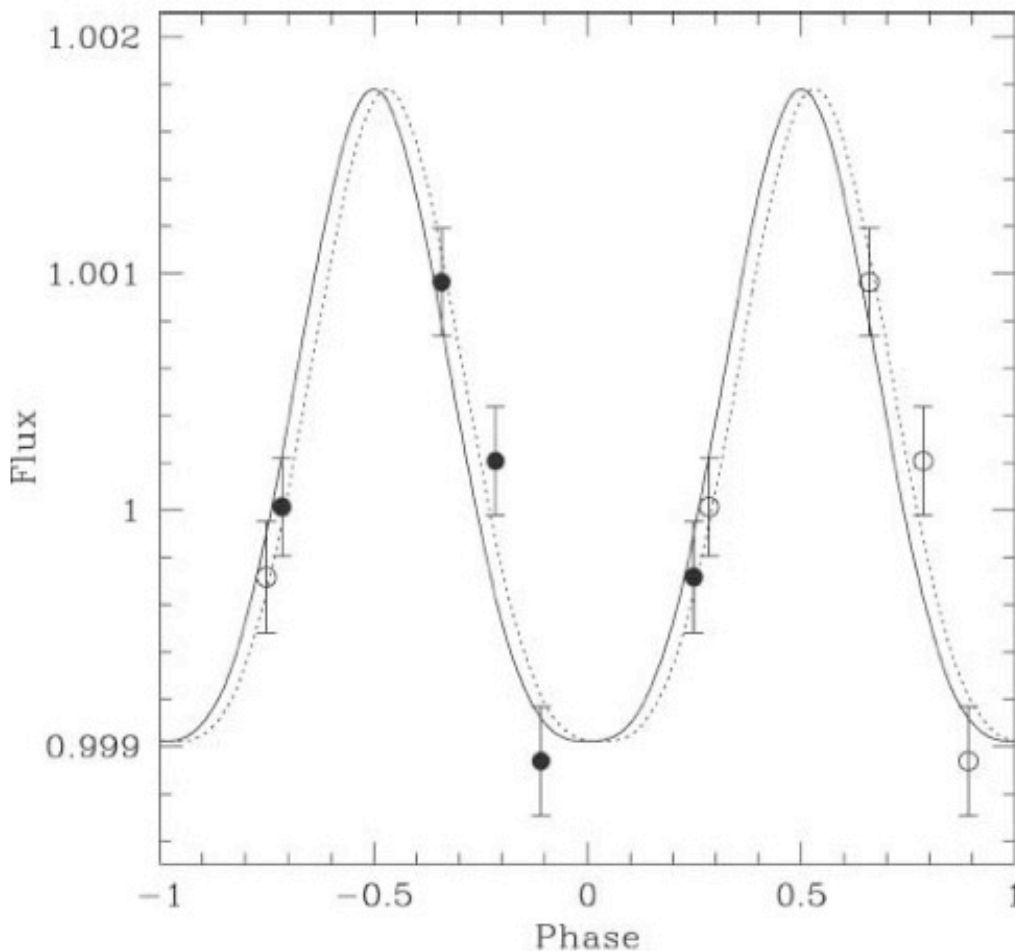
Harrington et al (2006) - μ And
strong day-night contrast - **little atmospheric transport**



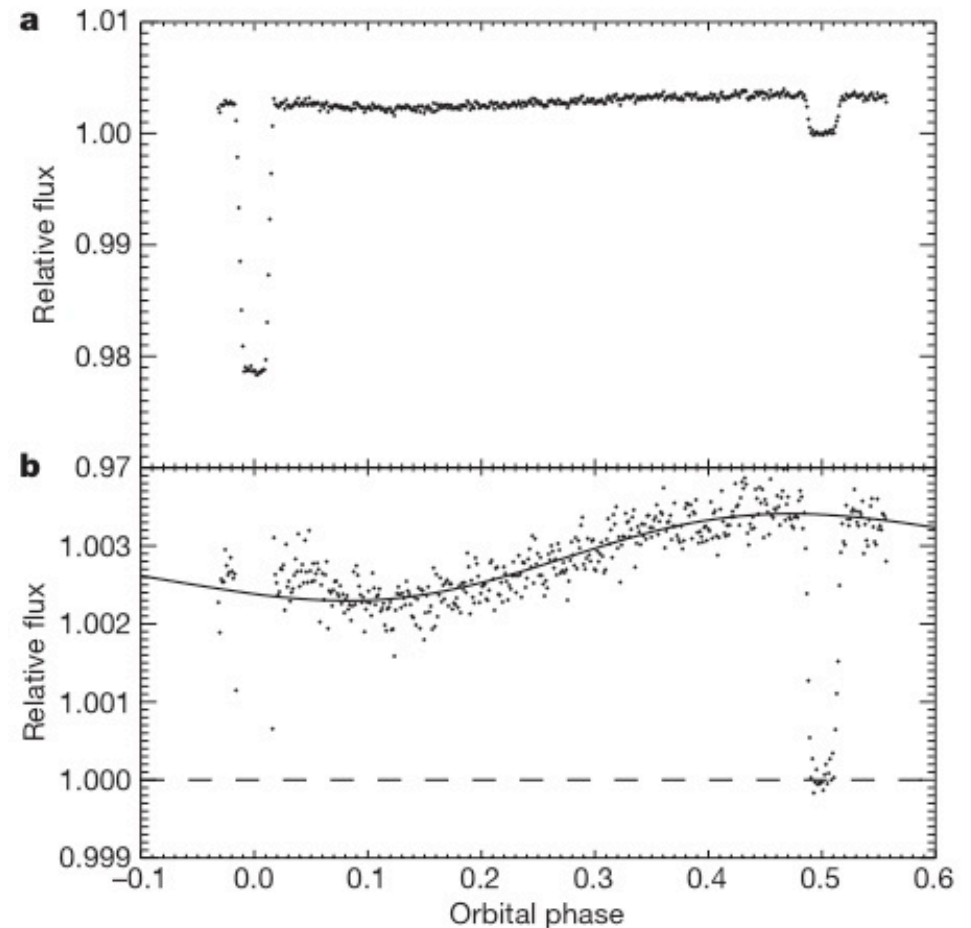
Atmospheric composition and dynamics

Phase curves, which can be measured for transiting and non-transiting planets, probe **thermal emission (IR)** or **reflected and scattered light (visible)**.

Harrington et al (2006) - μ And
strong day-night contrast - **little atmospheric transport**



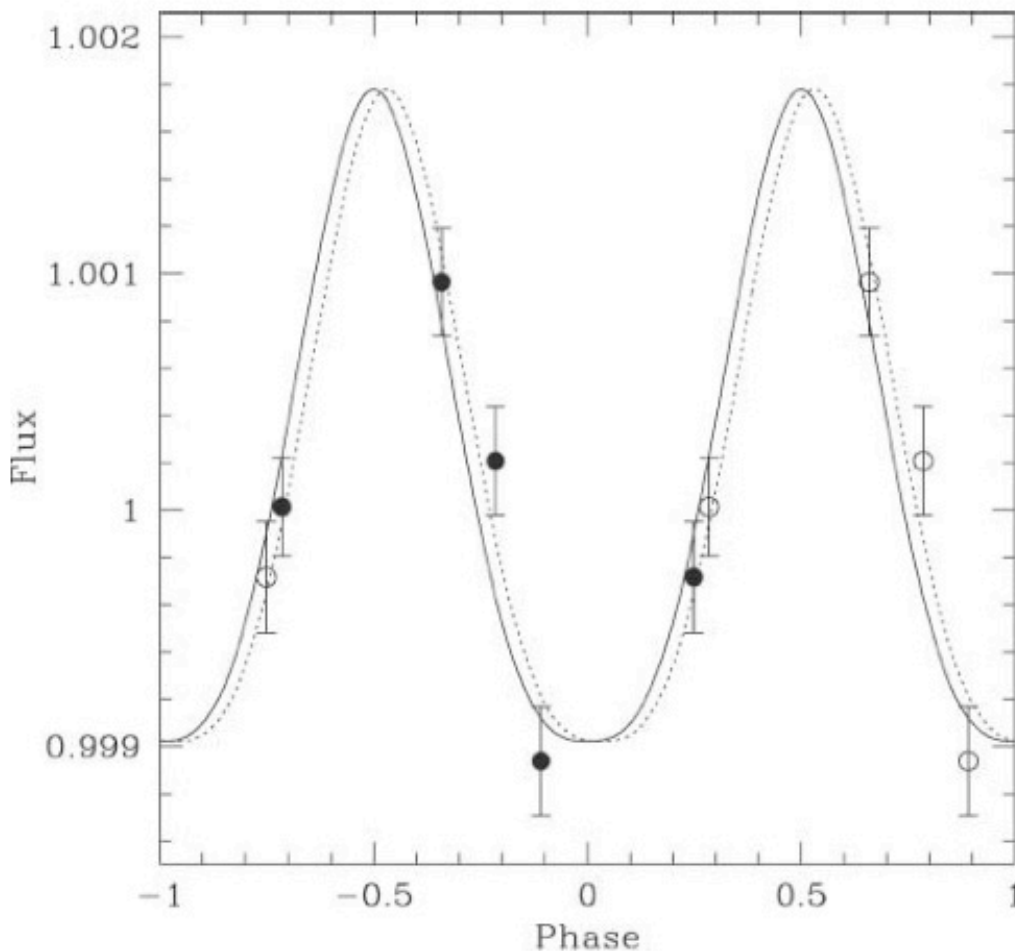
Knutson et al (2006) - HD 189733
weak day night contrast, phase offset - **large-scale transport**



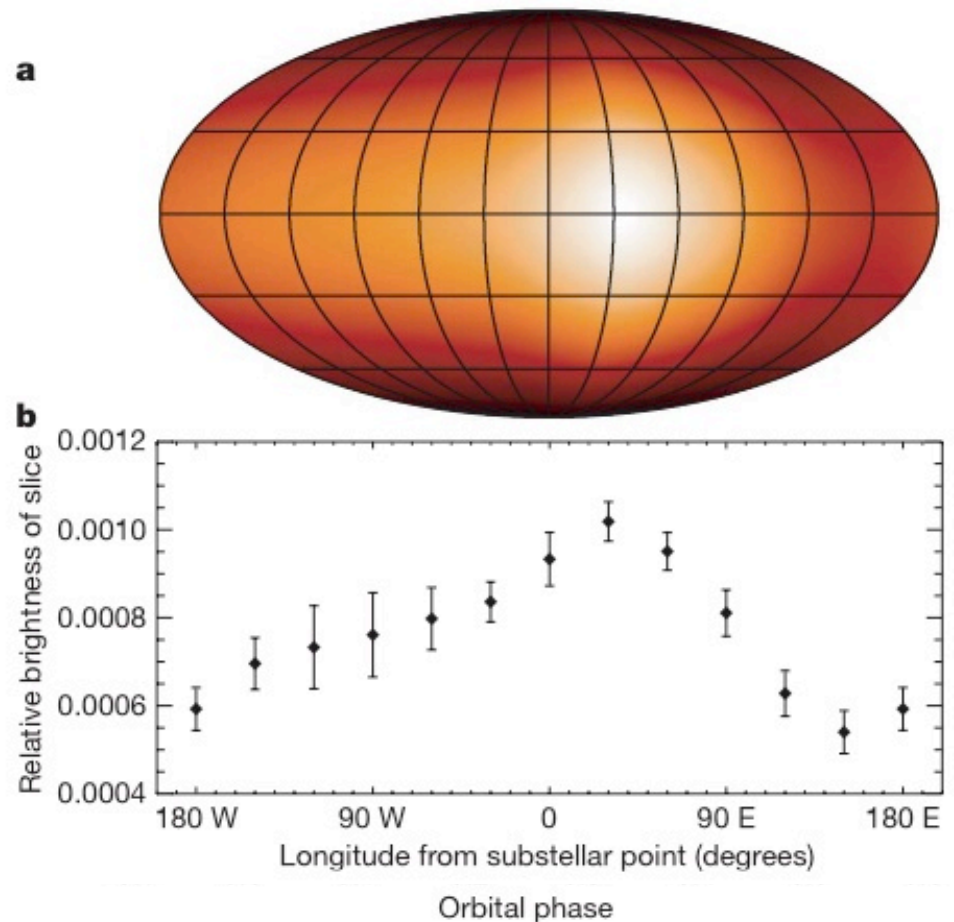
Atmospheric composition and dynamics

Phase curves, which can be measured for transiting and non-transiting planets, probe **thermal emission (IR)** or **reflected and scattered light (visible)**.

Harrington et al (2006) - μ And
strong day-night contrast - **little atmospheric transport**



Knutson et al (2006) - HD 189733
weak day night contrast, phase offset - **large-scale transport**



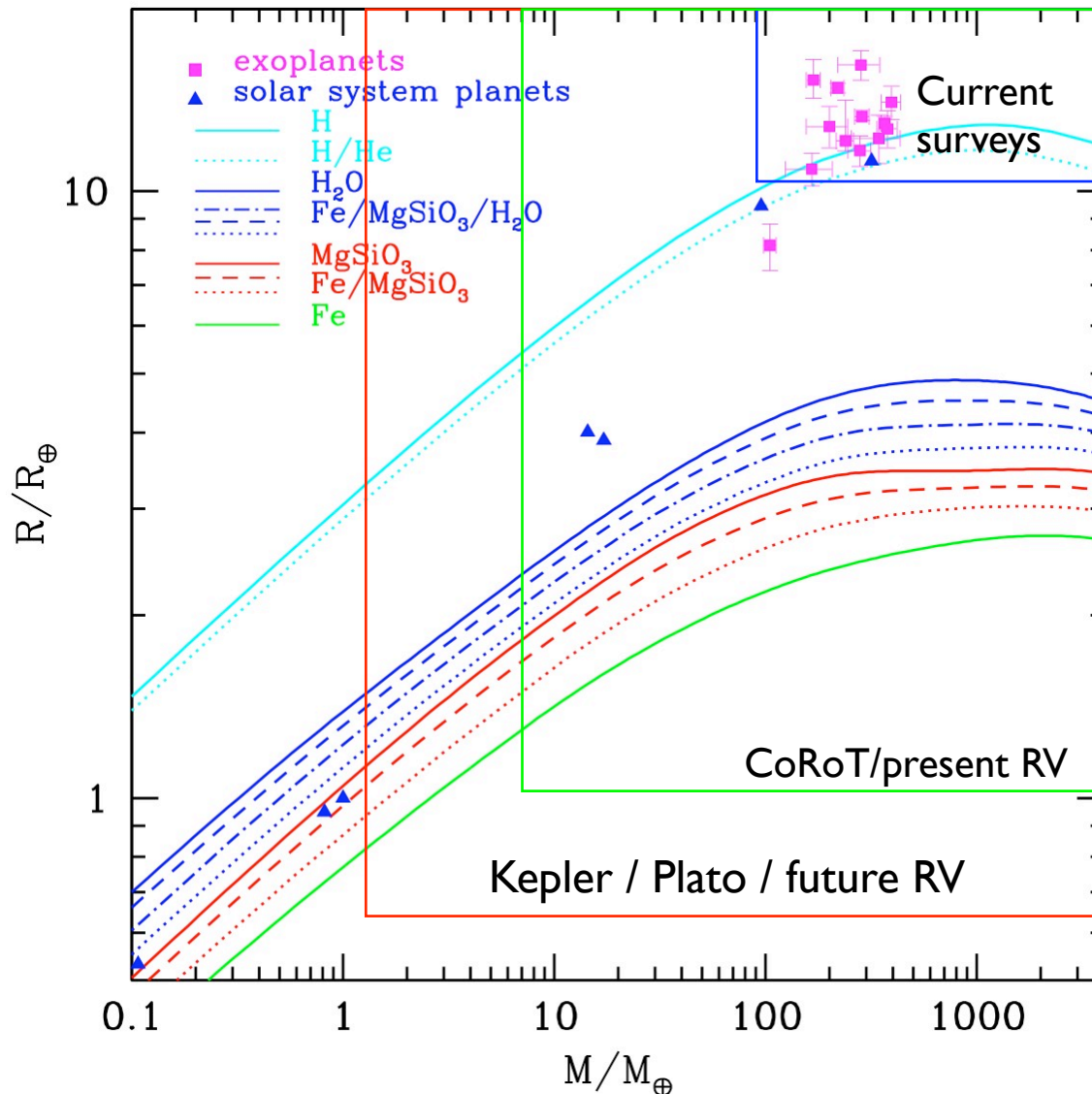
Why build CoRoT?

2. space = terrestrial planets +
more physics

Reaching the terrestrial and habitable regimes

Space means **higher precision**, less correlated noise, and long, **uninterrupted time-series**: detect shallower and rarer transits, i.e. **smaller and colder planets**.

Seager et al. (2007) - simple hydrostatic structure calculations



A word of caution: the mass - radius relation is degenerate for ocean and terrestrial planets (Adams et al. 2008, Baraffe et al. 2008)

At best, CoRoT is expected to reach ~2 Earth radii, i.e. 3-4 Earth masses, for very short period orbits, and larger planets out to weeks or months.

Improving statistics

Over 120,000 stars will be monitored for months.

Fressin et al (2007): **planet catch simulations** based on pre-launch simulated data, known properties of the RV planet population and realistic Galactic stellar population model:

Over the lifetime of the mission, simulations suggest that CoRoT should detect **60-70 Jupiter- or Saturn-mass** planets and **20-25 Neptune-mass planets or super-Earths**.

The simulations are being recalibrated to incorporate the actual properties of the data as we speak.

Improving statistics

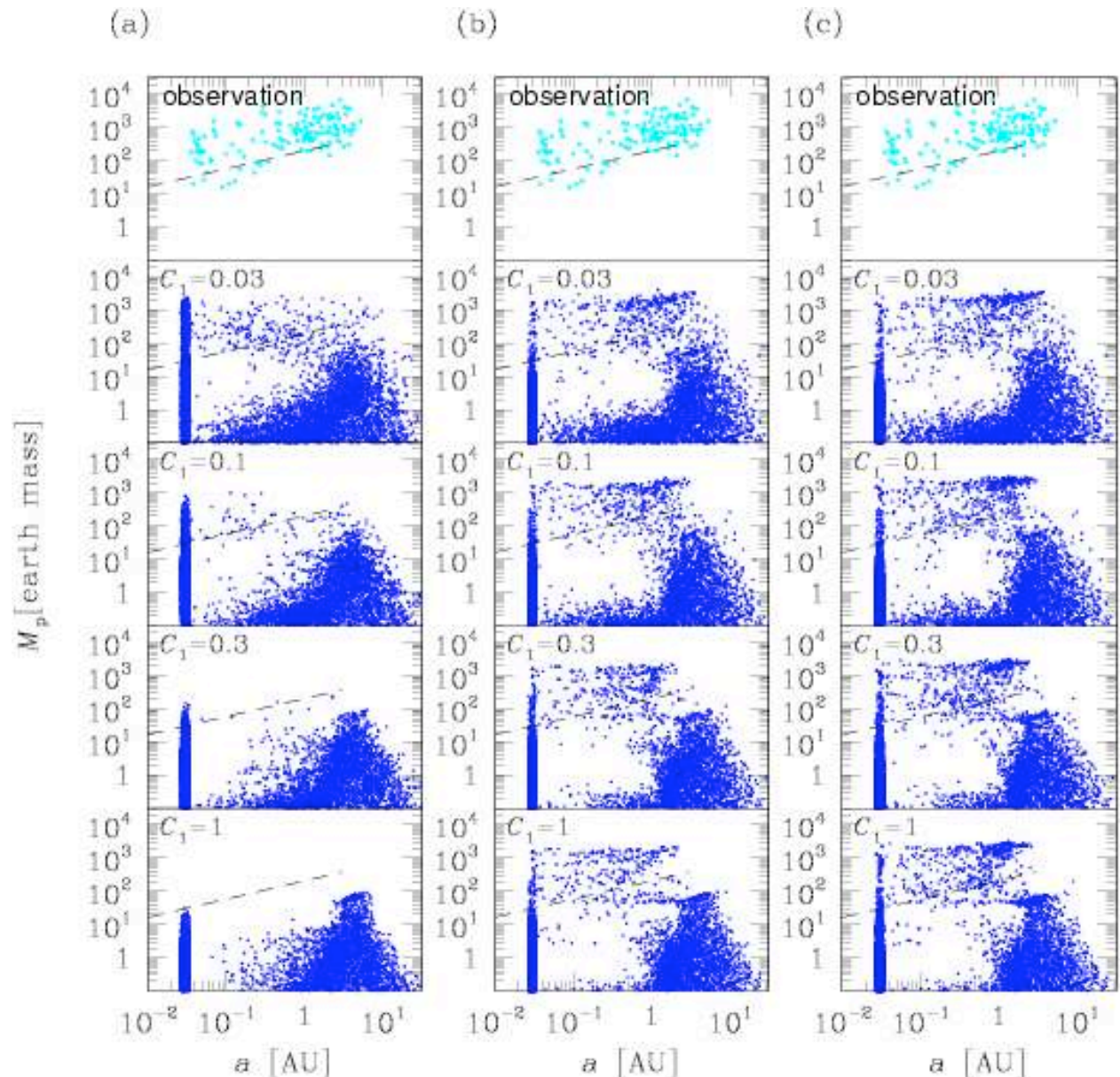
Over 120,000 stars will be monitored for months.

Fressin et al (2007): **planet catch simulations** based on pre-launch simulated data, known properties of the RV planet population and realistic Galactic stellar population model:

Over the lifetime of the mission, simulations suggest that CoRoT should detect **60-70 Jupiter- or Saturn-mass planets** and **20-25 Neptune-mass planets or super-Earths**.

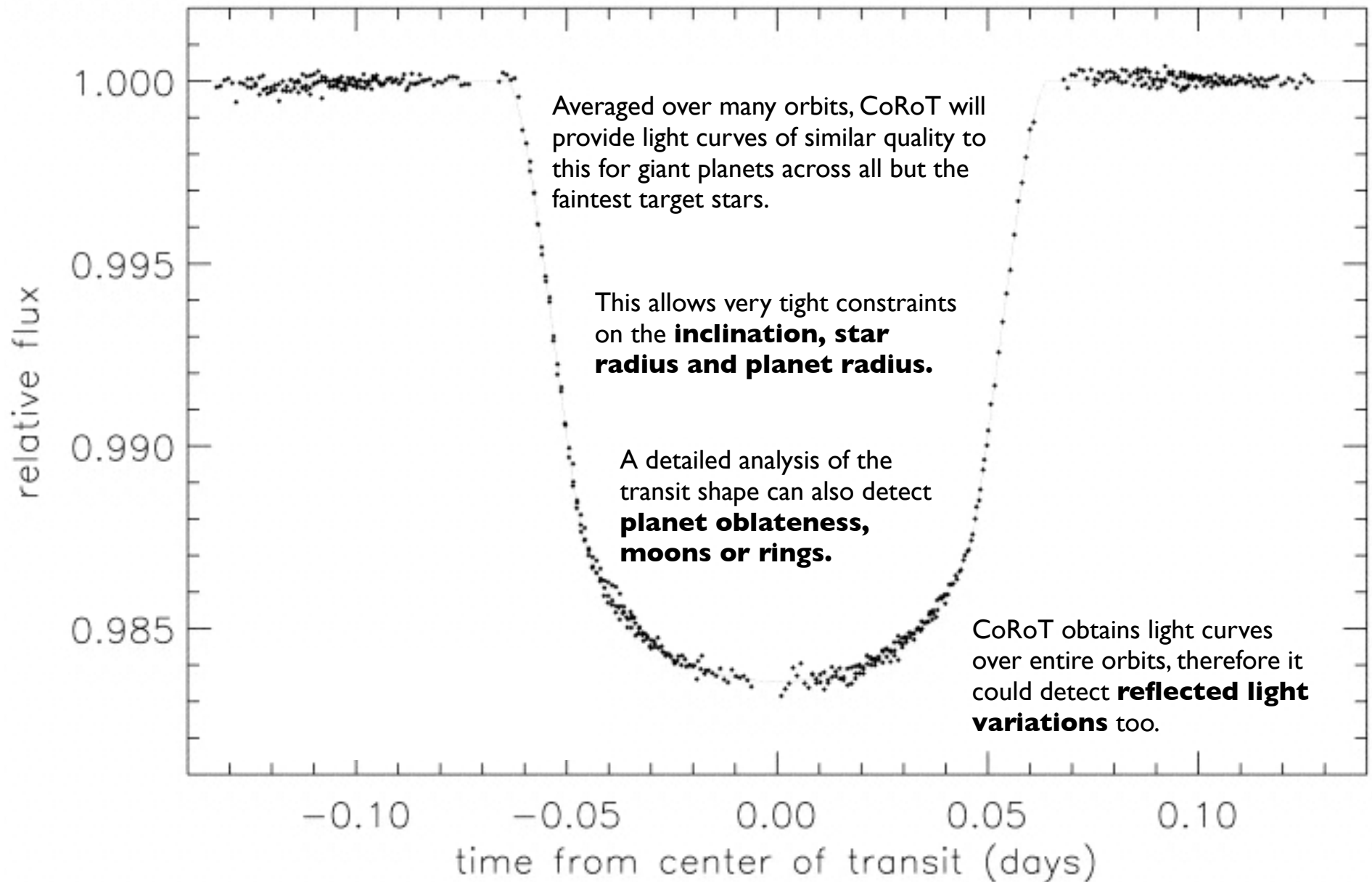
The simulations are being recalibrated to incorporate the actual properties of the data as we speak.

Simulated planet populations (Ida & Lin 2008)

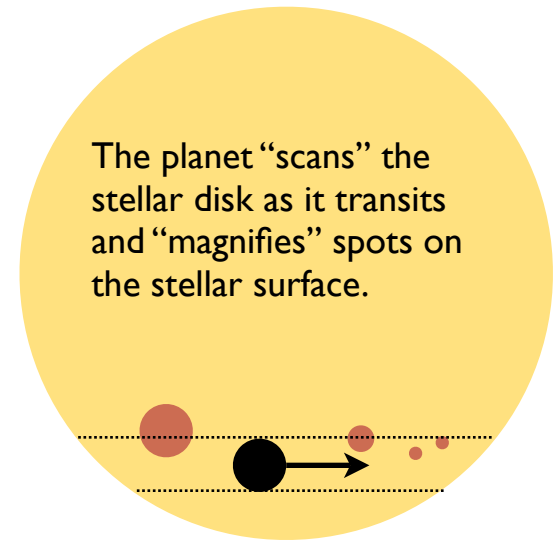
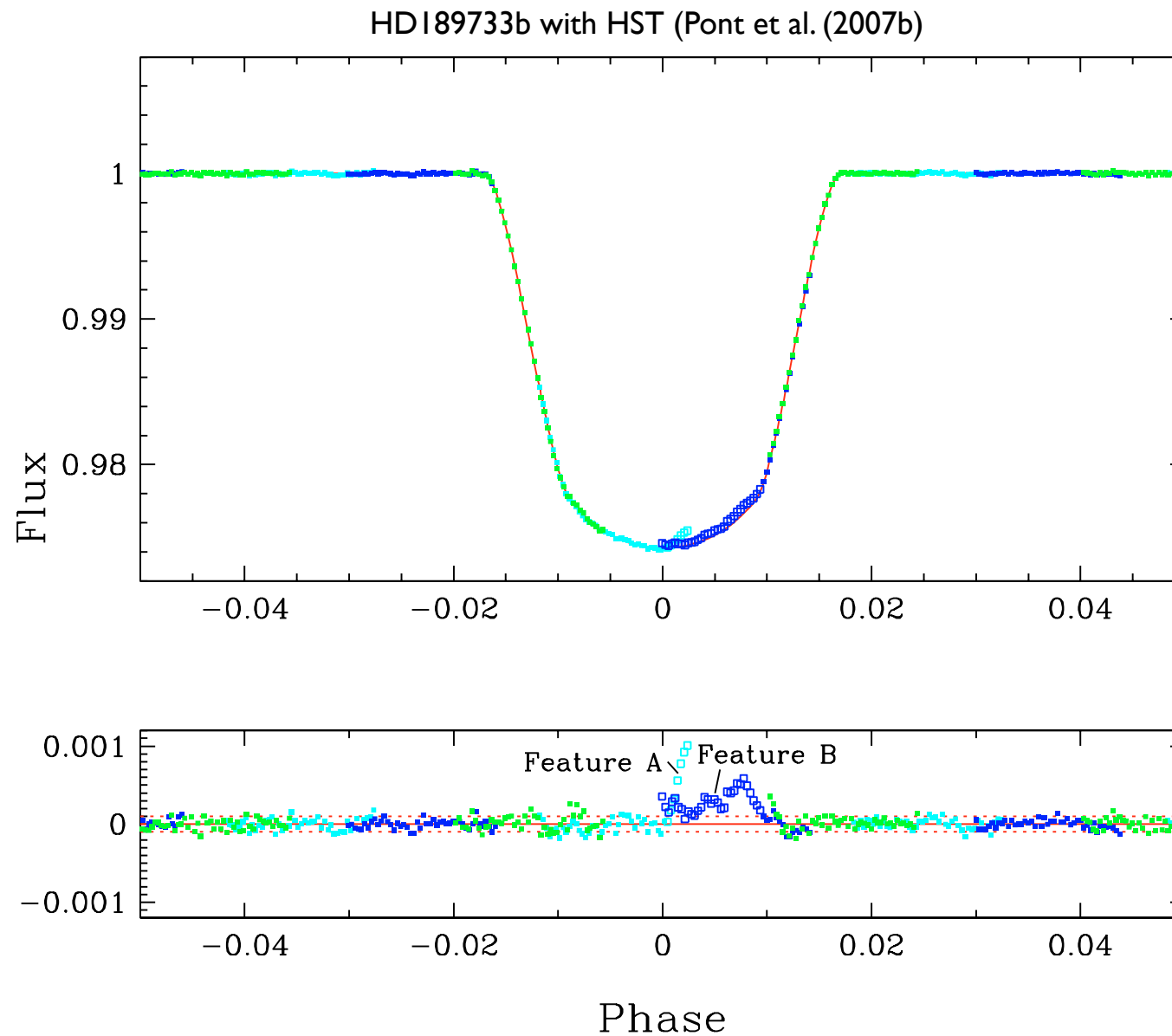


Ultraprecise light curves

HD209458b with HST (Brown et al. 2000)



Ultraprecise light curves

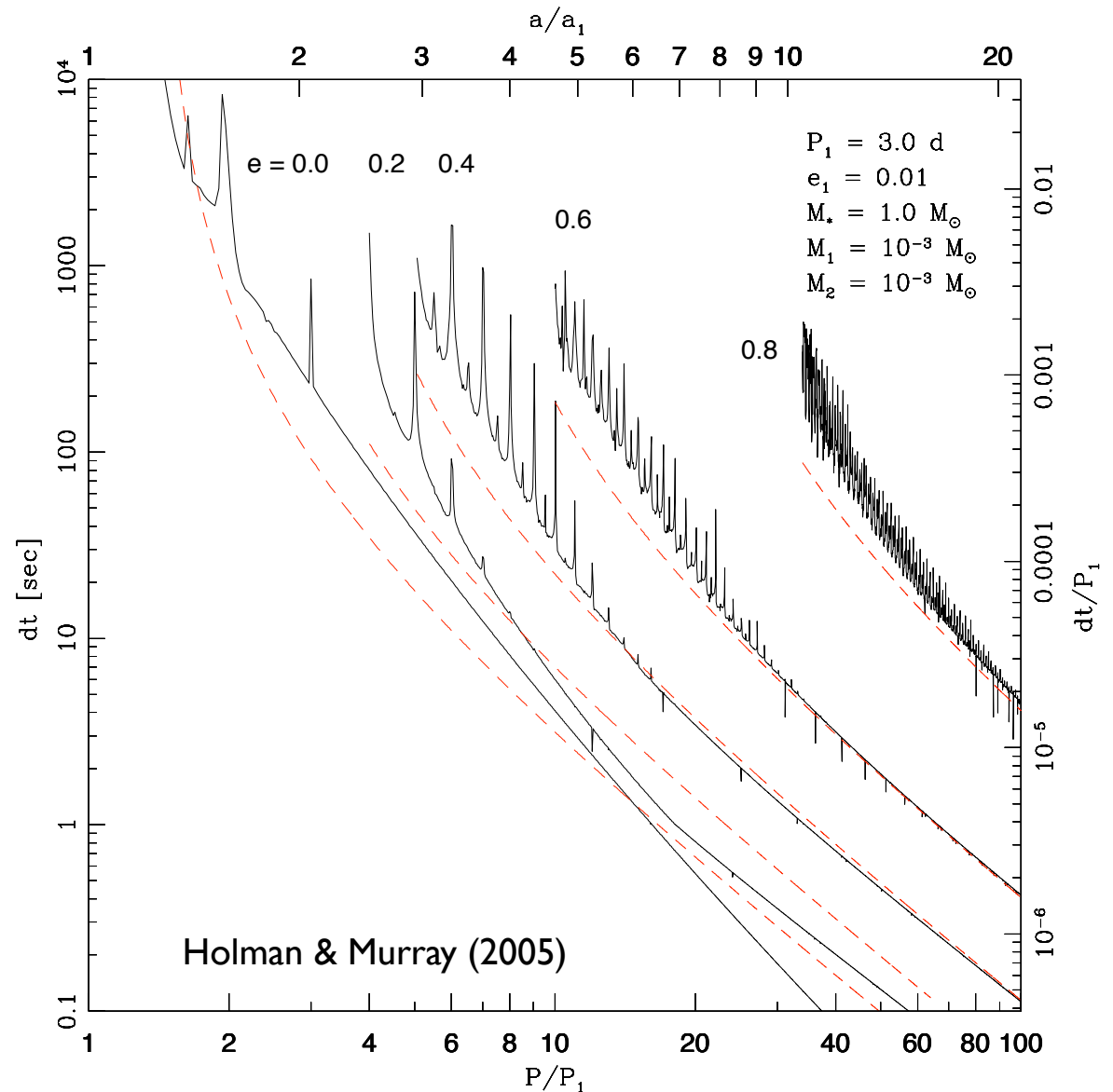


Potentially, this can be a tracer of **star-planet magnetic interaction** - as can the out-of-transit variability if it is synchronous with the planet's orbit.

Transit timing variations

If there are **other planets** in addition to the one whose transits have been detected, they will **dynamically perturb** the transiting planet's orbit, causing small deviations in from strict periodicity

This can potentially be used to detect Earth mass planets in systems containing giant planets



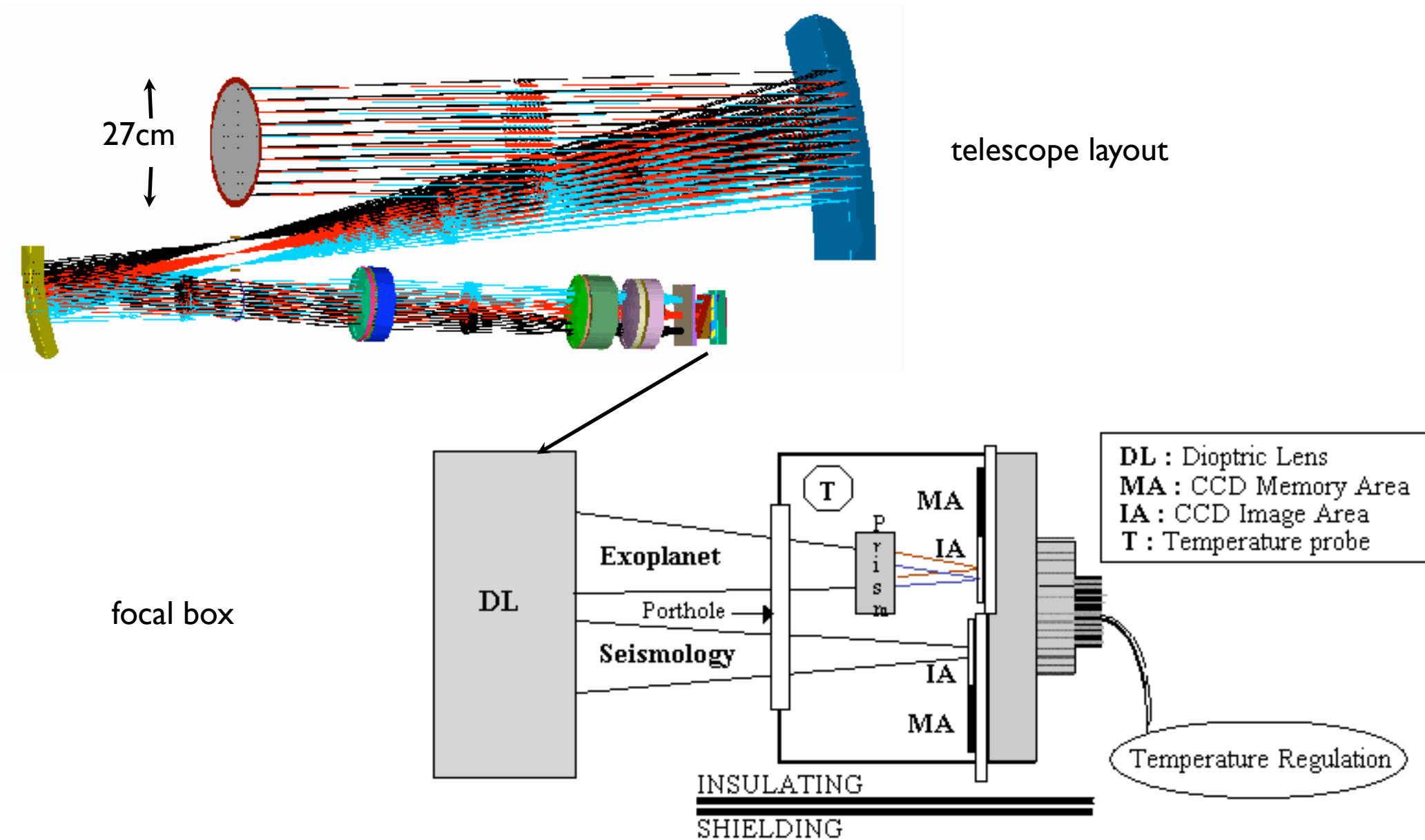
How does CoRoT
work?

The satellite

- PI: Annie Baglin, LESIA, Meudon
- CNES PROTEUS bus
- 27cm aperture telescope
- Soyuz II-Ib launcher from Baikonour
- Polar orbit
- 2.5 year minimum lifetime



Payload

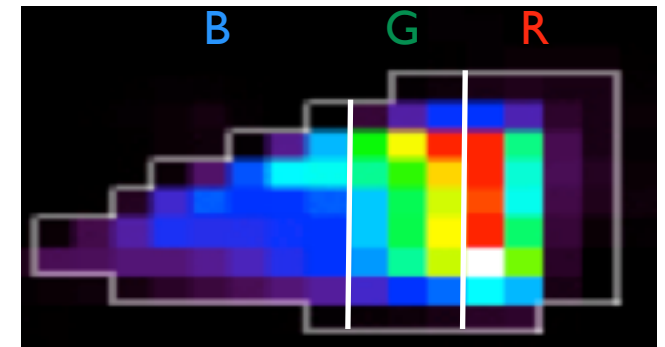
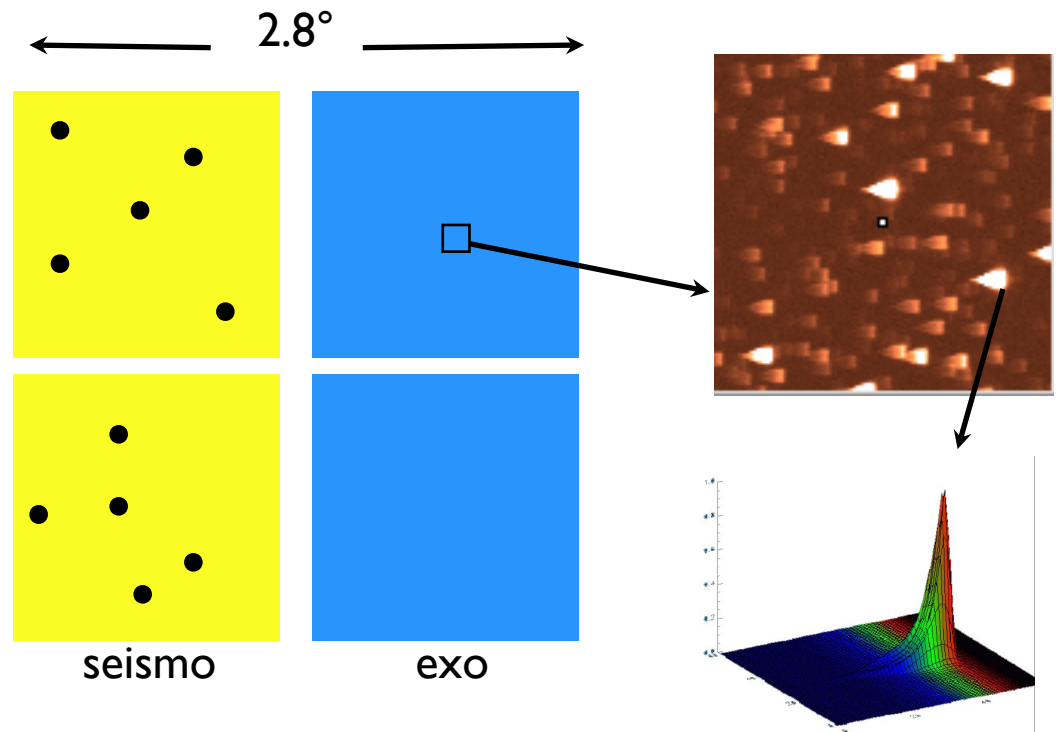


27 December 2006



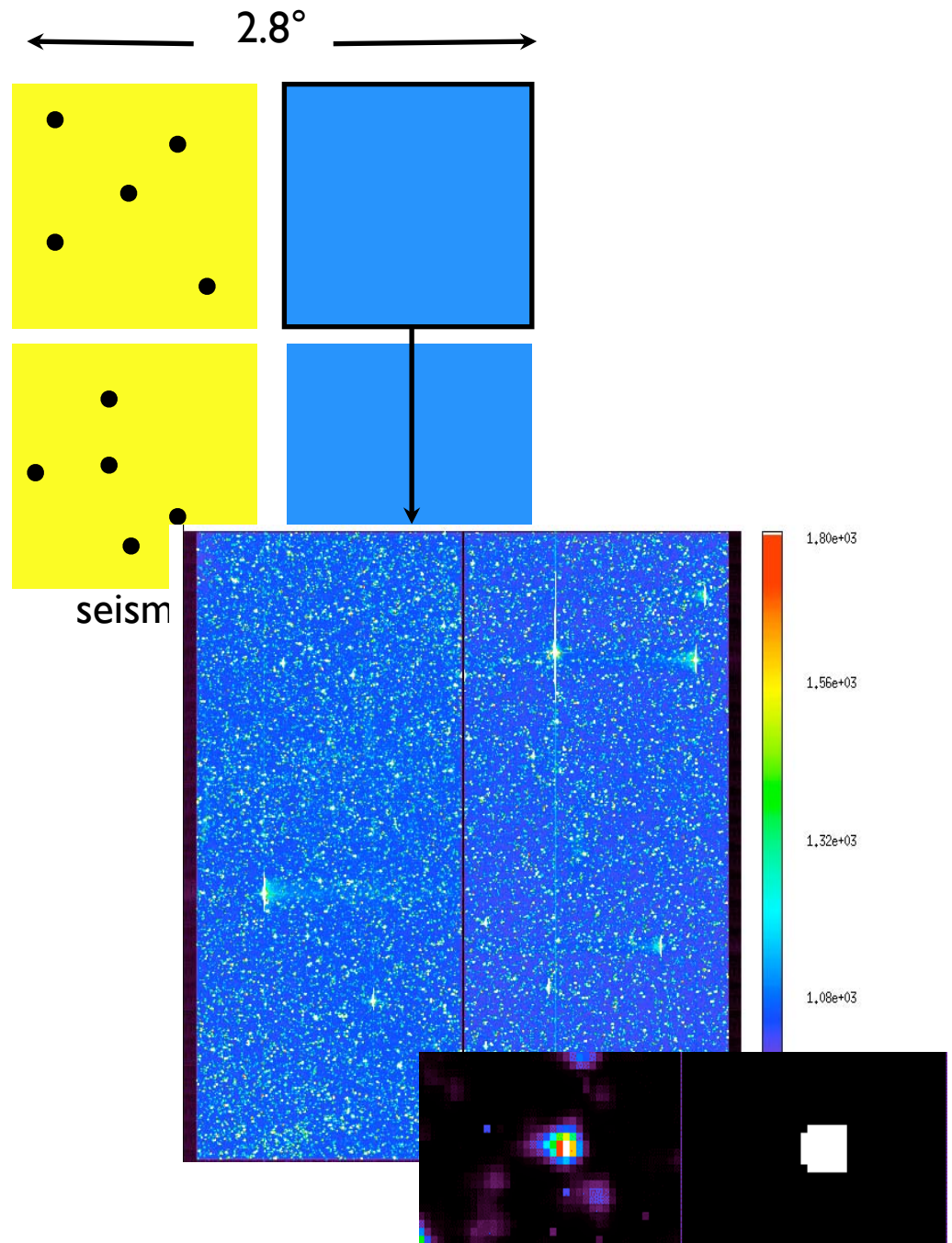
Exo field

- Exo field
 - up to 6000 LCs / CCD
 - $11.5 < m_V < 16$
 - 512s sampling (32s for 500 objects / CCD)
 - 3 colours for ~ 4500 objects / CCD with $m_V < 15$
- some small background windows
- up to 40 10x15 pixel windows
- on-board aperture photometry using mask selected from 256 templates based on one initial long integration image



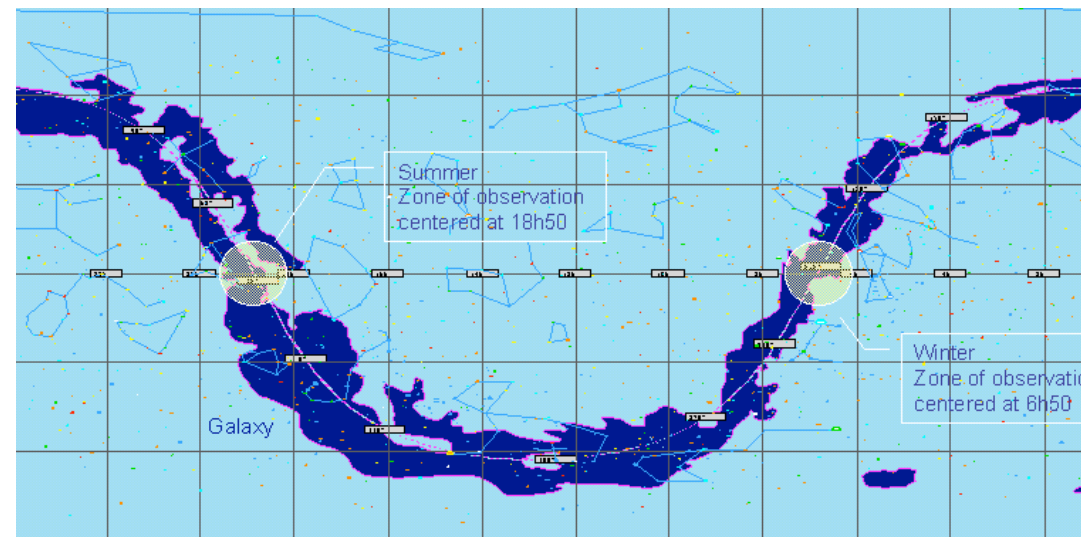
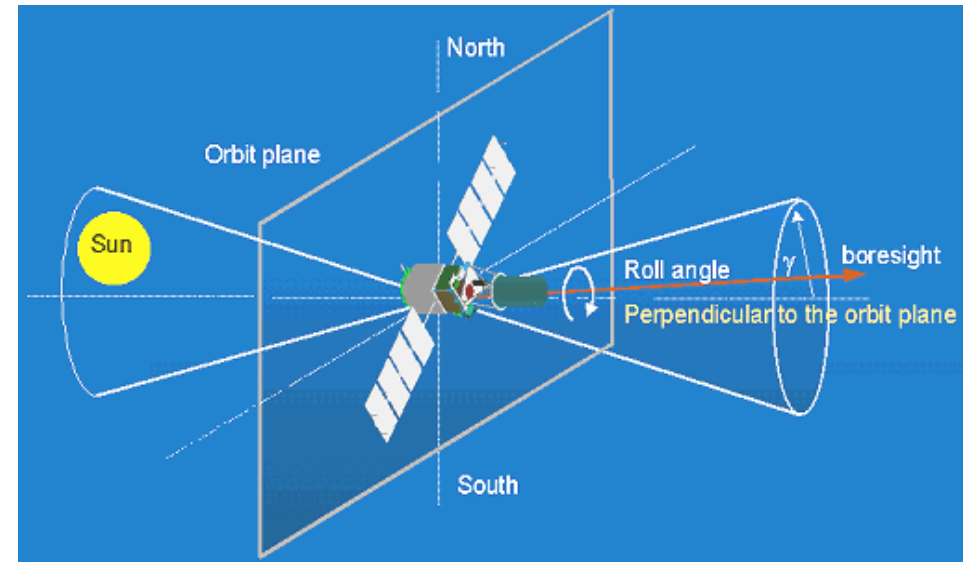
Exo field

- Exo field
 - up to 6000 LCs / CCD
 - $11.5 < m_V < 16$
 - 512s sampling (32s for 500 objects / CCD)
 - 3 colours for ~ 4500 objects / CCD with $m_V < 15$
- some small background windows
- up to 40 10x15 pixel windows
- on-board aperture photometry using mask selected from 256 templates based on one initial long integration image



Observing strategy

- Sequence:
 - ~1 month commissioning
 - 1 initial run (early science, ~50d)
 - then 5 x (150d long run + 21d short run)
 - rotate satellite every 6 months
 - Currently doing 2nd long run
- Visibility zone
 - sun angle constraints imply 2 'CoRoT eyes'
 - 10° diameter, small drift over 2.5 yr lifetime
 - intersection of ecliptic & Galactic planes
 - field selection = compromise

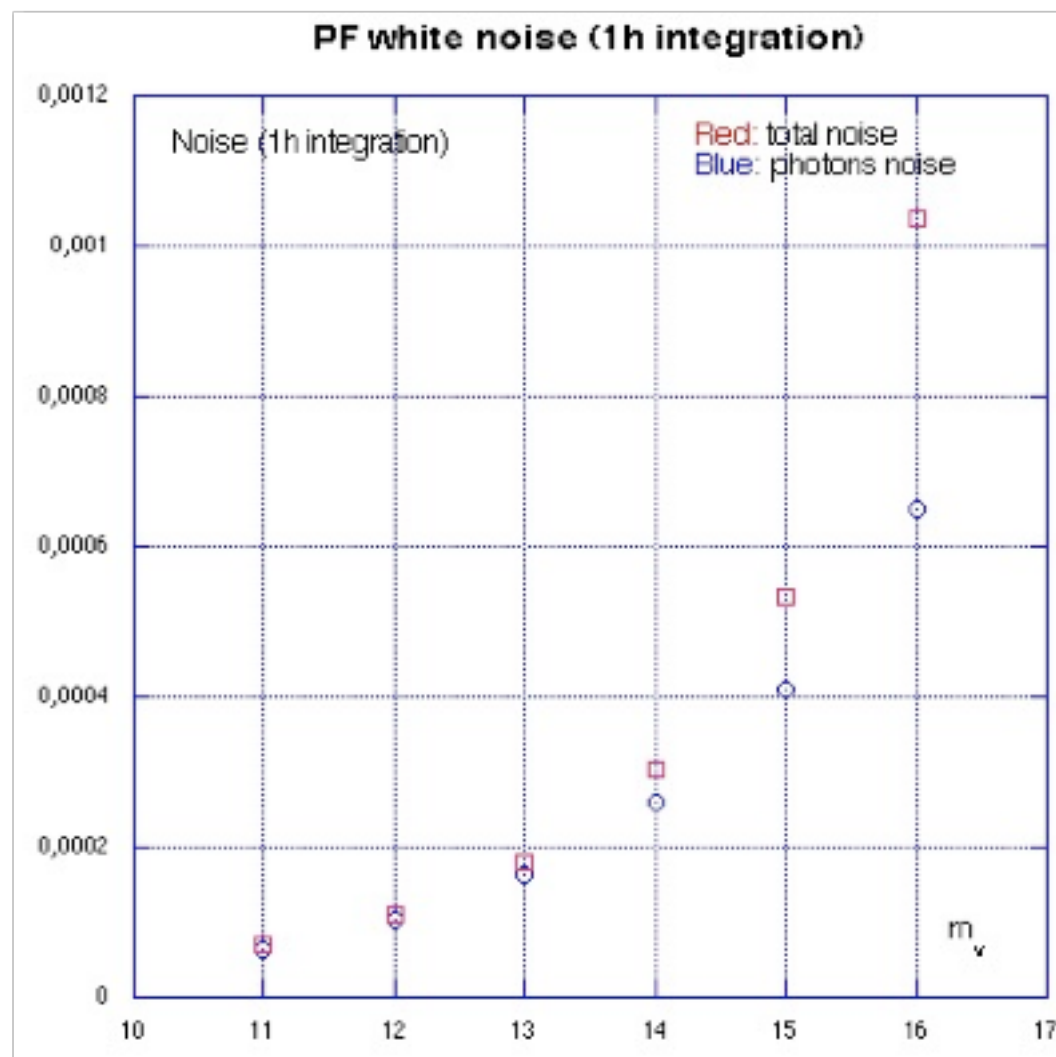


Field	Dur. (d)	RA	Dec	Rot* (°)
IR1	~60	06:50:25	-01:42:00	+14.96
LRc1	150	19:23:28.8	+00:28:48	+19.0
LRa1	150	06:46:48.0	-00:11:24	+7.3

*N-S direction: Rot = -5° in centre, +5° in anticentre

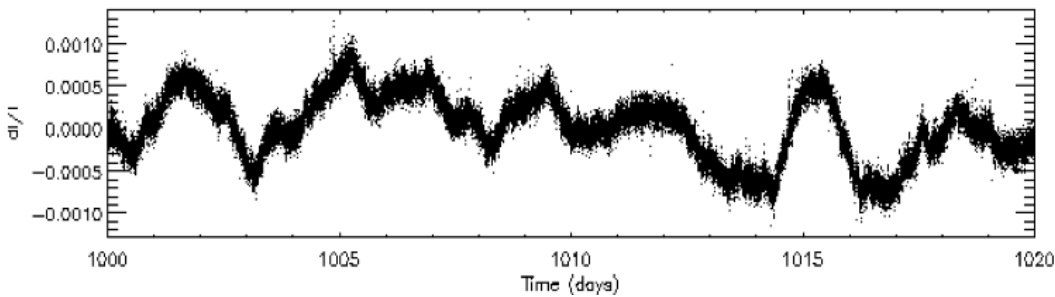
Exoplanet noise budget

- Nominal noise budget
 - white noise
 - readout, background, jitter
 - see plot
 - orbital period (6174s)
 - jitter, temperature, residual straylight
 - 120 ppm
- Stellar variability
 - few tens of ppm over transit timescale
- Correlated noise?
 - Blind test light curves contain 0.5 mmag red noise after detrending

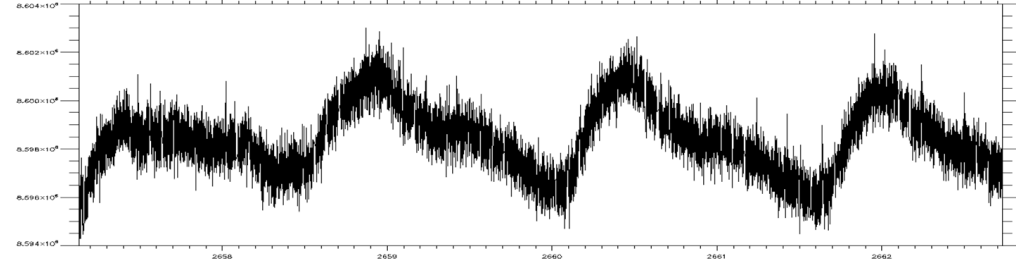


Example light curves from the seismo field

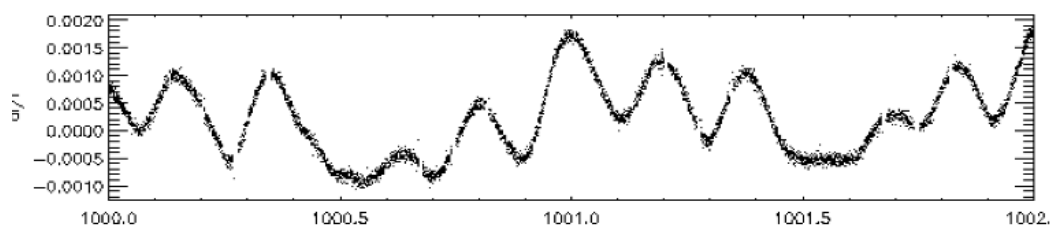
6th magnitude, F-type star, daily time-scales, few 10^{-3}



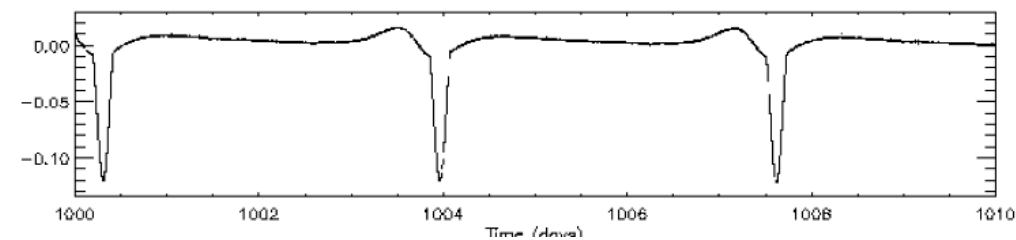
6th magnitude, Be star, daily time-scales



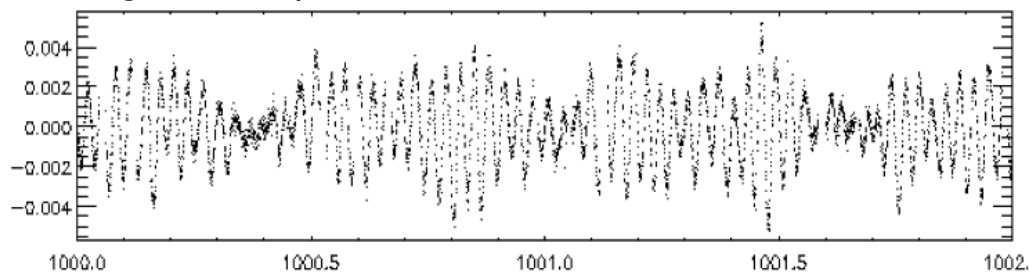
6th magnitude, few hours time-scales, few 10^{-3}



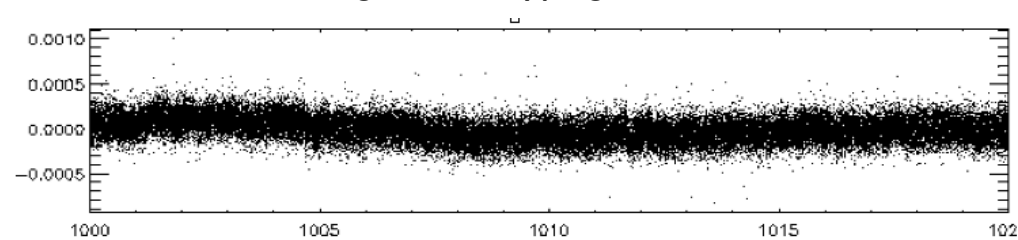
8th magnitude, B star, eclipsing binary



9th magnitude, suspected δ Scuti, few hours time-scales, few 10^{-3}



7th magnitude, F-type giant, few 10^{-4}



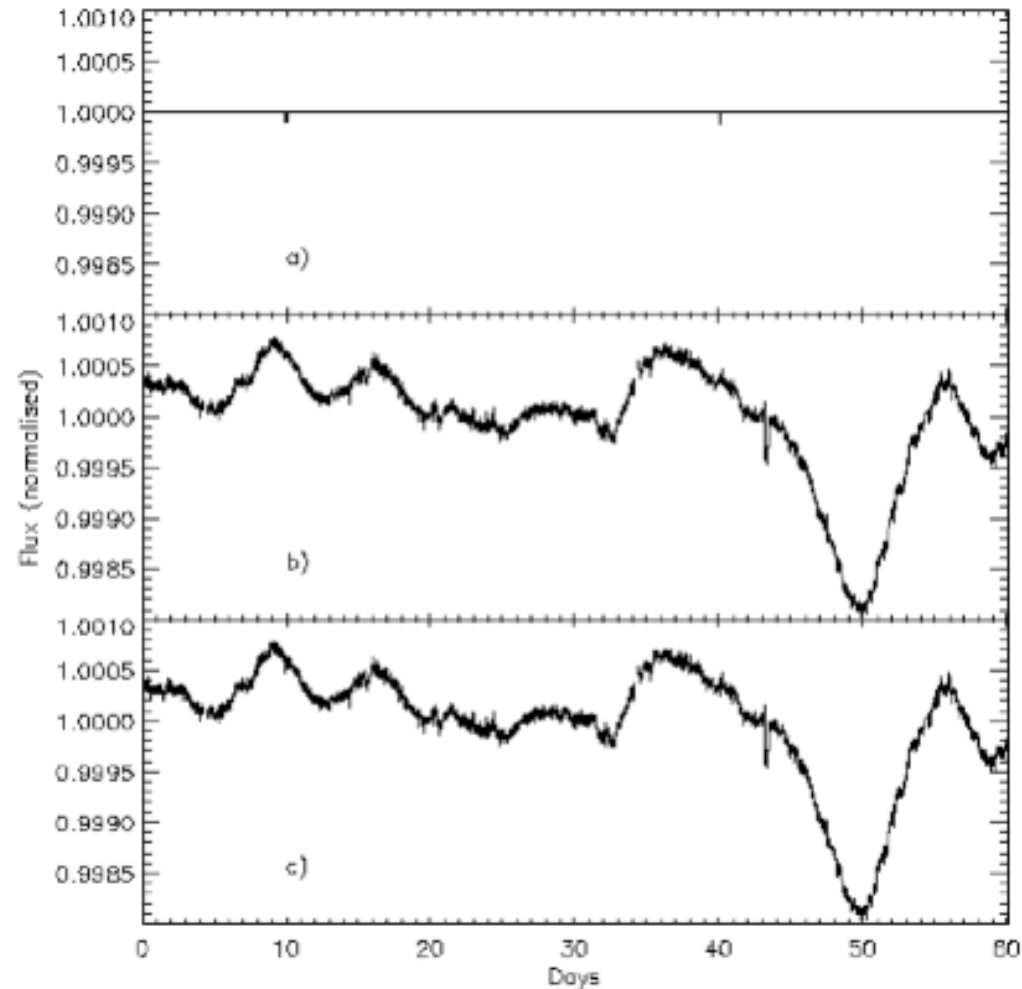
Detecting the planets

Steps in the detection process

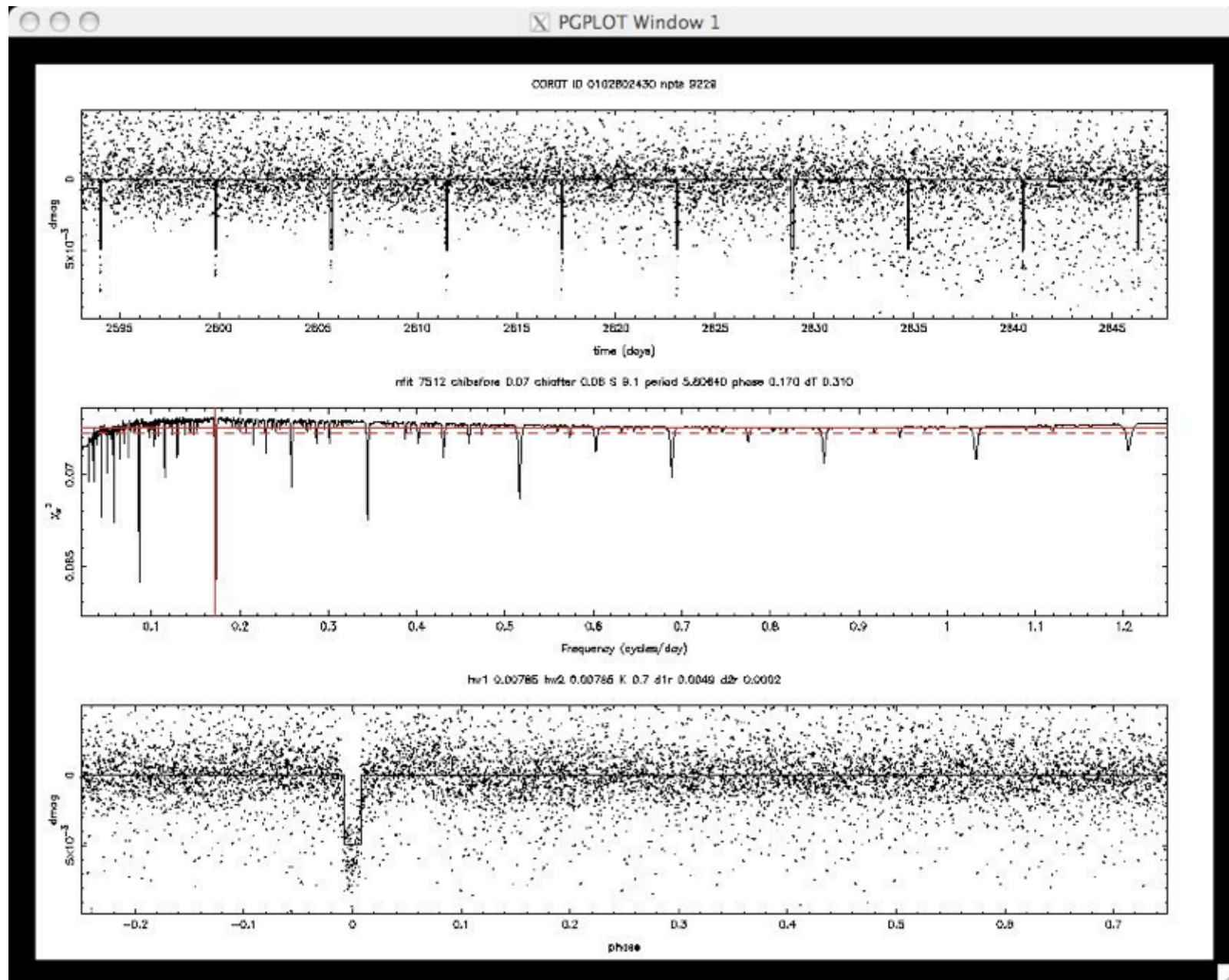
- Preprocessing
 - Identify and remove outliers
 - Correct for scattered light (satellite orbital period and daily timescales)
 - Identify and remove hot pixels
 - Evaluate flux measurement uncertainties
- Detection
 - Filter out stellar variability
 - Run transit search (most commonly using variants of the BLS algorithm of Kovacs, Zucker & Mazeh 2002)
 - Prioritise candidates
- Ground-based follow-up

Stellar micro-variability

- Rotational modulation & intrinsic evolution of surface structures (spots, faculae, granules)
 - Roughly $1/f$ noise spectrum
- Very ill characterised in stars other than the Sun
 - Attempts at predicting micro-variability for other stars (Aigrain, Favata & Gilmore 2004, Lanza et al. 2005)
 - Major ancillary science goal
- The main noise source for terrestrial transit detection from space
 - Temporal signature different from transits
 - Exploit to construct filters
 - Moutou et al. (2005): CoRoT detection limits in the presence of variability



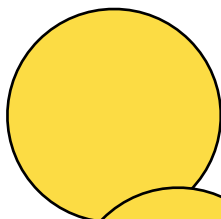
Transit detection



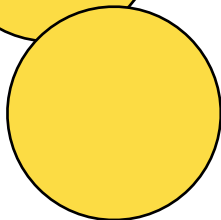
Algorithm of Aigrain & Irwin (2004) modified to allow secondaries and trapezoidal eclipses

Transit mimics

Transit mimics

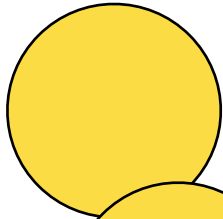


grazing eclipsing binary



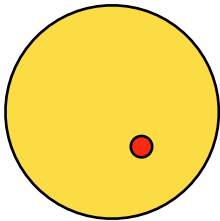
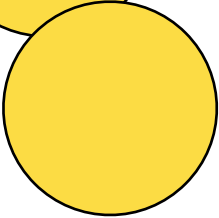
close inspection of light curve
SB2 spectrum
pair of RV measurements

Transit mimics



grazing eclipsing binary

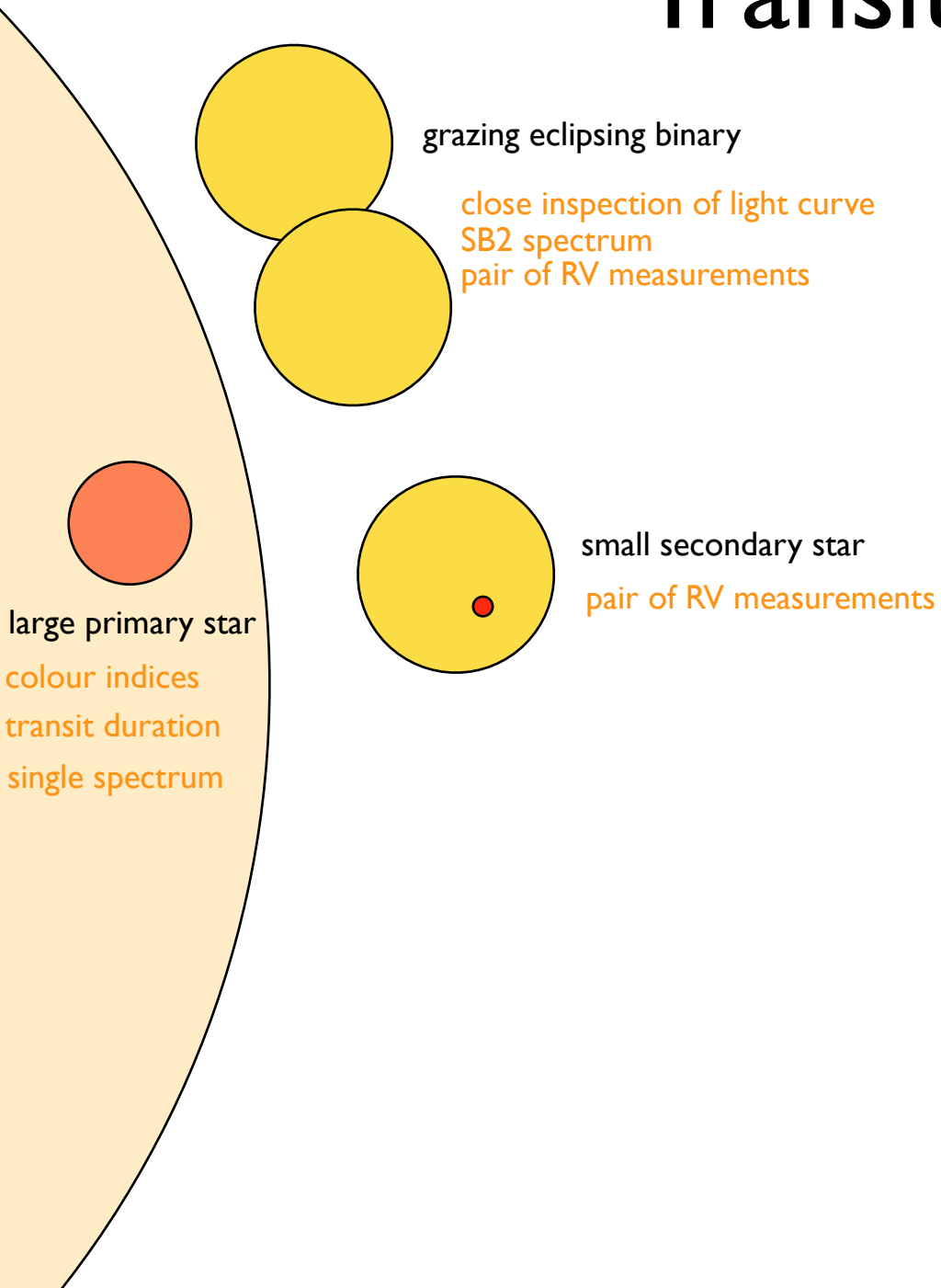
close inspection of light curve
SB2 spectrum
pair of RV measurements



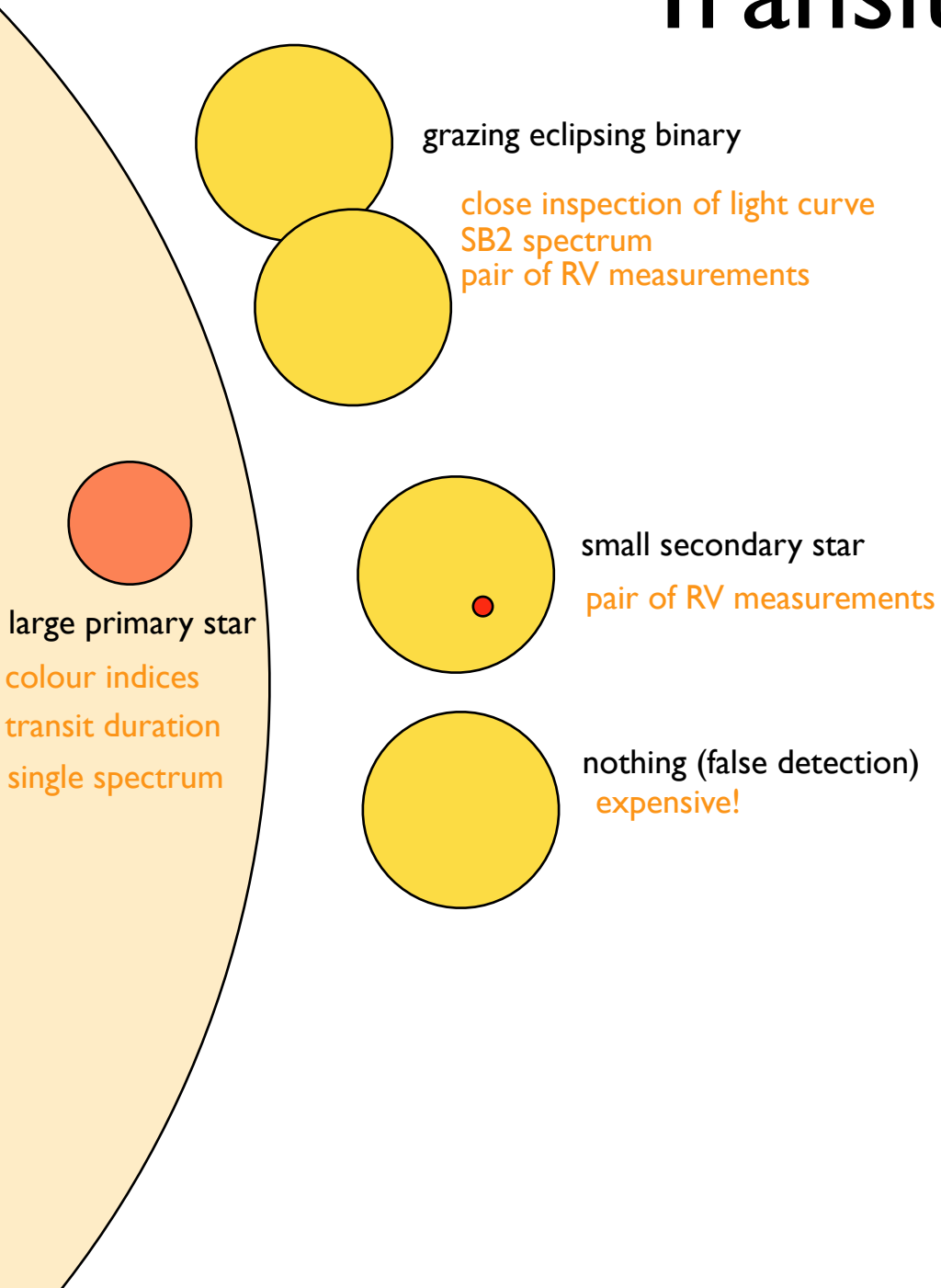
small secondary star

pair of RV measurements

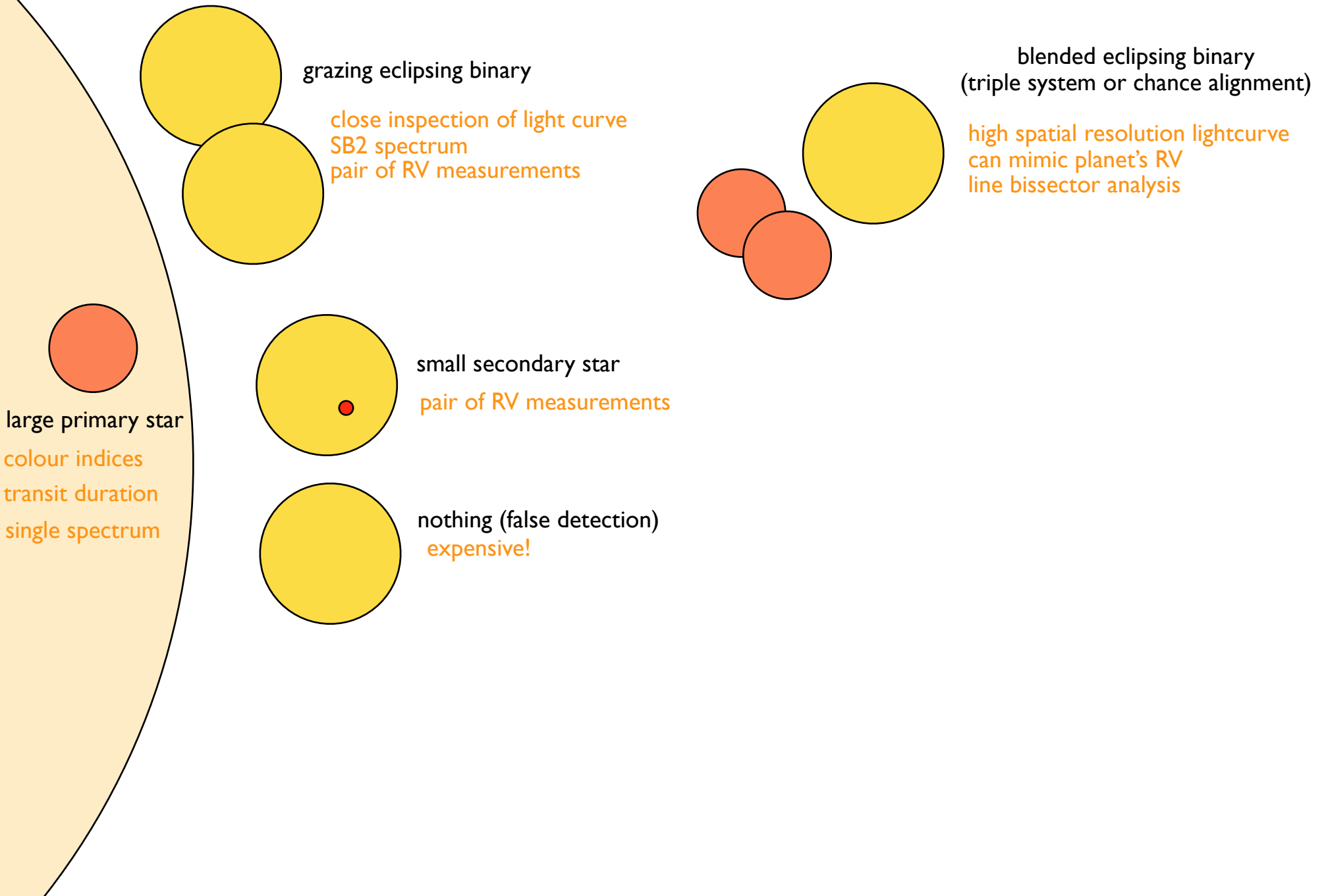
Transit mimics



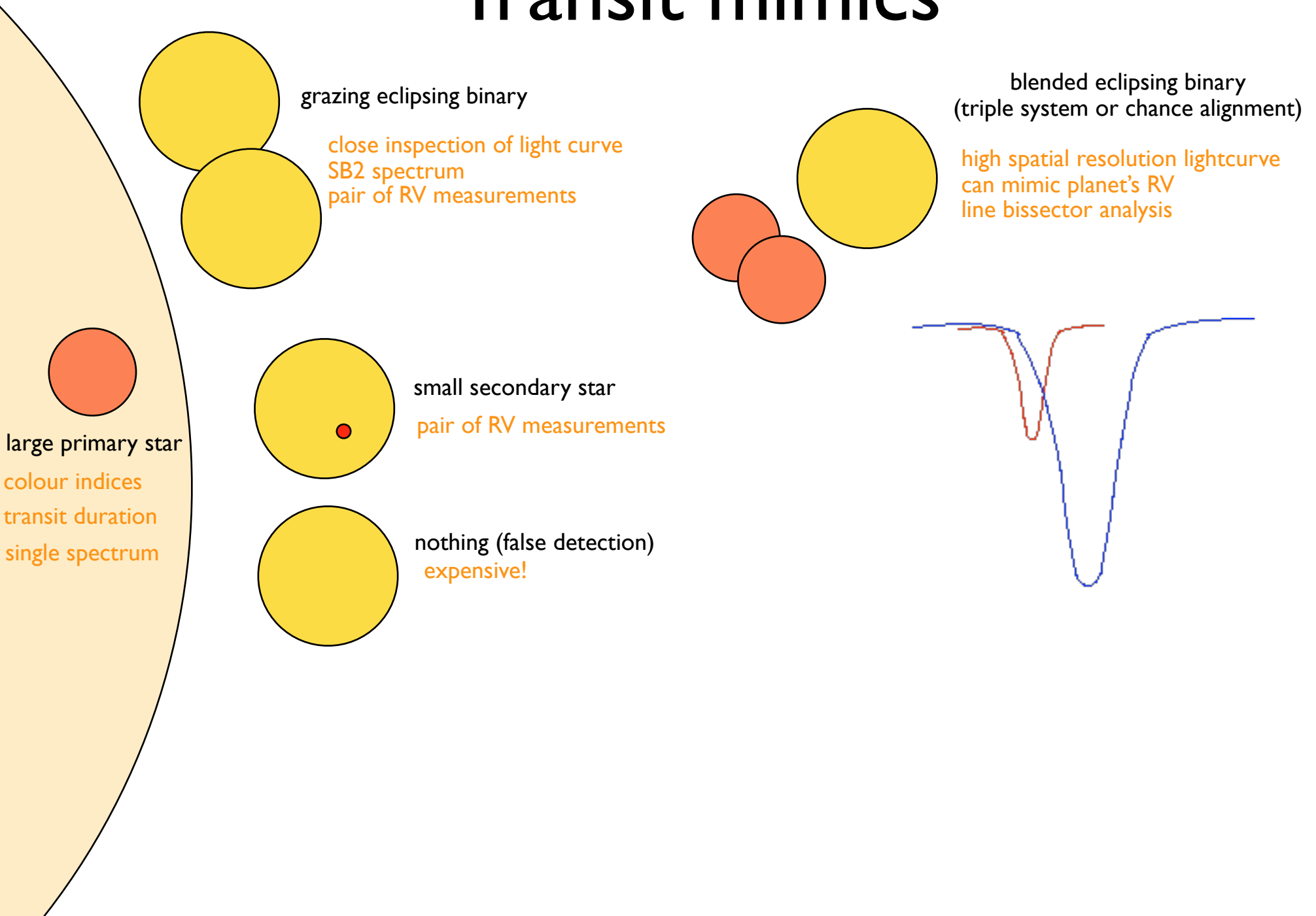
Transit mimics



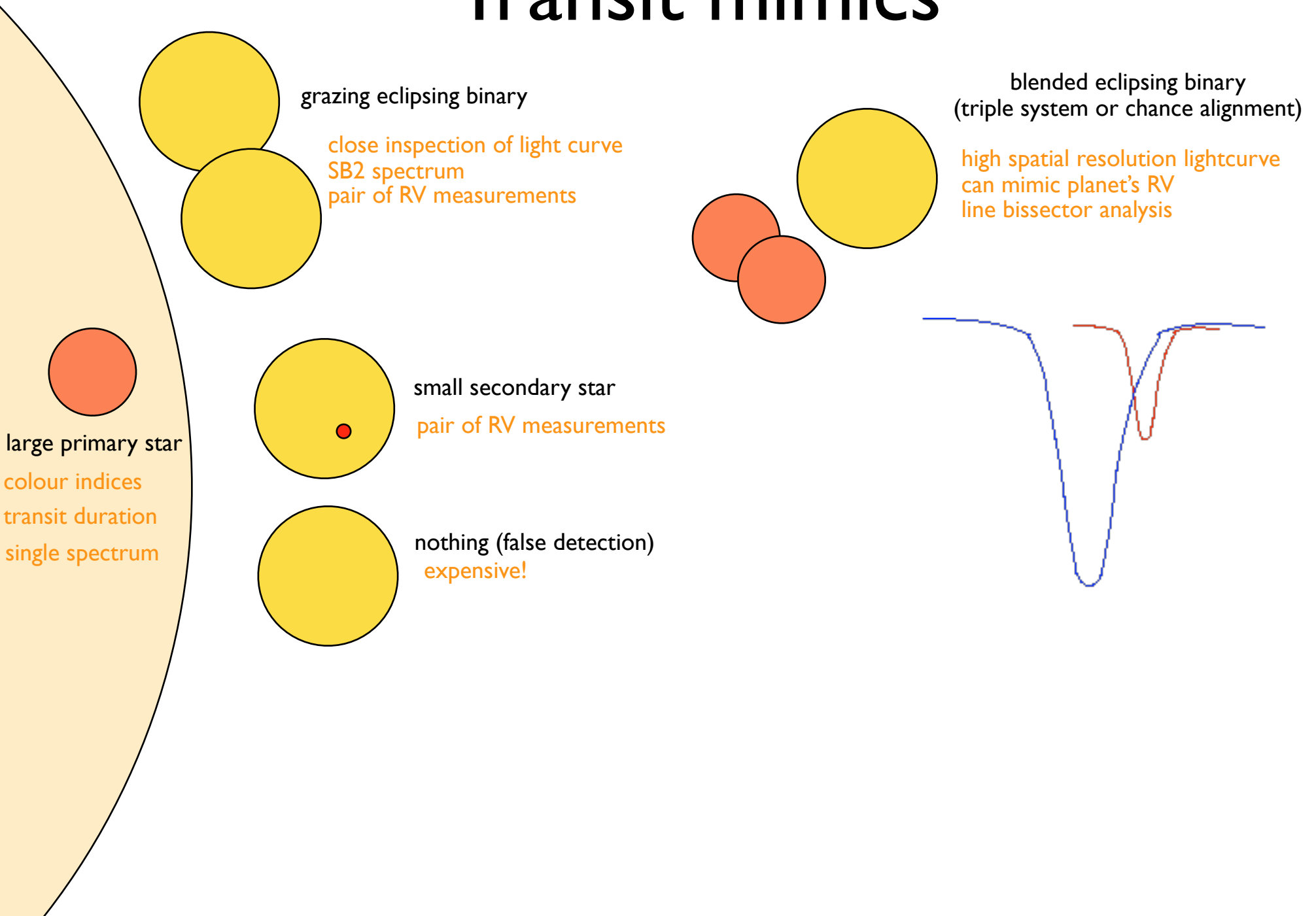
Transit mimics



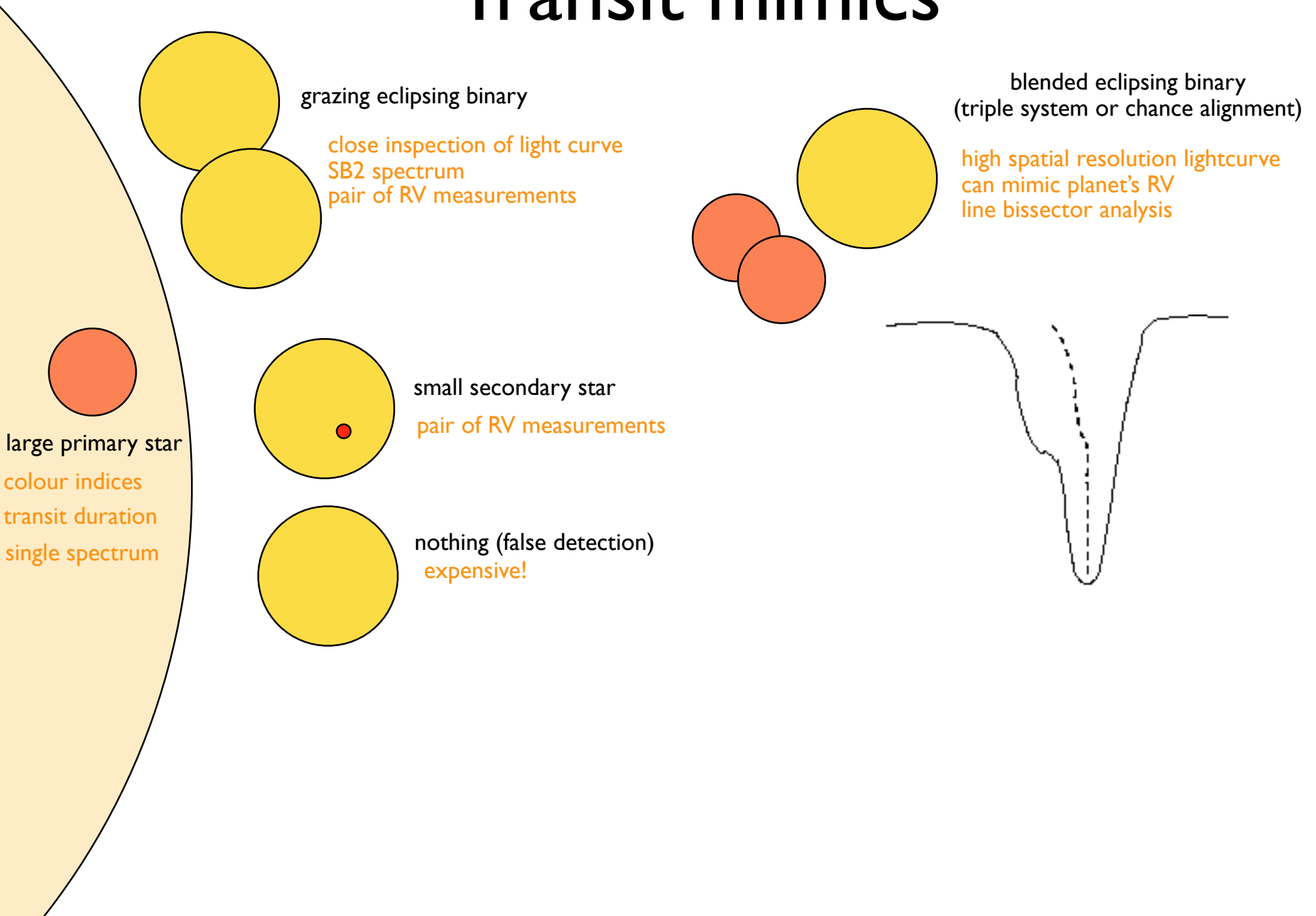
Transit mimics



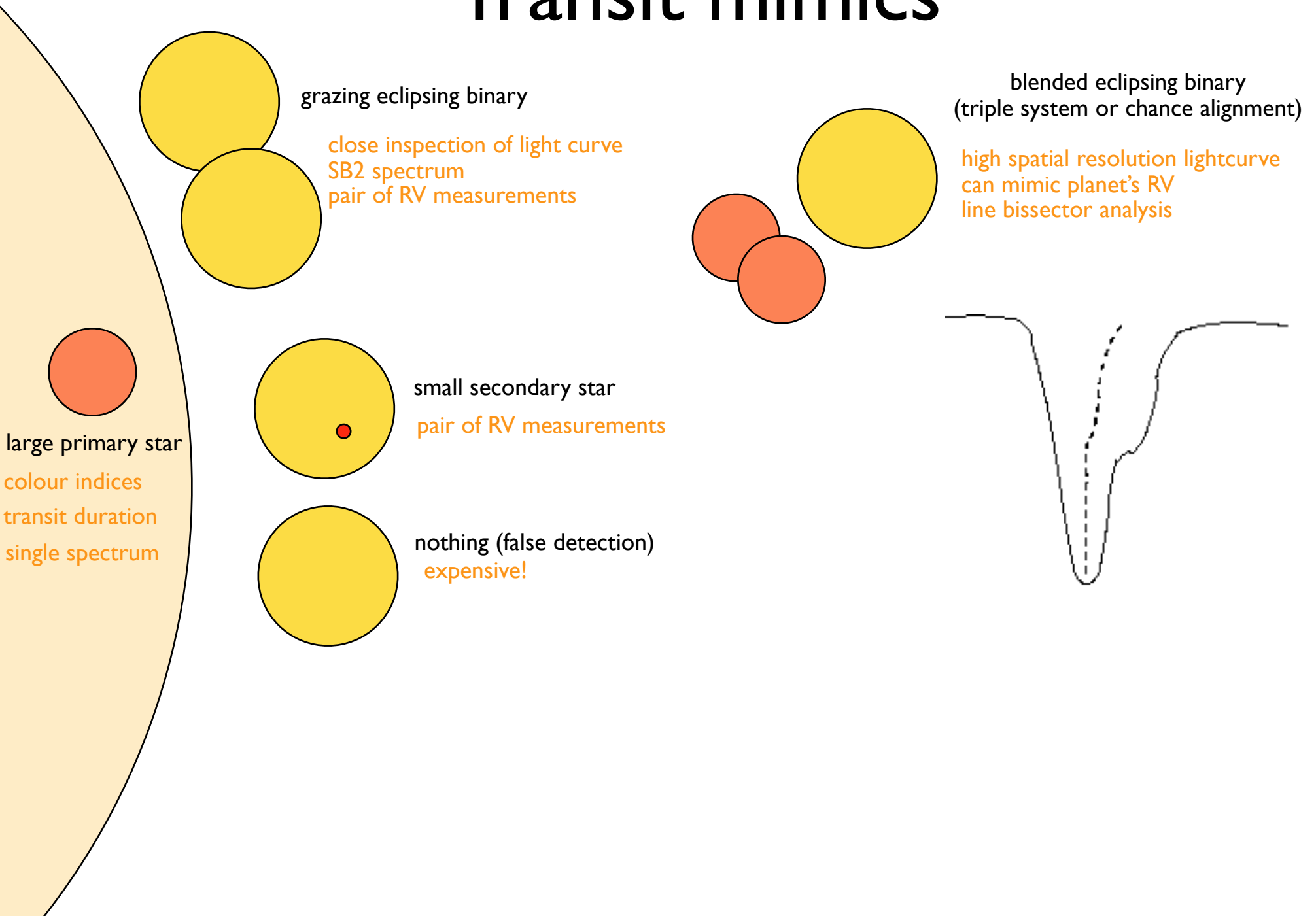
Transit mimics



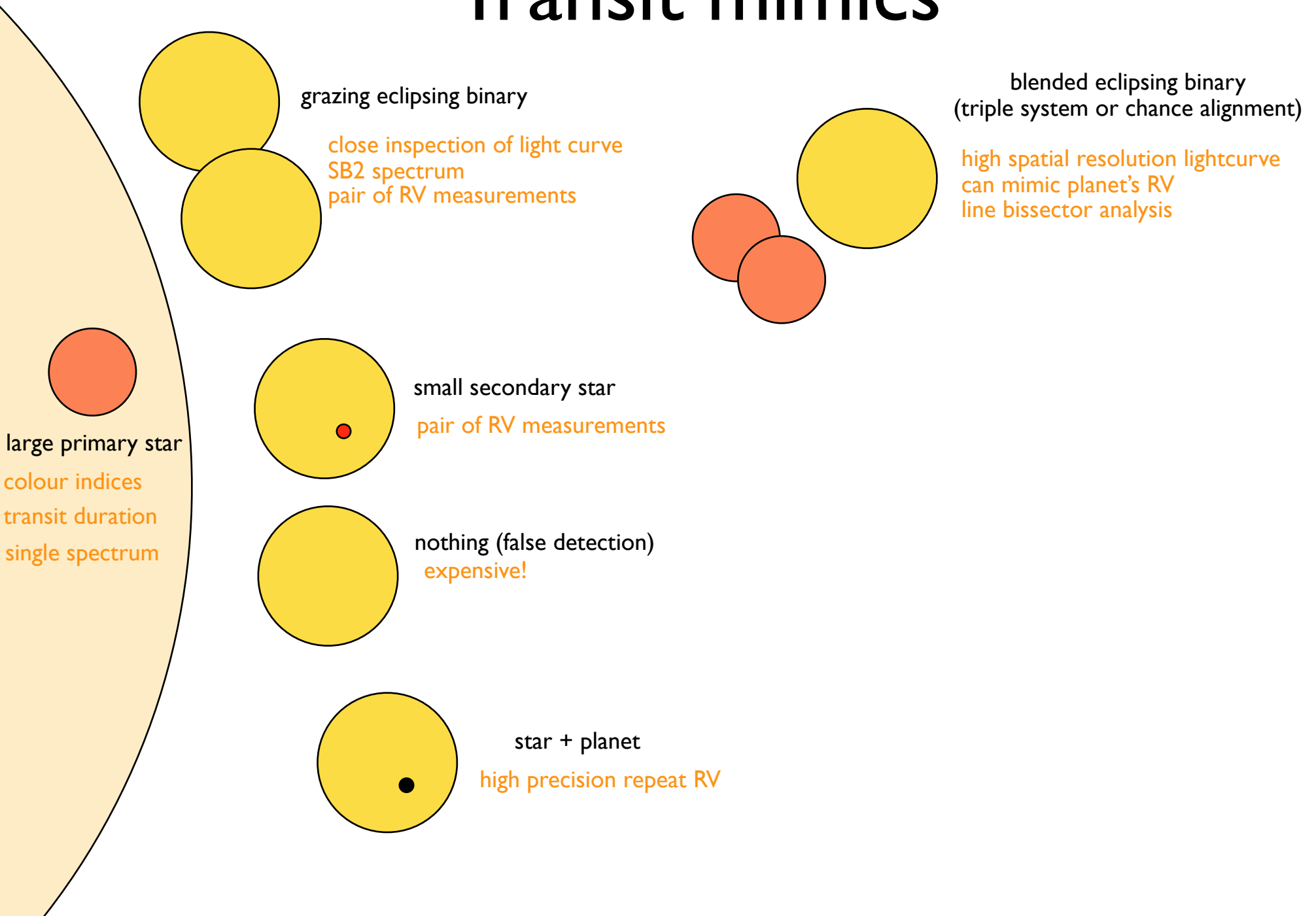
Transit mimics



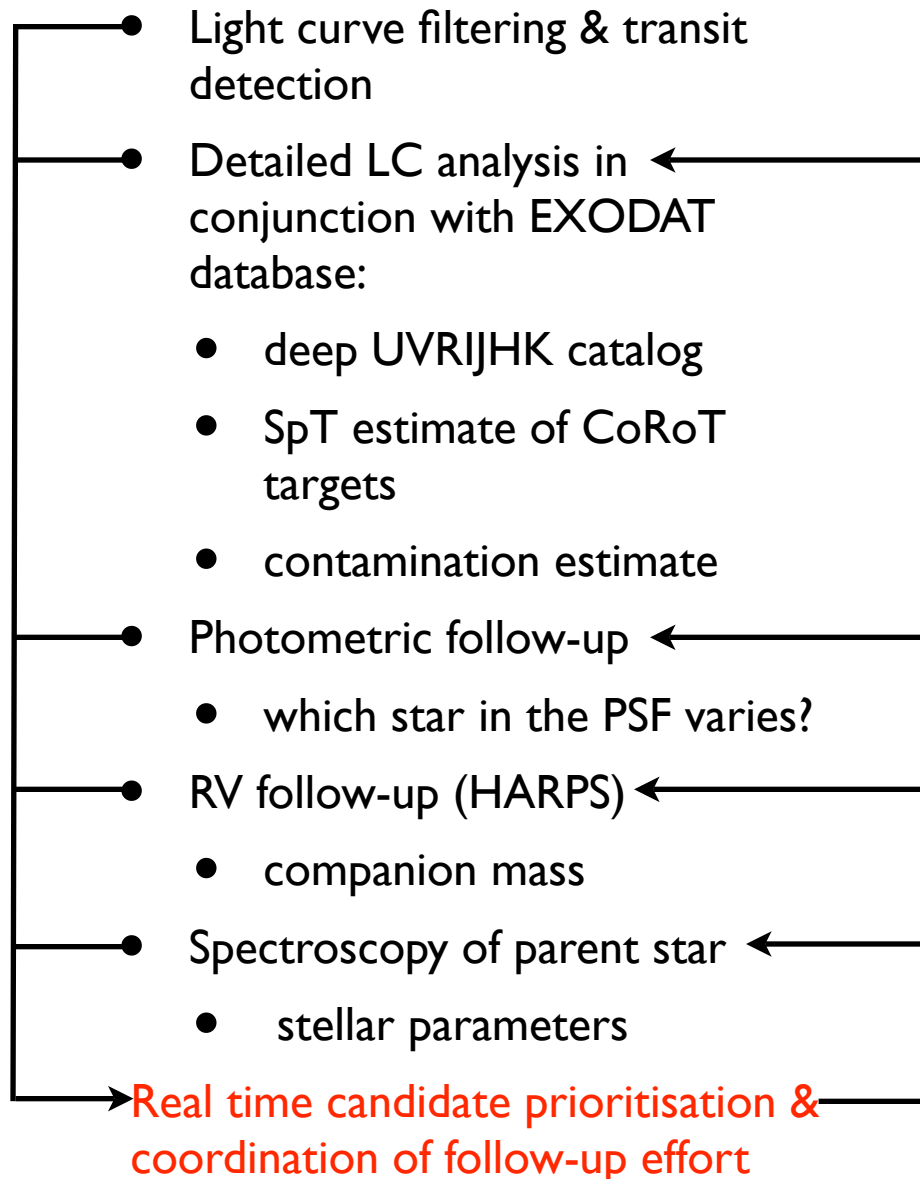
Transit mimics



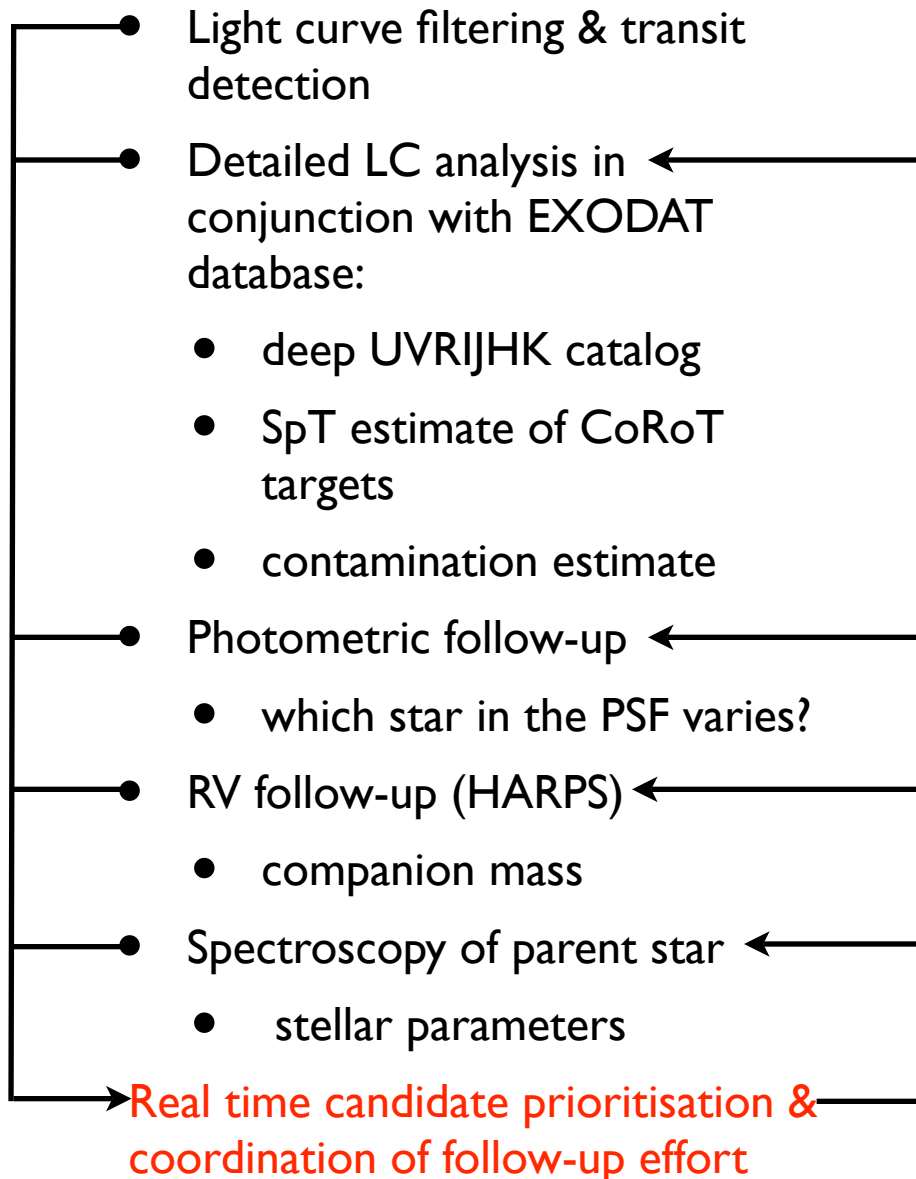
Transit mimics



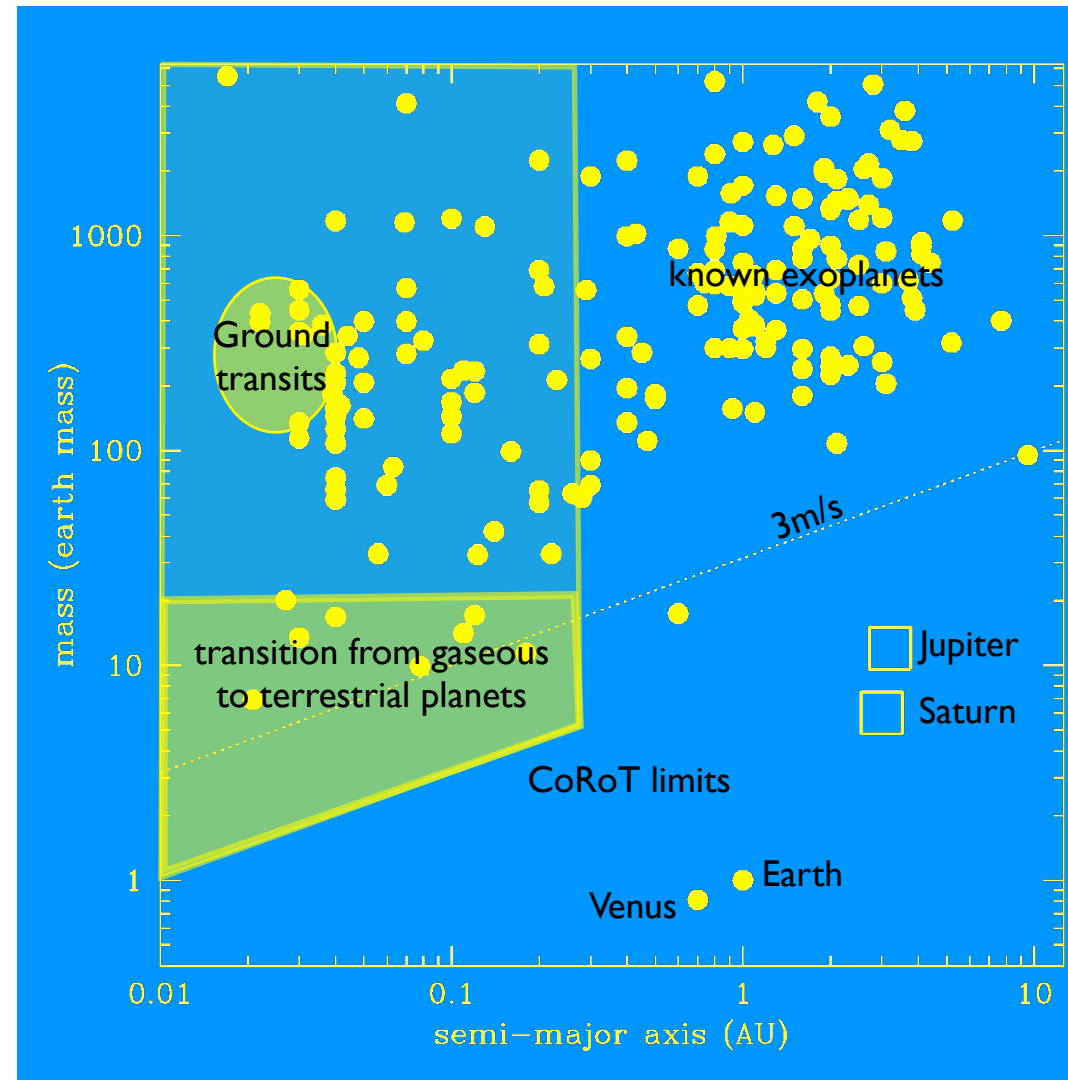
Follow-up



Follow-up



COROT is well matched to current RV facilities



CoRoT-exo-1b

a low density short-period planet around a G0V star

Barge et al. (2008, A&A submitted)

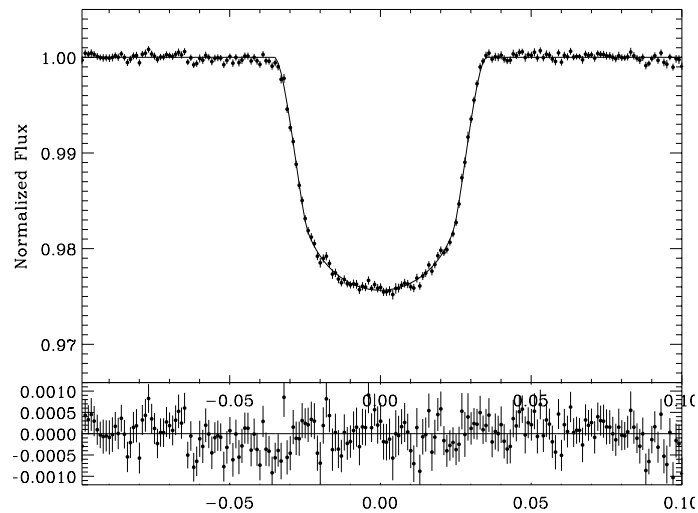


Fig. 1. Normalized and phase folded light curve of 36 transits of CoRoT-Exo-1b, and the residuals from the best-fit model. The bin size corresponds to 2.17min , and the 2σ error bars have been estimated from the dispersion of the data points inside each bin.

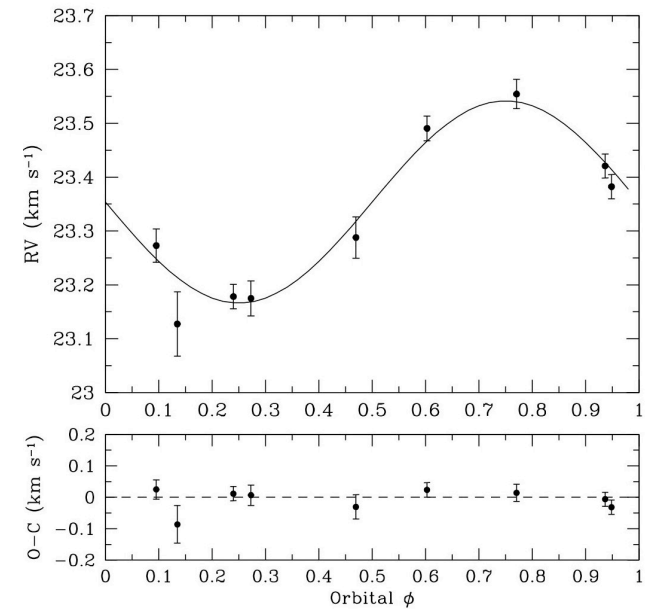


Fig. 2. Radial-velocity variations of CoRoT-Exo-1b versus phase from CoRoT's ephemeris. Top: the data fitted with a Keplerian circular orbit of semi-amplitude $K=188\text{ m s}^{-1}$ and a drift of 1.02 m s^{-1} per day; bottom: the O-C residuals to the fit

CoRoT-exo-1b

a low density short-period planet around a G0V star

Barge et al. (2008, A&A submitted)

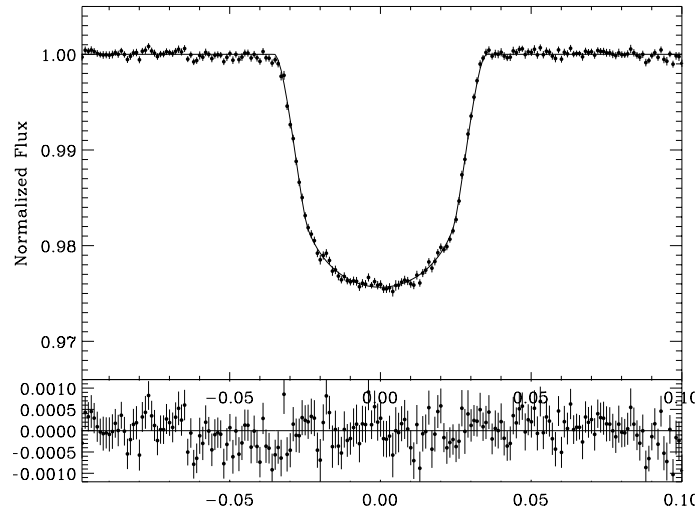


Fig. 1. Normalized and phase folded light curve of 36 transits of CoRoT-Exo-1b, and the residuals from the best-fit model. The bin size corresponds to 2.17min , and the 2σ error bars have been estimated from the dispersion of the data points inside each bin.

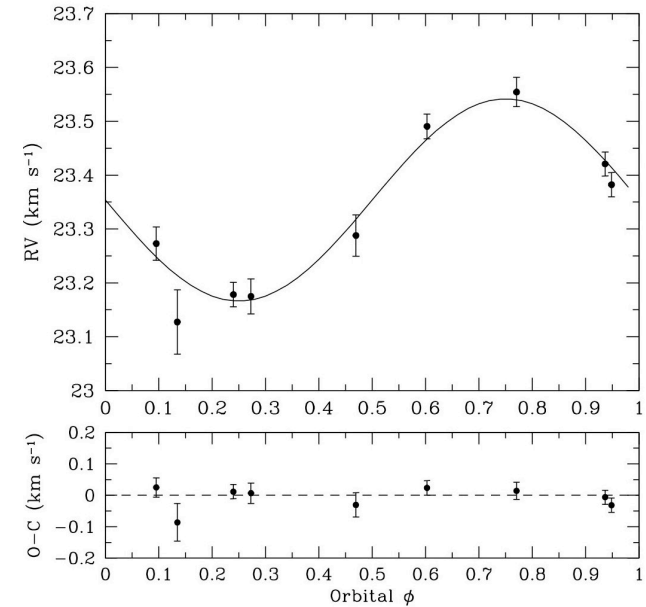


Fig. 2. Radial-velocity variations of CoRoT-Exo-1b versus phase from CoRoT's ephemeris. Top: the data fitted with a Keplerian circular orbit of semi-amplitude $K=188\text{ m s}^{-1}$ and a drift of 1.02 m s^{-1} per day; bottom: the O-C residuals to the fit

Orbital period (d)	$1.5089557 (\pm 0.0000064)$
Transit center (d)	$2454159.4532 (\pm 0.0001) - \text{HJD}$
V_0 (km/s)	23.354 ± 0.008
K (m/s)	188 ± 11
M_* : star mass (M_\odot)	$0.9 (\pm 0.1)$
R_* : star radius (R_\odot)	$1.09 (\pm 0.04)$
M_P : planet mass (M_{Jup})	$0.99 (\pm 0.09)$
R_P : planet radius (R_{Jup})	$1.47 (\pm 0.06)$
Planet mean density (g.cm^{-3})	$0.35 (\pm 0.06)$

CoRoT-exo-2b

a low transiting planet around a and active G star

Alonso et al., Bouchy et al (2008, A&A submitted)

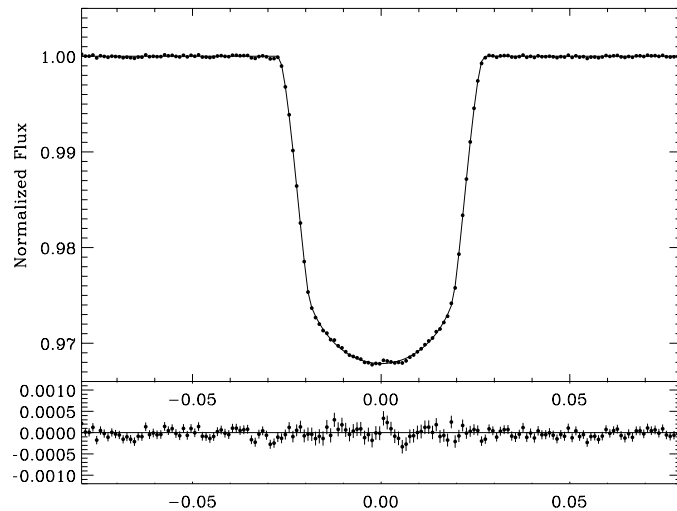


Fig. 2. Normalized and phase folded light curve of 78 transits of CoRoT-Exo-2b (top), and the residuals from the best-fit model (bottom). The bin size corresponds to 2.5 min, and the 1-sigma error bars have been estimated from the dispersion of the points inside each bin. The residuals of the in-transit points are larger due to the effect of successive planet occultations of stellar active regions.

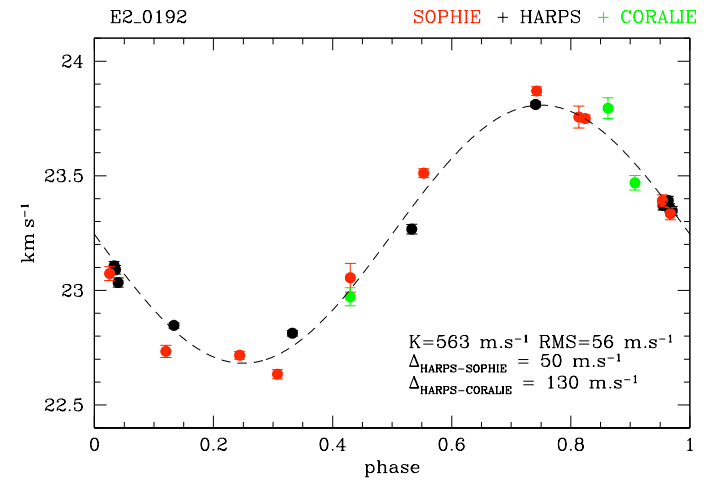


Fig. 3. Phase folded radial velocity measurements of CoRoT-Exo-2, together with the final fitted semi-amplitude (K) and the applied offsets between the instruments. Red points: SOPHIE, black points: HARPS, green points: CORALIE.

CoRoT-exo-2b

a low transiting planet around a and active G star

Alonso et al., Bouchy et al (2008, A&A submitted)

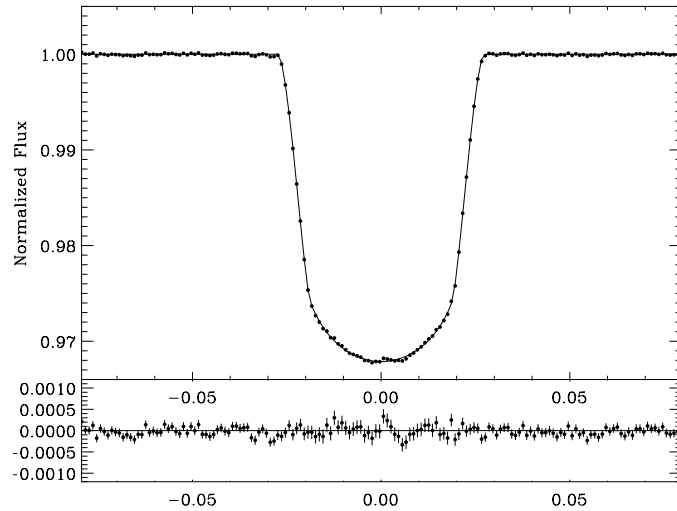


Fig. 2. Normalized and phase folded light curve of 78 transits of CoRoT-Exo-2b (top), and the residuals from the best-fit model (bottom). The bin size corresponds to 2.5 min, and the 1-sigma error bars have been estimated from the dispersion of the points inside each bin. The residuals of the in-transit points are larger due to the effect of successive planet occultations of stellar active regions.

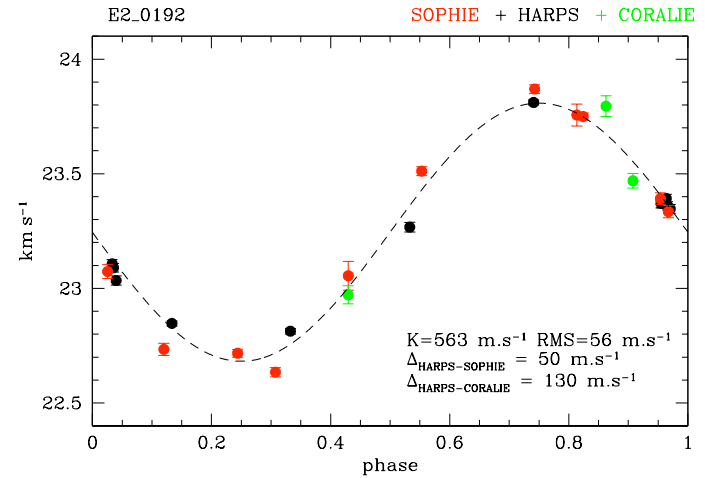


Fig. 3. Phase folded radial velocity measurements of CoRoT-Exo-2, together with the final fitted semi-amplitude (K) and the applied offsets between the instruments. Red points: SOPHIE, black points: HARPS, green points: CORALIE.

	Value	Error
P [d]	1.7429964	0.0000017
T_c [d]	2454237.53562	0.00014
V_0 [km/s]	23.245	0.010
K [km/s]	0.563	0.014
e	0	(fixed)
M_s [M_\odot]	0.97	0.06
R_s [R_\odot]	0.902	0.018
M_p [M_{Jup}]	3.31	0.16
R_p [R_{Jup}]	1.465	0.029
ρ_p [g/cm ³]	1.31	0.04

CoRoT-exo-2b

a low transiting planet around a and active G star

Alonso et al. (2008, A&A submitted)

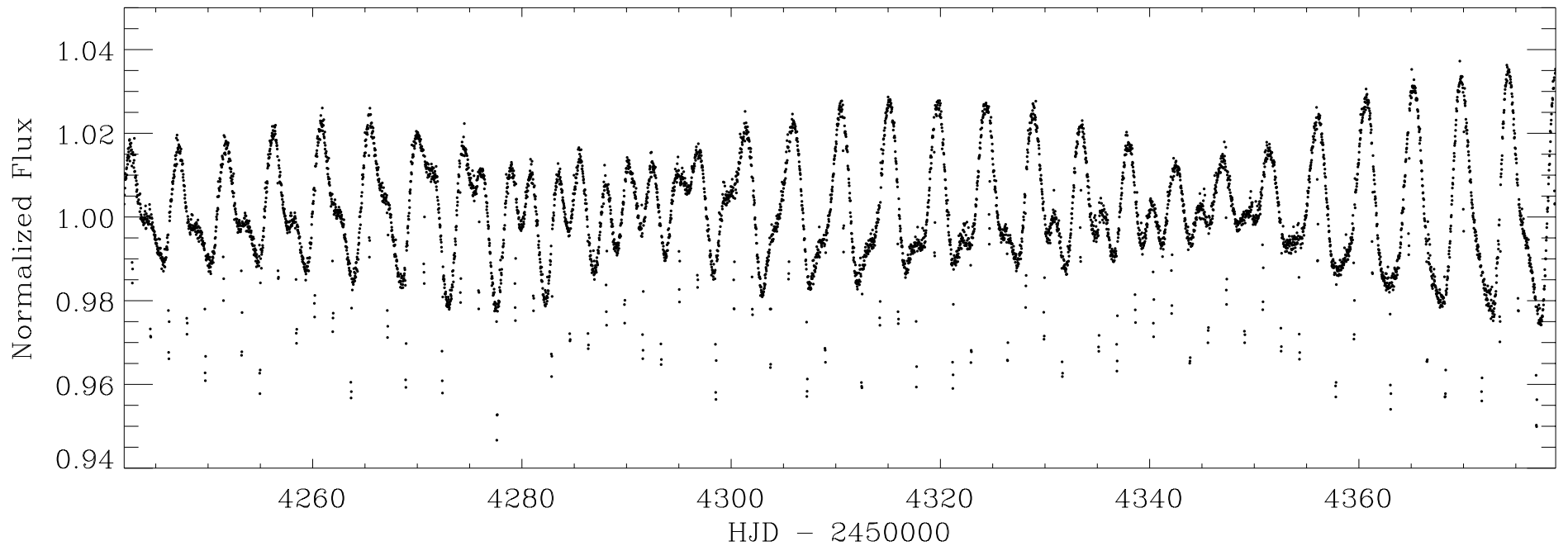


Fig. 1. Normalized flux of the CoRoT-Exo-2 star, showing a low frequency modulation due to the presence of spots on the stellar surface, and the 78 transits used to build the phase-folded transit of the Figure 2. For clarity purposes, data have been combined in 64-points bins.

CoRoT-exo-2b

a low transiting planet around a and active G star

Alonso et al. (2008, A&A submitted)

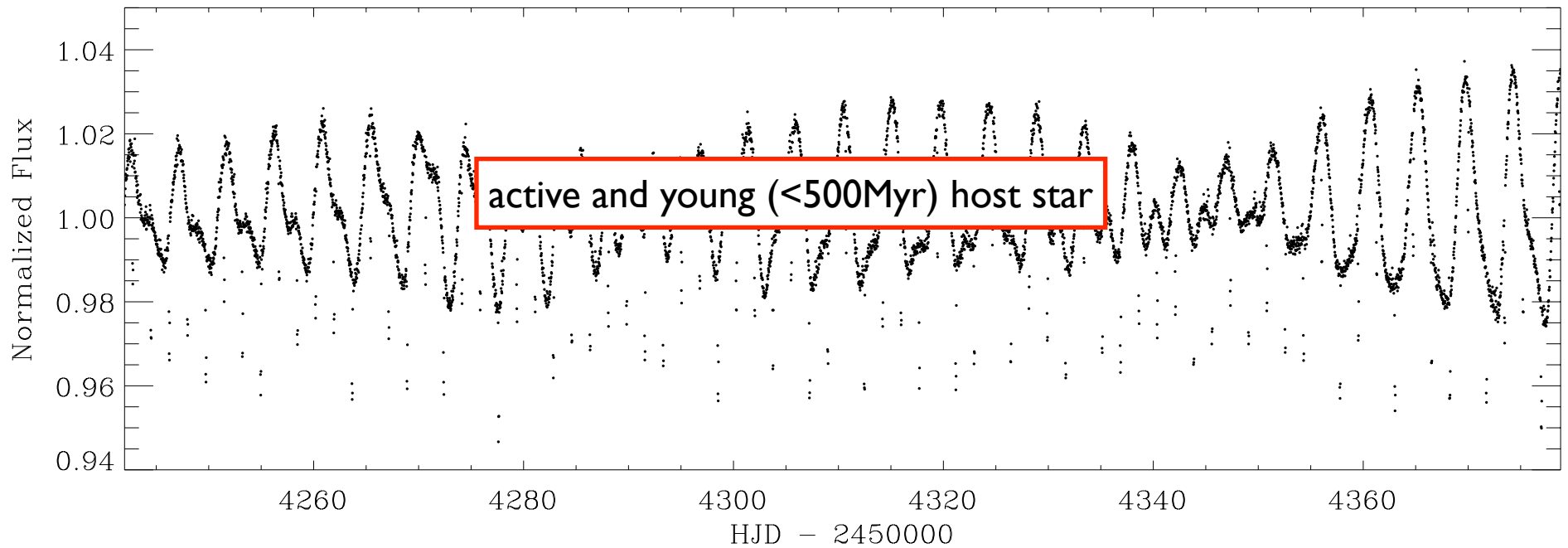


Fig. 1. Normalized flux of the CoRoT-Exo-2 star, showing a low frequency modulation due to the presence of spots on the stellar surface, and the 78 transits used to build the phase-folded transit of the Figure 2. For clarity purposes, data have been combined in 64-points bins.

CoRoT-exo-2b

a low transiting planet around a and active G star

Alonso et al. (2008, A&A submitted)

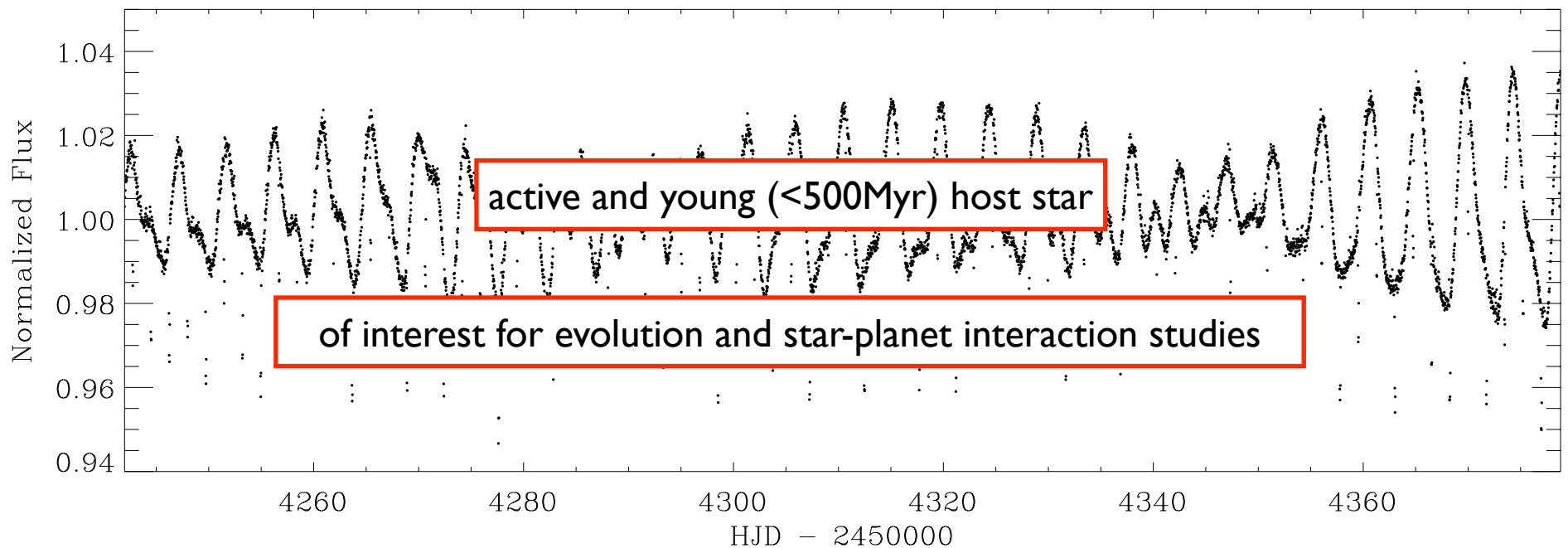


Fig. 1. Normalized flux of the CoRoT-Exo-2 star, showing a low frequency modulation due to the presence of spots on the stellar surface, and the 78 transits used to build the phase-folded transit of the Figure 2. For clarity purposes, data have been combined in 64-points bins.

CoRoT-exo-2b

spectroscopic transit with SOPHIE & HARPS

Bouchy et al. (2008, A&A submitted)

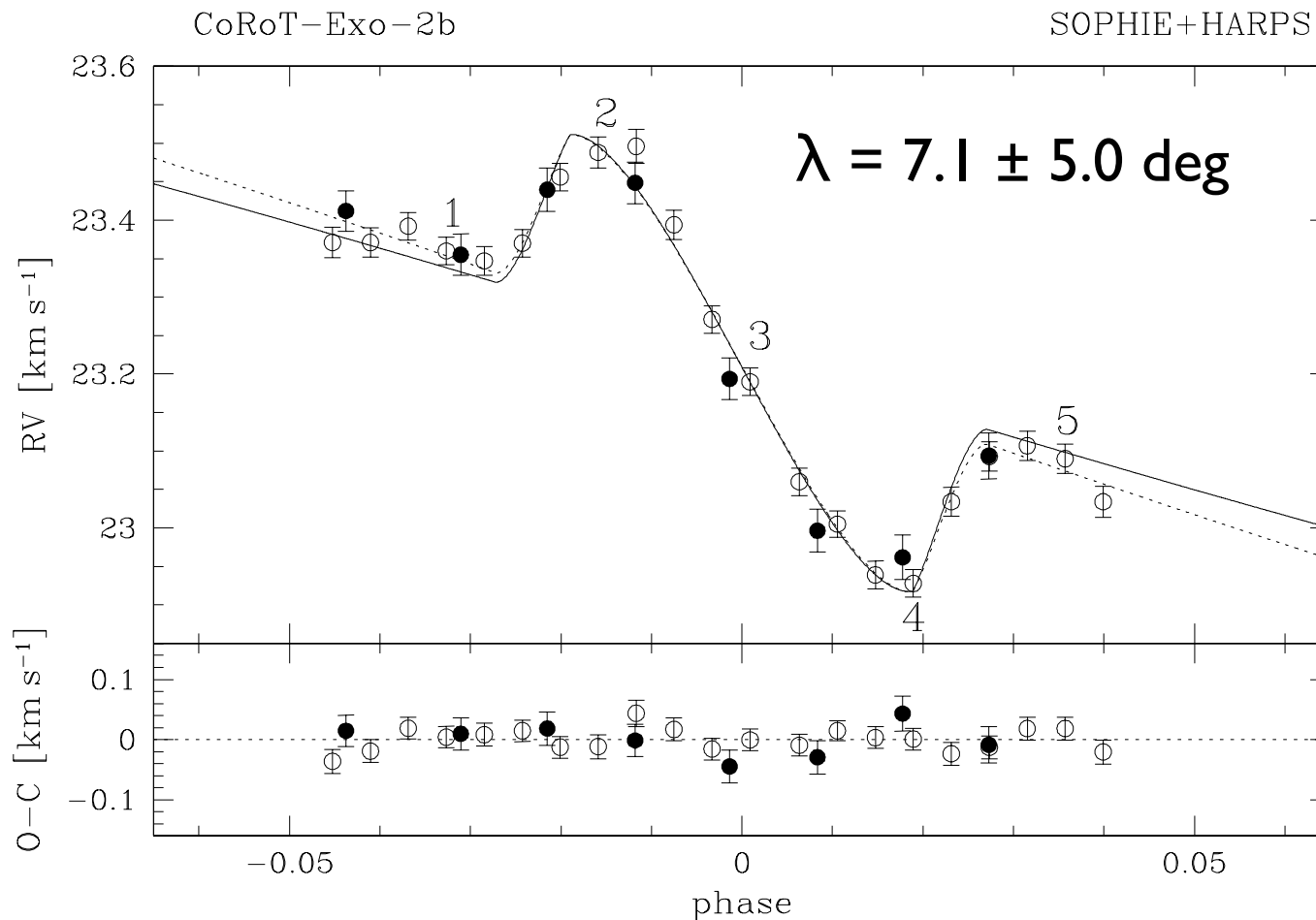
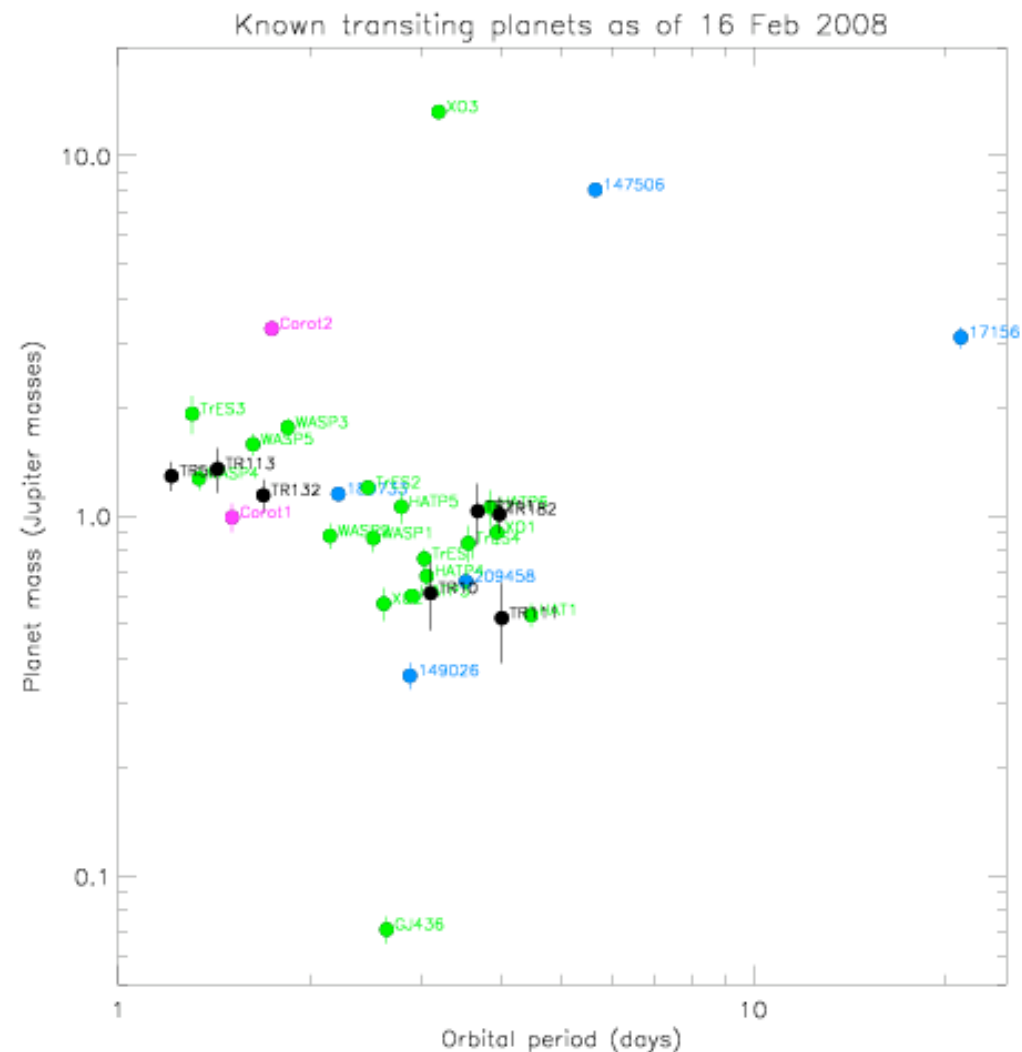
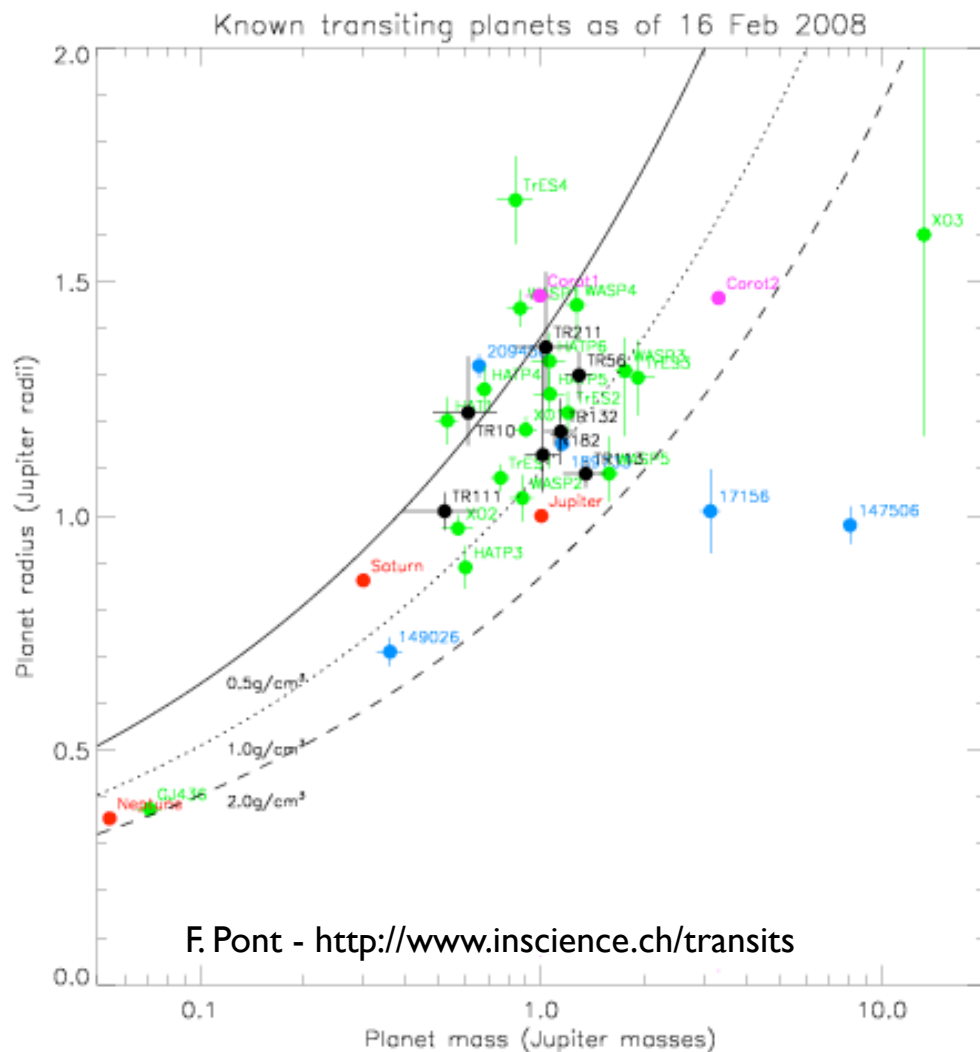
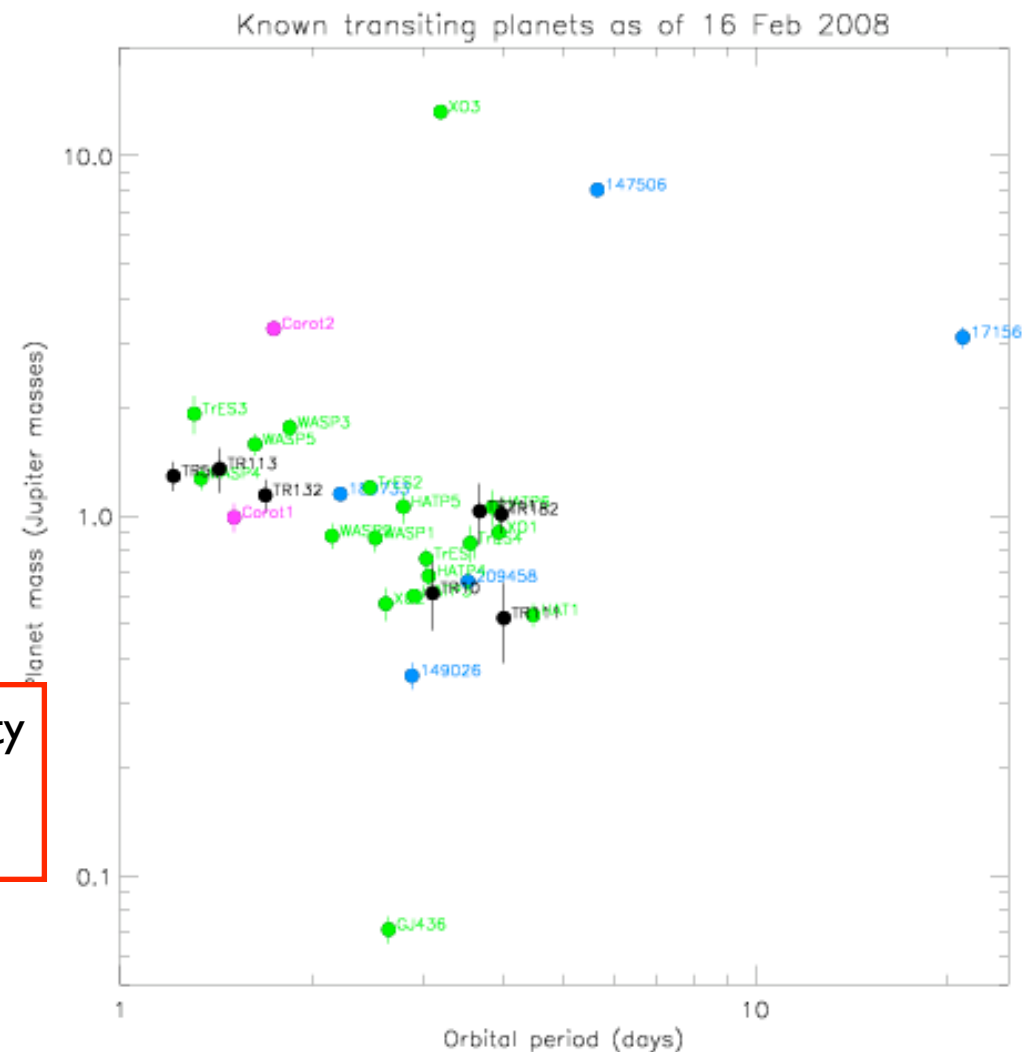
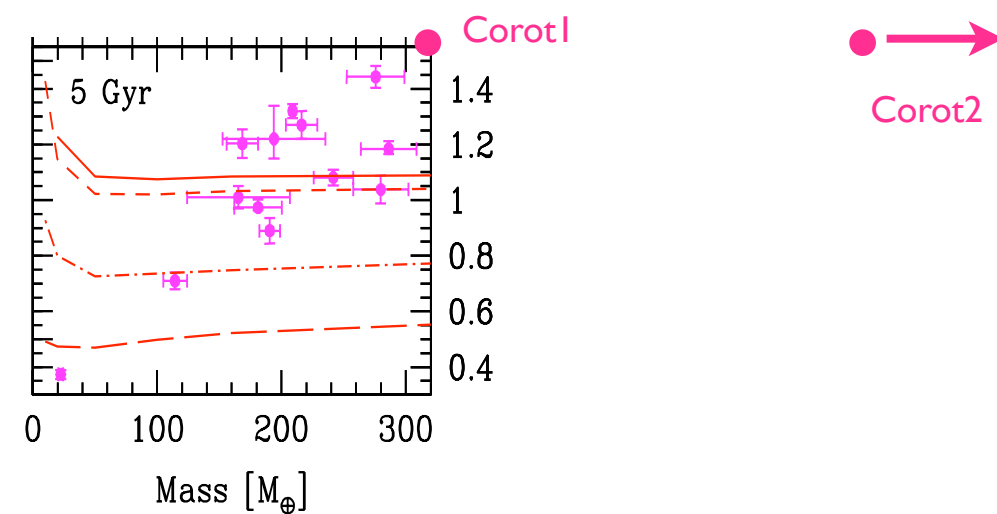
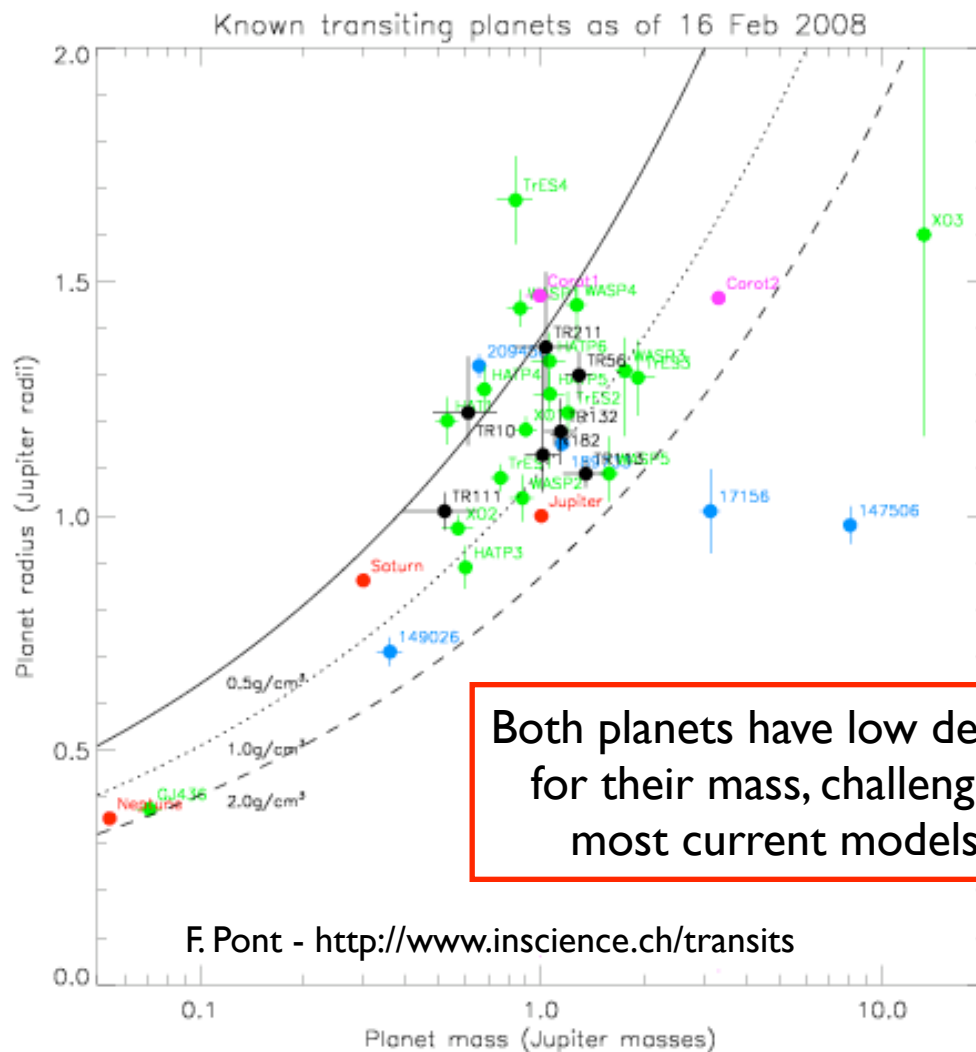


Fig. 1. Phase-folded radial velocity measurements of CoRoT-Exo-2 during the transit of the planet with SOPHIE (dark circle) and HARPS (open circle). The solid line corresponds to the Rossiter-McLaughlin model adjusted to these data assuming the semi-amplitude $K=563 \text{ m s}^{-1}$ from Alonso et al. (2008). The dotted line corresponds to the Rossiter-McLaughlin model with K as free parameters.

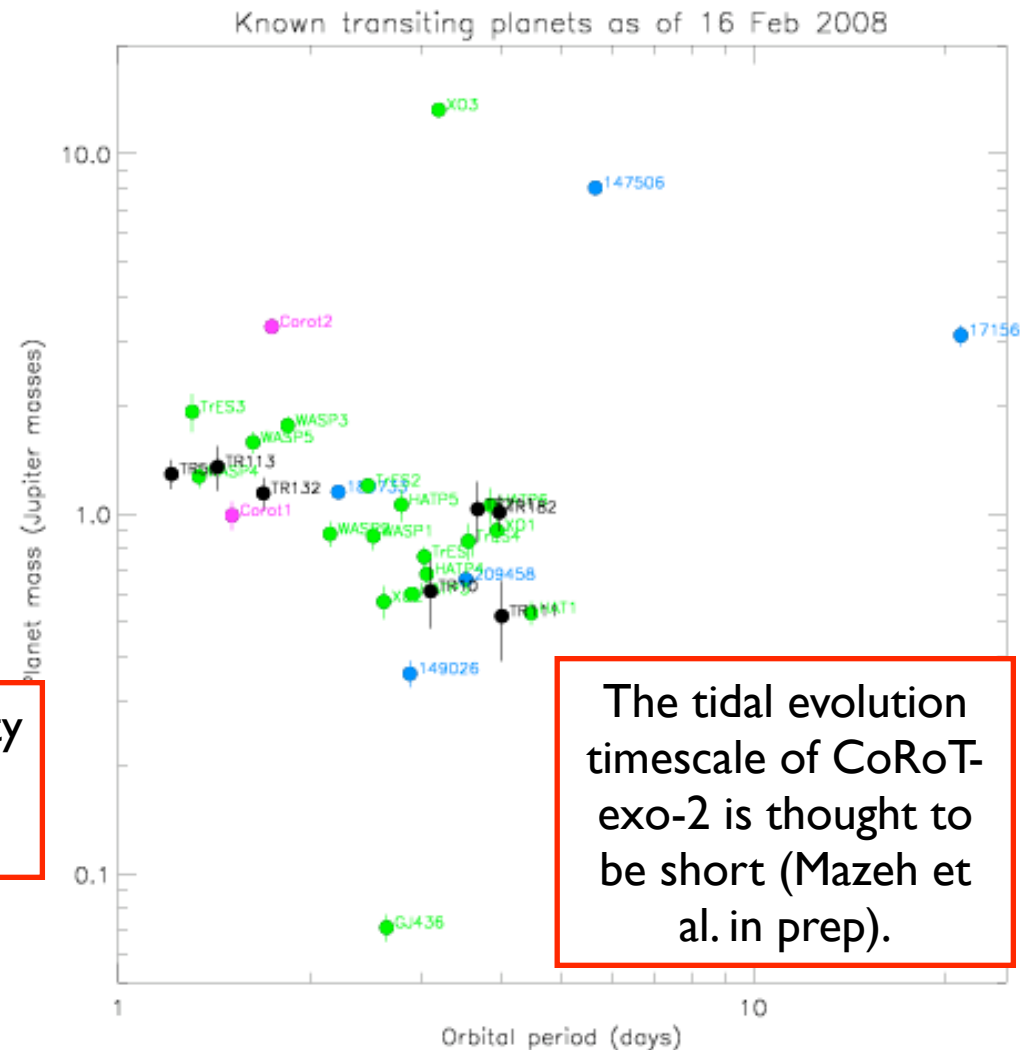
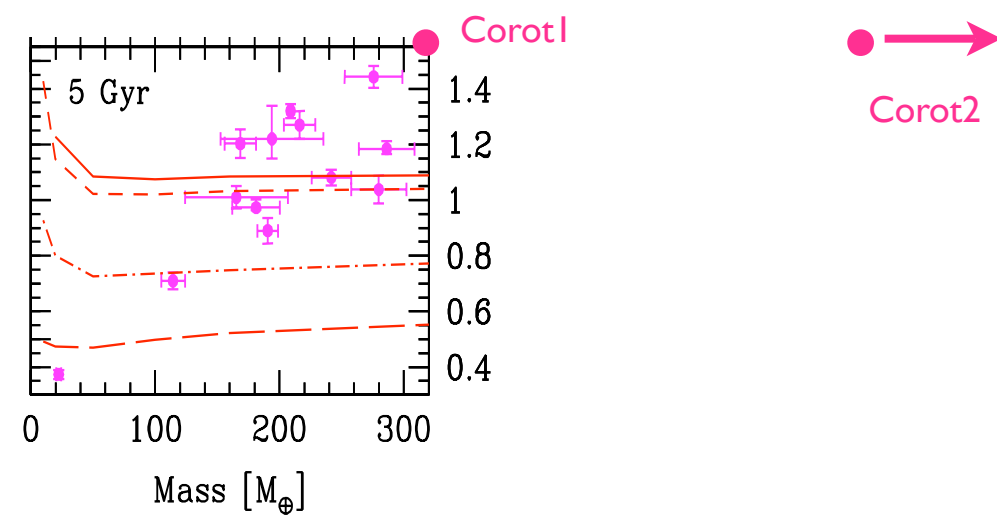
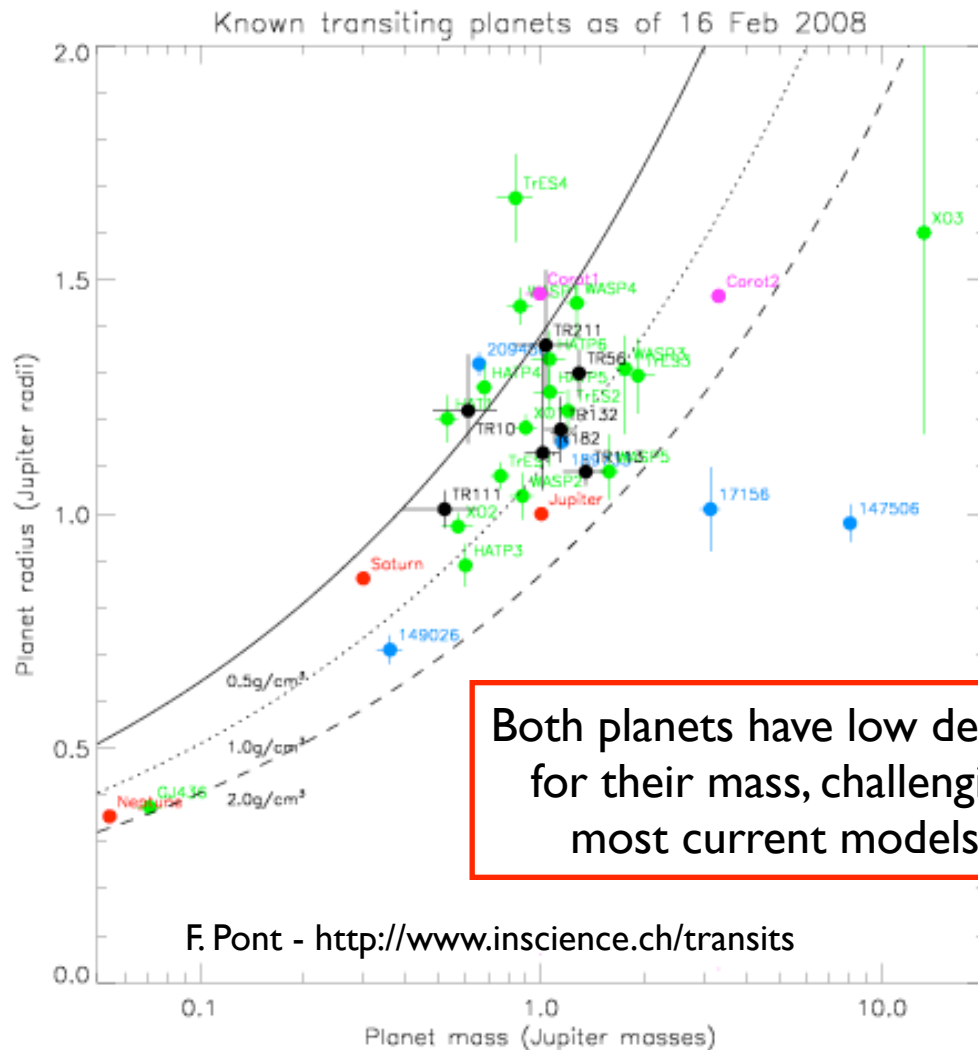
Mass-radius-period relations



Mass-radius-period relations



Mass-radius- period relations



The tidal evolution timescale of CoRoT-exo-2 is thought to be short (Mazeh et al. in prep).